International Journal of Solids and Structures 51 (2014) 2598–2619

Contents lists available at ScienceDirect

International Journal of Solids and Structures

journal homepage: www.elsevier.com/locate/ijsolstr

Bending solution of third-order orthotropic Reddy plates with asymmetric interfacial crack

András Szekrényes *

Budapest University of Technology and Economics, Department of Applied Mechanics, Műegyetem rkp. 5, Building MM, 1111 Budapest, Hungary

ARTICLE INFO

Article history:
Received 31 July 2013
Received in revised form 10 March 2014
Available online 8 April 2014

Keywords:
Delamination
Energy release rate
Third-order plate
Mixed mode II/III fracture
J-integral

ABSTRACT

In this paper Reddy's third-order shear deformable plate theory is applied to asymmetrically delaminated orthotropic composite plates under antiplane–inplane shear fracture mode. A double-plate system is utilized to capture the mechanical behavior of the uncracked plate portion. An assumed displacement field is used and modified in order to satisfy the traction-free conditions at the top and bottom plate boundaries. Moreover, the system of exact kinematic conditions was also implemented into the novel plate model. An important improvement of this work compared to previous papers is the continuity condition of the shear strains at the interface of the double-plate system. Applying these conditions it is shown that the nineteen parameters of the third-order displacement field can be reduced to nine. Using the simplified displacement field the governing equations are derived, as well. The solution of a simply-supported delaminated plate is presented using the state-space model and the displacement, strain and stress fields are determined, respectively. The energy release rate and mode mixity distributions are calculated using the 3D *J*-integral. The analytical results are compared to those by finite element computations and it is concluded that the present model is the most accurate one among the previous plate theory-based approaches.

1. Introduction

Laminated composite materials have a very wide range of application, beginning with car and bodywork construction, sport industry, prosthetic devices, airplanes and continuing with wind turbines, ships, pressure vessels, etc. (see e.g: Giannis et al., 2008; Chirica et al., 2011; Chirica, 2013). In all of these applications the small weight/high stiffness property is utilized. Unfortunately laminated materials are susceptible to delamination fracture (Andrews et al., 2009; Zhou et al., 2013; Kiani et al., 2013; Marat-Mendes and Freitas, 2013), e.g. as a result of low velocity impact and free edge effect. The resistance to delamination is characterized by experimental tests under different fracture modes. The main parameters of linear elastic fracture mechanics (LEFM) are the stress intensity factor (SIF) (Hills et al., 1996; Cherepanov, 1997; Anderson, 2005) and energy release rate (ERR) (Adams et al., 2000; Anderson, 2005), respectively. The fracture tests are carried out on different type of delamination specimens including mode-I (Hamed et al., 2006; Sorensen et al., 2007; Islam and Kapania, 2011; Kim et al., 2011; Peng et al., 2011; Romhany and Szebenyi, 2012; Jumel et al., 2011a; Salem et al., 2013), mode-II (Kutnar et al., 2008; Arrese et al., 2010; Argüelles et al., 2011; Rizov and Mladensky, 2012; Mladensky and Rizov, 2013b; Jumel et al., 2013; Budzik et al., 2013), mixed-mode I/II (Szekrényes, 2007b; Nikbakht and Choupani, 2008; Yoshihara and Satoh, 2009; Bennati et al., 2009; Kenane et al., 2010; Jumel et al., 2011b; da Silva et al., 2011; Fernández et al., 2013; Bennati et al., 2013a; Bennati et al., 2013b), mode-III (Rizov et al., 2006; Szekrényes, 2009a; de Moura et al., 2009; Marat-Mendes and Freitas, 2009; de Morais and Pereira, 2009; de Morais et al., 2011; Pereira et al., 2011; Suemasu and Tanikado, 2012; Johnston et al., 2012; Mehrabadi and Khosravan, 2013), mixed-mode I/III (Szekrényes, 2009b; Pereira and de Morais, 2009) mixed-mode II/III (Szekrényes, 2007a; de Morais and Pereira, 2008; Suemasu et al., 2010; Ho and Tay, 2011; Kondo et al., 2010, 2011; Nikbakht et al., 2010; Szekrényes, 2012a; Suemasu and Tanikado, 2012; Miura et al., 2012; Mehrabadi, 2013; Mladensky and Rizov, 2013a) and mixed-mode I/II/III (Davidson et al., 2010; Szekrényes, 2011; Davidson and Sediles, 2011) tests, respectively. In the former works beam and plate specimens are applied. While for beams the closed-form solutions are

* Tel.: +36 14631170; fax: +36 14633471.
E-mail address: szeki@mm.bme.hu
URL: http://www.mm.bme.hu/~szeki

http://dx.doi.org/10.1016/j.ijsolstr.2014.03.027
0020-7683/© 2014 Elsevier Ltd. All rights reserved.

available, for plates similar solutions exist only for some relatively simple systems (Lee and Tu, 1993; Saeedi et al., 2012a; Saeedi et al., 2012b). This paper puts emphasis essentially on the application of plate theories in fracture mechanics under mixed-mode II/III condition. In this respect the classical laminated plate theory (CLPT) (Reddy, 2004; Kollár and Springer, 2003; Kumar and Lal, 2012), first-order (FSDT) (Reddy, 2004; Yu, 2005; Kharazi et al., 2010; Thai and Choi, 2013), second-order (SSDT) (Shahrjerdi et al., 2010, 2011), general third-order (TSDT) and Reddy's third-order shear deformable theories are available (Reddy, 2004). These are the so-called equivalent single-layer theories (ESL). An important aspect of these approaches is that plane stress condition is assumed, therefore the transverse normal stress σ_z does not appear in the equations. The literature also offers the 3D elasticity solution and the layerwise or multilayer approaches (Reddy, 2004; Saeedi et al., 2012a,b; Batista, 2012; Ferreira et al., 2011; Massabò and Campi, 2013) (3D solutions). It has to be mentioned that there are some mixed analytical/numerical methods for the calculation of ERR in 3D structures (Sankar and Sonik, 1995; Davidson et al., 2000), as well. Concentrating on the pure analytical formulation of the problem of delaminated plates the precedents of the current work are the following:

- extension of the elastic interface model (e.g. Luo and Tong, 2009) for isotropic and orthotropic plates with midplane delamination (Szekrényes, 2012b, 2013b)
- application of classical, first-, second- and third-order plate theories to symmetrically delaminated orthotropic plates using interface constraints (Szekrényes, 2013a,c, in press)
- a refined model utilizing Reddy's third-order shear deformable plate theory for midplane delaminated orthotropic plates (Szekrényes, 2014b)
- introduction of the system of exact kinematic conditions (SEKC) for first-order (Szekrényes, 2013d) and second-order plates with asymmetric delamination

Based on these works it was shown that for plates with symmetric lay-up and midplane delamination the minimum requirement is the application of FSDT (Szekrényes, 2013a). Although the second- and third-order theories (Szekrényes, 2013c, in press, 2014b) provide some improvement, their main advantage can be exploited essentially if the delamination is not in the midplane of the plate. The latter case generates a complex strain and stress state around the delamination tip: the higher the order of the displacement field is, the higher the accuracy of the approach is. As a continuation of the previous researches, in this paper Reddy's third-order theory is extended to orthotropic plates with asymmetric interfacial delamination. The analysis is based on the SEKC requirements, which are complemented with the continuity of shear strains at the interface plane of the top and bottom layers of the double-plate model. Fig. 1 shows the main aspects of the problems investigated in this paper. The laminated plate contains a through-width delamination, which is parallel to the X–Y plane of the global coordinate system and in each case the direction of crack propagation is the global X axis. Four cases are presented in Fig. 1 including two different lay-ups. The governing equations are derived for asymmetrically delaminated plates and as an example a simply-supported plate is analyzed using the state-space formulation. The displacement and stress fields are determined and the distribution of the ERR along the delamination front is calculated by the 3D J-integral (e.g. Shivakumar and Raju, 1992; Mladensky and Rizov, 2013b) It is shown that the present approach is reasonable to obtain accurate results for asymmetrically delaminated plates.

2. The system of exact kinematic conditions

Let us assume a composite plate consisting of orthotropic plies, the plate contains an interfacial delamination between any plies as it is shown by Fig. 2. The local through-thickness coordinates are: $z^{(t)} \in (-t_t/2, t_t/2),\ z^{(b)} \in (-t_b/2, t_b/2)$, where t_t and t_b are the thicknesses of the top and bottom layers. The global coordinates are denoted by $X,\ Y$ and Z. The delamination divides the plate into a top and a bottom plate element, each is modeled by ESLs. In the delaminated portion (see Fig. 2(b)) the displacement field is discontinuous in the plane of the delamination, the top and bottom layers of the delaminated part can be modeled by traditional plate theories. In contrast the displacement field is continuous in the undelaminated region. Therefore, in this section the kinematic continuity conditions between the top and bottom layers of the undelaminated plate portion are formulated. In fact, the problem can be solved by any plate theory. Whichever theory is used the assumed displacement field of the undelaminated plate portion has to satisfy certain kinematic conditions. First, the components of the displacement vector are continuous across the interface plane. The requirements are:

$$(u_t, v_t, w_t)|_{z^{(t)}=-z_R^t} = (u_b, v_b, w_b)|_{z^{(b)}=t_b-z_R^b} \tag{1}$$

where $u,\ v$ and w are the components of the displacement vector, moreover z_R^b and z_R^t are the positions of the reference planes of the top and bottom plates, respectively. Second, we choose a global reference plane given by z_R (see Fig. 2) in the uncracked region (similarly to plates without discontinuities, Reddy, 2004). Depending on the thicknesses of top and bottom plates this condition involves two cases:

$$z_R \begin{cases} \leqslant t_b: & u_b|_{z^{(b)}=z_R-z_R^b} - u_0 = 0, \quad v_b|_{z^{(b)}=z_R-z_R^b} - v_0 = 0 \\ \geqslant t_b: & u_t|_{z^{(t)}=-(z_R^t-z_R+t_b)} - u_0 = 0, \quad v_t|_{z^{(t)}=-(z_R^t-z_R+t_b)} - v_0 = 0 \end{cases} \tag{2}$$

where z_R is the position of the reference plane in the uncracked portion, $u_0,\ v_0$ are the global constant in-plane displacements of the uncracked region because of the bending-stretching coupling. As it is shown by Fig. 2, the latter are the same for the top and bottom plates. For first- and second-order plates the conditions above are sufficient to develop a relatively accurate displacement field (Szekrényes, 2013d). However, for third-order plates even the transverse shear strains have to be continuous across the interface plane, involving the following conditions:

$$(\gamma_{xzt}, \gamma_{yzt})\Big|_{z^{(t)}=-z_R^t} = (\gamma_{xzb}, \gamma_{yzb})\Big|_{z^{(b)}=t_b-z_R^b} \tag{3}$$

Eqs. (1)–(3) are called the system of exact kinematic conditions (SEKC). As it is shown, there are seven conditions formulated. Since the neutral plane of laminated plates can be determined only in some particular cases (Nettles, 1991), it is convenient to choose the midplane of the plate to be the reference plane (Reddy, 2004, p. 113, Jones, 1999, p. 197). In this case Eqs. (1)–(3) reduce to:

$$(u_t, v_t, w_t)|_{z^{(t)}=-\frac{t_t}{2}} = (u_b, v_b, w_b)|_{z^{(b)}=\frac{t_b}{2}} \tag{4}$$

$$\frac{t_t+t_b}{2} \begin{cases} \leqslant t_b: & u_b|_{z^{(b)}=\frac{t_t}{2}} - u_0 = 0, \quad v_b|_{z^{(b)}=\frac{t_t}{2}} - v_0 = 0 \\ \geqslant t_b: & u_t|_{z^{(t)}=-\frac{t_b}{2}} - u_0 = 0, \quad v_t|_{z^{(t)}=-\frac{t_b}{2}} - v_0 = 0 \end{cases} \tag{5}$$

$$(\gamma_{xzt}, \gamma_{yzt})\Big|_{z^{(t)}=-\frac{t_t}{2}} = (\gamma_{xzb}, \gamma_{yzb})\Big|_{z^{(b)}=\frac{t_b}{2}} \tag{6}$$

In the sequel, the application of the SEKC to third-order Reddy plates is presented.

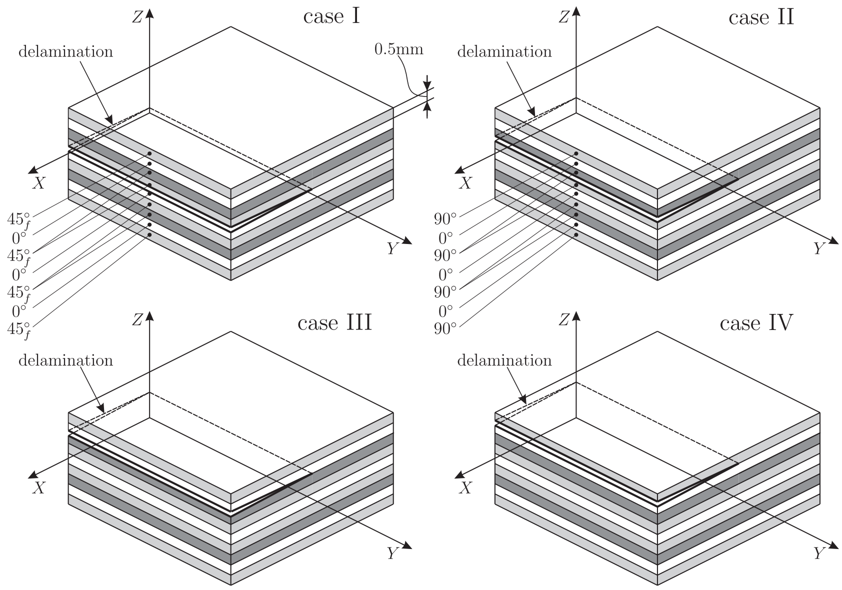

Fig. 1. Plate elements with orthotropic plies and the position of the delamination over the thickness of the plate.

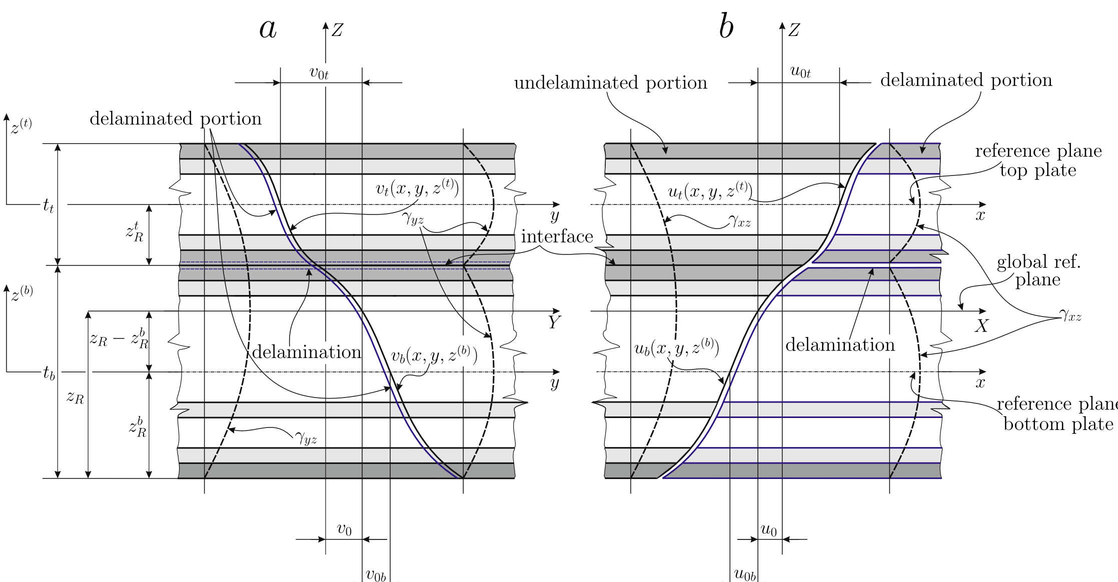

Fig. 2. Cross sections and deformation of the top and bottom plate elements of a delaminated plate in the Y–Z (a) and X–Z (b) planes.

3. Extension of Reddy's third-order theory to delaminated plates

In this section we develop the displacement field and the governing equations of the uncracked plate portion, the delaminated part can be modeled by the traditional TSDT by Reddy (Reddy, 2004, p. 671). The inplane displacements in the undelaminated portion of general third-order plates can be written as:

$$u_\delta(x,y,z^{(\delta)}) = u_0(x,y) + u_{0\delta}(x,y) + \theta_{x\delta}(x,y)\cdot z^{(\delta)} + \phi_{x\delta}(x,y) \cdot \left[z^{(\delta)}\right]^2 + \lambda_{x\delta}(x,y)\cdot\left[z^{(\delta)}\right]^3 \quad (7)$$

$$v_\delta(x,y,z^{(\delta)}) = v_0(x,y) + v_{0\delta}(x,y) + \theta_{y\delta}(x,y)\cdot z^{(\delta)} + \phi_{y\delta}(x,y) \cdot \left[z^{(\delta)}\right]^2 + \lambda_{y\delta}(x,y)\cdot\left[z^{(\delta)}\right]^3 \quad (8)$$

where δ takes t for the top and b for the bottom plate, respectively (refer to Fig. 2), furthermore $z^{(\delta)}$ is the local coordinate, u_0 and v_0 are the global (through-thickness) constant parts of the displacement functions, $u_{0\delta}$ and $v_{0\delta}$ are the local constant parts (refer to u_{0t}, u_{0b} and v_{0t}, v_{0b} in Fig. 2), $\theta_{x\delta}$ and $\theta_{y\delta}$ are the rotations about the x and y axes, $\phi_{x\delta}$ and $\phi_{y\delta}$ are the parameters of the second-order, $\lambda_{x\delta}$ and $\lambda_{y\delta}$ are the parameters of the third-order terms, respectively. It should be highlighted that the local constant components (or membrane components, u_{0t} and u_{0b} or v_{0t} and v_{0b} in Fig. 2) are different in magnitude for the top and bottom plates. These are very important to satisfy the SEKC requirements. Based on the intersection points between the local reference planes with the curve of the through-thickness displacement distribution in Fig. 2(b) it can be seen that u_{0t} and u_{0b} should be different in magnitude (geometric consideration). The magnitude of the u_{0t} and u_{0b} (and v_{0t}, v_{0b}) parameters would be the same only for a plate with symmetric lay-up and midplane delamination (Szekrényes, 2014b). It is assumed (see Eq. (1)) that the $w(x,y)$ deflections of the top and bottom plates are the same, and so, we have nineteen parameters altogether. Utilizing Eqs. (4)–(6) and the first case in Eq. (5), moreover taking the midplanes of the top and bottom plates to be the reference planes and finally using the

$$(\gamma_{xzt},\gamma_{yzt})\Big|_{z^{(t)}=\frac{t_t}{2}}=(\gamma_{xzb},\gamma_{yzb})\Big|_{z^{(b)}=\frac{-t_b}{2}}=0 \tag{9}$$

conditions to ensure traction-free top and bottom surfaces (Reddy, 2004, p. 673) it is possible to eliminate ten from the nineteen parameters. However, we can not choose arbitrarily that which ones of the displacement parameters are eliminated. The higher-order stress resultant denoted by P (see later) plays an important role in Reddy's theory (Reddy, 2004, p. 704), therefore the corresponding parameters denoted by λ in Eqs. (7) and (8) must be untouched. On the other hand it is seen that the higher-order stress resultant denoted by L (Szekrényes, 2013c) is eliminated from Reddy's plate theory. Therefore, the corresponding two quadratic parameters, given by ϕ can be eliminated. The next two parameters eliminated from Eqs. (7) and (8) are $u_{0\delta}$ and $v_{0\delta}$. Finally, the rotations of the top plate are also eliminated. Consequently, the remaining parameters are: u_0, v_0, θ_{xb}, θ_{yb}, λ_{xt}, λ_{yt}, λ_{xb}, λ_{yb} and the deflection w, respectively. Based on these concepts and Eqs. (4)–(8) the displacement fields of the uncracked portion becomes:

$$\{u_t\}=\{u_0\}+\{u_{0t}\}+\{u_{1t}\}\cdot z^{(t)}+\{u_{2t}\}\cdot\left[z^{(t)}\right]^2+\{u_{3t}\}\cdot\left[z^{(t)}\right]^3 \tag{10}$$

$$\{u_b\}=\{u_0\}+\{u_{0b}\}+\{u_{1b}\}\cdot z^{(b)}+\{u_{2b}\}\cdot\left[z^{(b)}\right]^2+\{u_{3b}\}\cdot\left[z^{(b)}\right]^3 \tag{11}$$

where $\{u_t\}^{\mathrm{T}}=\{u_t\quad v_t\}, \{u_{1t}\}^{\mathrm{T}}=\{u_{1t}\quad v_{1t}\}$, etc. Furthermore:

$$\{u_0\}=\begin{Bmatrix}u_0\\ v_0\end{Bmatrix},\quad \{u_{0t}\}=\Delta_t\begin{Bmatrix}\theta_{xb}\\ \theta_{yb}\end{Bmatrix}+\Phi_t\begin{Bmatrix}\lambda_{xt}\\ \lambda_{yt}\end{Bmatrix}+\Gamma_t\begin{Bmatrix}\lambda_{xb}\\ \lambda_{yb}\end{Bmatrix}+\Lambda_t\begin{Bmatrix}\frac{\partial w}{\partial x}\\ \frac{\partial w}{\partial y}\end{Bmatrix}$$
$$\{u_{1t}\}=\begin{Bmatrix}\theta_{xb}\\ \theta_{yb}\end{Bmatrix}+\Pi_t\begin{Bmatrix}\lambda_{xt}\\ \lambda_{yt}\end{Bmatrix}+\Sigma_t\begin{Bmatrix}\lambda_{xb}\\ \lambda_{yb}\end{Bmatrix}$$
$$\{u_{2t}\}=\Omega_t\begin{Bmatrix}\theta_{xb}\\ \theta_{yb}\end{Bmatrix}+\Psi_t\begin{Bmatrix}\lambda_{xt}\\ \lambda_{yt}\end{Bmatrix}+\Omega_t\begin{Bmatrix}\frac{\partial w}{\partial x}\\ \frac{\partial w}{\partial y}\end{Bmatrix},\quad \{u_{3t}\}=\begin{Bmatrix}\lambda_{xt}\\ \lambda_{yt}\end{Bmatrix} \tag{12}$$

and:

$$\{u_{0b}\}=\Delta_b\begin{Bmatrix}\theta_{xb}\\ \theta_{yb}\end{Bmatrix}+\Gamma_b\begin{Bmatrix}\lambda_{xb}\\ \lambda_{yb}\end{Bmatrix}+\Lambda_b\begin{Bmatrix}\frac{\partial w}{\partial x}\\ \frac{\partial w}{\partial y}\end{Bmatrix},\quad \{u_{1b}\}=\begin{Bmatrix}\theta_{xb}\\ \theta_{yb}\end{Bmatrix}$$
$$\{u_{2b}\}=\Omega_b\begin{Bmatrix}\theta_{xb}\\ \theta_{yb}\end{Bmatrix}+\Psi_b\begin{Bmatrix}\lambda_{xb}\\ \lambda_{yb}\end{Bmatrix}+\Omega_b\begin{Bmatrix}\frac{\partial w}{\partial x}\\ \frac{\partial w}{\partial y}\end{Bmatrix},\quad \{u_{3b}\}=\begin{Bmatrix}\lambda_{xb}\\ \lambda_{yb}\end{Bmatrix} \tag{13}$$

where: $\Delta_t=\frac{1}{4t_b}(3t_b^2+t_tt_b-t_t^2)$, $\Phi_t=-\frac{1}{4}t_t^3$, $\Gamma_t=\frac{1}{16}(2t_t+t_b)(5t_b^2-t_tt_b-t_t^2)$, $\Lambda_t=\frac{1}{4t_b}(t_b^2+t_tt_b-t_t^2)$, $\Pi_t=-\frac{3}{4}t_t^2$, $\Sigma_t=\frac{3}{4}t_b^2$, $\Omega_t=-\frac{1}{t_t}$, $\Psi_t=-\frac{3t_b^2}{4t_t}$, $\Delta_b=-\frac{t_t}{4t_b}(2t_b+t_t)$, $\Gamma_b=-\frac{t_t^2}{16}(3t_b+2t_t)$, $\Lambda_b=-\frac{t_t^2}{4t_b}$, $\Omega_b=\frac{1}{t_b}$, $\Psi_b=\frac{3}{4}t_b$.

It must be highlighted again that the SEKC requirements are essentially related to the uncracked portion of the plate. The parameters that were eliminated in Eqs. (10) and (11) (u_{0t}, v_{0t}, u_{0b}, v_{0b}, ϕ_{xt}, ϕ_{yt}, ϕ_{xb}, ϕ_{yb}, θ_{xt} and θ_{yt}) became the functions of the remaining parameters (θ_{xb}, θ_{yb}, λ_{xt}, λ_{yt}, λ_{xb}, λ_{yb} and w) in accordance with the second, third and fourth expressions in Eq. (12), moreover in accordance with the first and third expressions in Eq. (13). It is important that u_0 are v_0 are also remaining (independent) parameters.

The strain field is obtained by using the basic equations of linear elasticity (Chou and Pagano, 1967):

$$\begin{Bmatrix}\varepsilon_x\\ \varepsilon_y\\ \gamma_{xy}\end{Bmatrix}_{(\delta)}=\begin{Bmatrix}\frac{\partial u_0}{\partial x}\\ \frac{\partial v_0}{\partial y}\\ \frac{\partial u_0}{\partial y}+\frac{\partial v_0}{\partial x}\end{Bmatrix}+\begin{Bmatrix}\varepsilon_x^{(0)}\\ \varepsilon_y^{(0)}\\ \gamma_{xy}^{(0)}\end{Bmatrix}_{(\delta)}+z^{(\delta)}\cdot\begin{Bmatrix}\varepsilon_x^{(1)}\\ \varepsilon_y^{(1)}\\ \gamma_{xy}^{(1)}\end{Bmatrix}_{(\delta)}+\left[z^{(\delta)}\right]^2\cdot\begin{Bmatrix}\varepsilon_x^{(2)}\\ \varepsilon_y^{(2)}\\ \gamma_{xy}^{(2)}\end{Bmatrix}_{(\delta)}+\left[z^{(\delta)}\right]^3\cdot\begin{Bmatrix}\varepsilon_x^{(3)}\\ \varepsilon_y^{(3)}\\ \gamma_{xy}^{(3)}\end{Bmatrix}_{(\delta)} \tag{14}$$

$$\begin{Bmatrix}\gamma_{xz}\\ \gamma_{yz}\end{Bmatrix}_{(\delta)}=\begin{Bmatrix}\gamma_{xz}^{(0)}\\ \gamma_{yz}^{(0)}\end{Bmatrix}_{(\delta)}+z^{(\delta)}\cdot\begin{Bmatrix}\gamma_{xz}^{(1)}\\ \gamma_{yz}^{(1)}\end{Bmatrix}_{(\delta)}+\left[z^{(\delta)}\right]^2\cdot\begin{Bmatrix}\gamma_{xz}^{(2)}\\ \gamma_{yz}^{(2)}\end{Bmatrix}_{(\delta)} \tag{15}$$

where the terms with superscript "0" are the constant strains:

$$\begin{Bmatrix}\varepsilon_x^{(0)}\\ \varepsilon_y^{(0)}\\ \gamma_{xy}^{(0)}\end{Bmatrix}_{(t)}=\Delta_t\begin{Bmatrix}\varepsilon_x^{(1)}\\ \varepsilon_y^{(1)}\\ \gamma_{xy}^{(1)}\end{Bmatrix}_{(b)}+\Phi_t\begin{Bmatrix}\varepsilon_x^{(3)}\\ \varepsilon_y^{(3)}\\ \gamma_{xy}^{(3)}\end{Bmatrix}_{(t)}+\Gamma_t\begin{Bmatrix}\varepsilon_x^{(3)}\\ \varepsilon_y^{(3)}\\ \gamma_{xy}^{(3)}\end{Bmatrix}_{(b)}+\Lambda_t\begin{Bmatrix}\frac{\partial^2 w}{\partial x^2}\\ \frac{\partial^2 w}{\partial y^2}\\ 2\frac{\partial^2 w}{\partial x\partial y}\end{Bmatrix} \tag{16}$$

$$\begin{Bmatrix}\varepsilon_x^{(0)}\\ \varepsilon_y^{(0)}\\ \gamma_{xy}^{(0)}\end{Bmatrix}_{(b)}=\Delta_b\begin{Bmatrix}\varepsilon_x^{(1)}\\ \varepsilon_y^{(1)}\\ \gamma_{xy}^{(1)}\end{Bmatrix}_{(b)}+\Gamma_b\begin{Bmatrix}\varepsilon_x^{(3)}\\ \varepsilon_y^{(3)}\\ \gamma_{xy}^{(3)}\end{Bmatrix}_{(b)}+\Lambda_b\begin{Bmatrix}\frac{\partial^2 w}{\partial x^2}\\ \frac{\partial^2 w}{\partial y^2}\\ 2\frac{\partial^2 w}{\partial x\partial y}\end{Bmatrix} \tag{17}$$

The first-, second- and third-order strains are defined as:

$$\begin{Bmatrix}\varepsilon_x^{(1)}\\ \varepsilon_y^{(1)}\\ \gamma_{xy}^{(1)}\end{Bmatrix}_{(t)}=\begin{Bmatrix}\varepsilon_x^{(1)}\\ \varepsilon_y^{(1)}\\ \gamma_{xy}^{(1)}\end{Bmatrix}_{(b)}+\Pi_t\begin{Bmatrix}\varepsilon_x^{(3)}\\ \varepsilon_y^{(3)}\\ \gamma_{xy}^{(3)}\end{Bmatrix}_{(t)}+\Sigma_t\begin{Bmatrix}\varepsilon_x^{(3)}\\ \varepsilon_y^{(3)}\\ \gamma_{xy}^{(3)}\end{Bmatrix}_{(b)} \tag{18}$$

$$\begin{Bmatrix}\varepsilon_x^{(1)}\\ \varepsilon_y^{(1)}\\ \gamma_{xy}^{(1)}\end{Bmatrix}_{(b)}=\begin{Bmatrix}\frac{\partial\theta_x}{\partial x}\\ \frac{\partial\theta_y}{\partial y}\\ \frac{\partial\theta_x}{\partial y}+\frac{\partial\theta_y}{\partial x}\end{Bmatrix}_{(b)} \tag{19}$$

$$\begin{Bmatrix}\varepsilon_x^{(2)}\\ \varepsilon_y^{(2)}\\ \gamma_{xy}^{(2)}\end{Bmatrix}_{(\delta)}=\Omega_{(\delta)}\begin{Bmatrix}\varepsilon_x^{(1)}\\ \varepsilon_y^{(1)}\\ \gamma_{xy}^{(1)}\end{Bmatrix}_{(b)}+\Psi_{(\delta)}\begin{Bmatrix}\varepsilon_x^{(3)}\\ \varepsilon_y^{(3)}\\ \gamma_{xy}^{(3)}\end{Bmatrix}_{(b)}+\Omega_{(\delta)}\begin{Bmatrix}\frac{\partial^2 w}{\partial x^2}\\ \frac{\partial^2 w}{\partial y^2}\\ 2\frac{\partial^2 w}{\partial x\partial y}\end{Bmatrix} \tag{20}$$

$$\begin{Bmatrix}\varepsilon_x^{(3)}\\ \varepsilon_y^{(3)}\\ \gamma_{xy}^{(3)}\end{Bmatrix}_{(\delta)}=\begin{Bmatrix}\frac{\partial\lambda_x}{\partial x}\\ \frac{\partial\lambda_y}{\partial y}\\ \frac{\partial\lambda_x}{\partial y}+\frac{\partial\lambda_y}{\partial x}\end{Bmatrix}_{(\delta)} \tag{21}$$

Finally the shear strains are given by the following equations:

$$\begin{Bmatrix}\gamma_{xz}^{(0)}\\ \gamma_{yz}^{(0)}\end{Bmatrix}_{(t)}=\begin{Bmatrix}\theta_x+\frac{\partial w}{\partial x}\\ \theta_y+\frac{\partial w}{\partial y}\end{Bmatrix}_{(b)}+\Pi_t\begin{Bmatrix}\lambda_x\\ \lambda_y\end{Bmatrix}_{(b)}+\Sigma_t\begin{Bmatrix}\lambda_x\\ \lambda_y\end{Bmatrix}_{(t)} \tag{22}$$

$$\begin{Bmatrix}\gamma_{xz}^{(0)}\\ \gamma_{yz}^{(0)}\end{Bmatrix}_{(b)}=\begin{Bmatrix}\theta_x+\frac{\partial w}{\partial x}\\ \theta_y+\frac{\partial w}{\partial y}\end{Bmatrix}_{(b)} \tag{23}$$

$$\begin{Bmatrix}\gamma_{xz}^{(1)}\\ \gamma_{yz}^{(1)}\end{Bmatrix}_{(\delta)}=2\Omega_{(\delta)}\begin{Bmatrix}\theta_x+\frac{\partial w}{\partial x}\\ \theta_y+\frac{\partial w}{\partial y}\end{Bmatrix}_{(b)}+2\Psi_{(\delta)}\begin{Bmatrix}\lambda_x\\ \lambda_y\end{Bmatrix}_{(b)} \tag{24}$$

$$\begin{Bmatrix}\gamma_{xz}^{(2)}\\ \gamma_{yz}^{(2)}\end{Bmatrix}_{(\delta)}=3\begin{Bmatrix}\lambda_x\\ \lambda_y\end{Bmatrix}_{(\delta)} \tag{25}$$

The relationship among the stress resultants and the strain field parameters of third-order plates is (Reddy, 2004):

$$\begin{Bmatrix} \{N\} \\ \{M\} \\ \{L\} \\ \{P\} \end{Bmatrix}_{(\delta)} = \begin{bmatrix} [A] & [B] & [D] & [E] \\ [B] & [D] & [E] & [F] \\ [D] & [E] & [F] & [G] \\ [E] & [F] & [G] & [H] \end{bmatrix}_{(\delta)} \begin{Bmatrix} \{\varepsilon^{(0)}\} \\ \{\varepsilon^{(1)}\} \\ \{\varepsilon^{(2)}\} \\ \{\varepsilon^{(3)}\} \end{Bmatrix}_{(\delta)} \tag{26}$$

$$\begin{Bmatrix} \{Q\} \\ \{R\} \\ \{S\} \end{Bmatrix}_{(\delta)} = \begin{bmatrix} [A]^* & [B]^* & [D]^* \\ [B]^* & [D]^* & [E]^* \\ [D]^* & [E]^* & [F]^* \end{bmatrix} \begin{Bmatrix} \{\gamma^{(0)}\} \\ \{\gamma^{(1)}\} \\ \{\gamma^{(2)}\} \end{Bmatrix}_{(\delta)} \tag{27}$$

where:

$$[..]^* = \begin{bmatrix} (.)_{55} & 0 \\ 0 & (.)_{44} \end{bmatrix} \tag{28}$$

Moreover: $\{N\}^{\mathrm{T}}_{(\delta)} = \{N_x \quad N_y \quad N_{xy}\}_{(\delta)}$ is the vector of in-plane forces, $\{M\}^{\mathrm{T}}_{(\delta)} = \{M_x \quad M_y \quad M_{xy}\}_{(\delta)}$ is the vector of bending and twisting moments, $\{Q\}^{\mathrm{T}}_{(\delta)} = \{Q_x \quad Q_y\}_{(\delta)}$ is the vector of transverse shear forces, and finally $\{L\}^{\mathrm{T}}_{(\delta)} = \{L_x \quad L_y \quad L_{xy}\}_{(\delta)}$, $\{P\}^{\mathrm{T}}_{(\delta)} = \{P_x \quad P_y \quad P_{xy}\}_{(\delta)}$ and $\{R\}^{\mathrm{T}}_{(\delta)} = \{R_x \quad R_y\}_{(\delta)}$, $\{S\}^{\mathrm{T}}_{(\delta)} = \{S_x \quad S_y\}_{(\delta)}$ are the vectors of higher-order stress resultants. The stress resultants are defined as:

$$\begin{Bmatrix} N_{\alpha\beta} \\ M_{\alpha\beta} \\ L_{\alpha\beta} \\ P_{\alpha\beta} \end{Bmatrix}_{(\delta)} = \int_{-t_\delta/2}^{t_\delta/2} \sigma_{\alpha\beta} \begin{Bmatrix} 1 \\ z \\ z^2 \\ z^3 \end{Bmatrix}^{(\delta)} dz^{(\delta)}$$
$$\begin{Bmatrix} Q_\alpha \\ R_\alpha \\ S_\alpha \end{Bmatrix}_{(\delta)} = \int_{-t_\delta/2}^{t_\delta/2} \sigma_{\alpha z} \begin{Bmatrix} 1 \\ z \\ z^2 \end{Bmatrix}^{(\delta)} dz^{(\delta)} \tag{29}$$

where the symbols α and β take x or y. The extensional, coupling, bending and higher-order stiffnesses can be defined as (Reddy, 2004):

$$(A_{ij}, B_{ij}, D_{ij}, E_{ij}, F_{ij}, G_{ij}, H_{ij})_{(\delta)} = \sum_{k=1}^{N_l} \int_{z_k}^{z_{k+1}} \bar{C}_{ij}^{(k)} (1, z, z^2, z^3, z^4, z^5, z^6)^{(\delta)} dz^{(\delta)} \tag{30}$$

The stiffnesses above are calculated with respect to the local reference planes of the top and bottom plates (refer to Fig. 2). The application of the principle of virtual work (Reddy, 2004, p. 674) makes it possible to obtain the Euler–Lagrange equations (equilibrium equations) in the following forms:

$$\frac{\partial N_{xt}}{\partial x} + \frac{\partial N_{xyt}}{\partial y} + \frac{\partial N_{xb}}{\partial x} + \frac{\partial N_{xyb}}{\partial y} = 0 \tag{31}$$

$$\frac{\partial N_{xyt}}{\partial x} + \frac{\partial N_{yt}}{\partial y} + \frac{\partial N_{xyb}}{\partial x} + \frac{\partial N_{yb}}{\partial y} = 0 \tag{32}$$

$$\frac{\partial P_{xt}}{\partial x} + \frac{\partial P_{xyt}}{\partial y} + \Phi_t \left(\frac{\partial N_{xt}}{\partial x} + \frac{\partial N_{xyt}}{\partial y} \right) + \Phi_b \left(\frac{\partial N_{xb}}{\partial x} + \frac{\partial N_{xyb}}{\partial y} \right) + \Pi_t \left(\frac{\partial M_{xt}}{\partial x} + \frac{\partial M_{xyt}}{\partial y} \right) - \Pi_t Q_{xt} - 3S_{xt} = 0 \tag{33}$$

$$\frac{\partial P_{xyt}}{\partial x} + \frac{\partial P_{yt}}{\partial y} + \Phi_t \left(\frac{\partial N_{xyt}}{\partial x} + \frac{\partial N_{yt}}{\partial y} \right) + \Phi_b \left(\frac{\partial N_{xyb}}{\partial x} + \frac{\partial N_{yb}}{\partial y} \right) + \Pi_t \left(\frac{\partial M_{xyt}}{\partial x} + \frac{\partial M_{yt}}{\partial y} \right) - \Pi_t Q_{yt} - 3S_{yt} = 0 \tag{34}$$

$$\frac{\partial \hat{M}_{xt}}{\partial x} + \frac{\partial \hat{M}_{xyt}}{\partial y} - \hat{Q}_{xt} + \frac{\partial \hat{M}_{xb}}{\partial x} + \frac{\partial \hat{M}_{xyb}}{\partial y} - \hat{Q}_{xb} = 0 \tag{35}$$

$$\frac{\partial \hat{M}_{yt}}{\partial y} + \frac{\partial \hat{M}_{xyt}}{\partial x} - \hat{Q}_{yt} + \frac{\partial \hat{M}_{yb}}{\partial y} + \frac{\partial \hat{M}_{xyb}}{\partial x} - \hat{Q}_{yb} = 0 \tag{36}$$

$$\frac{\partial P_{xb}}{\partial x} + \frac{\partial P_{xyb}}{\partial y} + \Gamma_b \left(\frac{\partial N_{xb}}{\partial x} + \frac{\partial N_{xyb}}{\partial y} \right) + \Psi_b \left(\frac{\partial L_{xb}}{\partial x} + \frac{\partial L_{xyb}}{\partial y} \right) + \Sigma_t \left(\frac{\partial M_{xt}}{\partial x} + \frac{\partial M_{xyt}}{\partial y} \right) + \Gamma_t \left(\frac{\partial N_{xt}}{\partial x} + \frac{\partial N_{xyt}}{\partial y} \right) + \Psi_t \left(\frac{\partial L_{xt}}{\partial x} + \frac{\partial L_{xyt}}{\partial y} \right) - \Psi_b R_{xb} - 3S_{xb} - \Sigma_t Q_{xt} - 2\Psi_t R_{xt} = 0 \tag{37}$$

$$\frac{\partial P_{xyb}}{\partial x} + \frac{\partial P_{yb}}{\partial y} + \Gamma_b \left(\frac{\partial N_{xyb}}{\partial x} + \frac{\partial N_{yb}}{\partial y} \right) + \Psi_b \left(\frac{\partial L_{xyb}}{\partial x} + \frac{\partial L_{yb}}{\partial y} \right) + \Sigma_t \left(\frac{\partial M_{xyt}}{\partial x} + \frac{\partial M_{yt}}{\partial y} \right) + \Gamma_t \left(\frac{\partial N_{xyt}}{\partial x} + \frac{\partial N_{yt}}{\partial y} \right) + \Psi_t \left(\frac{\partial L_{xyt}}{\partial x} + \frac{\partial L_{yt}}{\partial y} \right) - \Psi_b R_{yb} - 3S_{yb} - \Sigma_t Q_{yt} - 2\Psi_t R_{yt} = 0 \tag{38}$$

$$\frac{\partial \hat{Q}_{xt}}{\partial x} + \frac{\partial \hat{Q}_{yt}}{\partial y} + \frac{\partial \hat{Q}_{xb}}{\partial x} + \frac{\partial \hat{Q}_{yb}}{\partial y} + q = 0 \tag{39}$$

where the equivalent stress resultants are denoted by the hat. The equivalent bending and twisting moments are:

$$\begin{Bmatrix} \hat{M}_x \\ \hat{M}_y \\ \hat{M}_{xy} \end{Bmatrix}_{(\delta)} = \begin{Bmatrix} M_x \\ M_y \\ M_{xy} \end{Bmatrix}_{(\delta)} + (\Delta_\delta - \Lambda_\delta) \begin{Bmatrix} N_x \\ N_y \\ N_{xy} \end{Bmatrix}_{(\delta)} \tag{40}$$

Moreover, the equivalent shear forces become:

$$\hat{Q}_{x\delta} = Q_{x\delta} + 2\Omega_\delta R_{x\delta} - \Lambda_\delta \left(\frac{\partial N_{x\delta}}{\partial x} + \frac{\partial N_{xy\delta}}{\partial y} \right) - \Omega_\delta \left(\frac{\partial L_{x\delta}}{\partial x} + \frac{\partial L_{xy\delta}}{\partial y} \right) \tag{41}$$

$$\hat{Q}_{y\delta} = Q_{y\delta} + 2\Omega_\delta R_{y\delta} - \Lambda_\delta \left(\frac{\partial N_{xy\delta}}{\partial x} + \frac{\partial N_{y\delta}}{\partial y} \right) - \Omega_\delta \left(\frac{\partial L_{xy\delta}}{\partial x} + \frac{\partial L_{y\delta}}{\partial y} \right) \tag{42}$$

As it can be seen there is significant coupling among the stress resultants. Taking Eqs. (26) and (27) back into (31)–(39) we obtain the governing PDE system in terms of the displacement parameters:

$$\underline{M}_1^T \underline{U}_1 = 0, \quad \underline{M}_2^T \underline{U}_2 = 0$$
$$\underline{\underline{M}}_i \underline{U}_i = \underline{0}, \ i = 3, 4, \quad \underline{M}_5^T \underline{U}_5 + q = 0 \tag{43}$$

where $q = q(x, y)$ is the function of external load, moreover:

$$\underline{M}_1 = (a_1 \quad \cdots \quad a_{14})^T, \quad \underline{M}_2 = (b_1 \quad \cdots \quad b_{14})^T$$
$$\underline{\underline{M}}_3 = \begin{pmatrix} c_1 & \ldots & c_{18} \\ e_1 & \cdots & e_{18} \\ g_1 & \cdots & g_{18} \end{pmatrix}, \quad \underline{\underline{M}}_4 = \begin{pmatrix} d_1 & \ldots & d_{18} \\ f_1 & \cdots & f_{18} \\ h_1 & \cdots & h_{18} \end{pmatrix} \tag{44}$$
$$\underline{M}_5 = (j_1 \quad \cdots \quad j_{27})^T$$

where the constants denoted by a–h and j are given in Appendix A. The vectors $\underline{U}_i$, $i = 1, 2, 3, 4$ and 5 are defined as:

$$\underline{U}_1 = \left[\frac{\partial^2 u_0}{\partial x^2} \quad \frac{\partial^2 u_0}{\partial y^2} \quad \frac{\partial^2 v_0}{\partial x \partial y} \quad \frac{\partial^2 \theta_{xb}}{\partial x^2} \quad \frac{\partial^2 \theta_{xb}}{\partial y^2} \quad \frac{\partial^2 \theta_{yb}}{\partial x \partial y} \quad \frac{\partial^2 \lambda_{xt}}{\partial x^2} \quad \frac{\partial^2 \lambda_{xt}}{\partial y^2} \quad \frac{\partial^2 \lambda_{yt}}{\partial x \partial y} \quad \frac{\partial^2 \lambda_{xb}}{\partial x^2} \quad \frac{\partial^2 \lambda_{xb}}{\partial y^2} \quad \frac{\partial^2 \lambda_{yb}}{\partial x \partial y} \quad \frac{\partial^3 w}{\partial x^3} \quad \frac{\partial^3 w}{\partial x \partial y^2} \right]^T \tag{45}$$

$$\underline{U}_2 = \left\{ \frac{\partial^2 u_0}{\partial x \partial y} \quad \frac{\partial^2 v_0}{\partial x^2} \quad \frac{\partial^2 v_0}{\partial y^2} \quad \frac{\partial^2 \theta_{xb}}{\partial x \partial y} \quad \frac{\partial^2 \theta_{yb}}{\partial x^2} \quad \frac{\partial^2 \theta_{yb}}{\partial y^2} \quad \frac{\partial^2 \lambda_{xt}}{\partial x \partial y} \quad \frac{\partial^2 \lambda_{yt}}{\partial x^2} \quad \frac{\partial^2 \lambda_{yt}}{\partial y^2} \quad \frac{\partial^2 \lambda_{xb}}{\partial x \partial y} \quad \frac{\partial^2 \lambda_{yb}}{\partial x^2} \quad \frac{\partial^2 \lambda_{yb}}{\partial y^2} \quad \frac{\partial^3 w}{\partial x^2 \partial y} \quad \frac{\partial^3 w}{\partial y^3} \right\}^T \tag{46}$$

$$\underline{U}_3 = \left\{ \frac{\partial^2 u_0}{\partial x^2} \quad \frac{\partial^2 u_0}{\partial y^2} \quad \frac{\partial^2 v_0}{\partial x \partial y} \quad \theta_{xb} \quad \frac{\partial^2 \theta_{xb}}{\partial x^2} \quad \frac{\partial^2 \theta_{xb}}{\partial y^2} \quad \frac{\partial^2 \theta_{yb}}{\partial x \partial y} \quad \lambda_{xt} \quad \frac{\partial^2 \lambda_{xt}}{\partial x^2} \quad \frac{\partial^2 \lambda_{xt}}{\partial y^2} \quad \frac{\partial^2 \lambda_{yt}}{\partial x \partial y} \quad \lambda_{xb} \quad \frac{\partial^2 \lambda_{xb}}{\partial x^2} \quad \frac{\partial^2 \lambda_{xb}}{\partial y^2} \quad \frac{\partial^2 \lambda_{yb}}{\partial x \partial y} \quad \frac{\partial w}{\partial x} \quad \frac{\partial^3 w}{\partial x^3} \quad \frac{\partial^3 w}{\partial x \partial y^2} \right\}^T \tag{47}$$

$$\underline{U}_4 = \left\{ \frac{\partial^2 u_0}{\partial x \partial y} \quad \frac{\partial^2 v_0}{\partial x^2} \quad \frac{\partial^2 v_0}{\partial y^2} \quad \frac{\partial^2 \theta_{xb}}{\partial x \partial y} \quad \theta_{yb} \quad \frac{\partial^2 \theta_{yb}}{\partial x^2} \quad \frac{\partial^2 \theta_{yb}}{\partial y^2} \quad \frac{\partial^2 \lambda_{xt}}{\partial x \partial y} \quad \lambda_{yt} \quad \frac{\partial^2 \lambda_{yt}}{\partial x^2} \quad \frac{\partial^2 \lambda_{yt}}{\partial y^2} \quad \frac{\partial^2 \lambda_{xb}}{\partial x \partial y} \quad \lambda_{yb} \quad \frac{\partial^2 \lambda_{yb}}{\partial x^2} \quad \frac{\partial^2 \lambda_{yb}}{\partial y^2} \quad \frac{\partial^3 w}{\partial x^2 \partial y} \quad \frac{\partial^3 w}{\partial y^3} \quad \frac{\partial w}{\partial y} \right\}^T \tag{48}$$

$$\underline{U}_5 = \left\{ \frac{\partial^3 u_0}{\partial x^3} \quad \frac{\partial^2 u_0}{\partial x \partial y^2} \quad \frac{\partial^2 v_0}{\partial x^2 \partial y} \quad \frac{\partial^2 v_0}{\partial y^3} \quad \frac{\partial \theta_{xb}}{\partial x} \quad \frac{\partial^3 \theta_{xb}}{\partial x^3} \quad \frac{\partial^3 \theta_{xb}}{\partial x \partial y^2} \quad \frac{\partial \theta_{yb}}{\partial y} \quad \frac{\partial^3 \theta_{yb}}{\partial x^2 \partial y} \quad \frac{\partial^3 \theta_{yb}}{\partial y^3} \quad \frac{\partial \lambda_{xt}}{\partial x} \quad \frac{\partial^3 \lambda_{xt}}{\partial x^3} \quad \frac{\partial^3 \lambda_{xt}}{\partial x \partial y^2} \quad \frac{\partial \lambda_{yt}}{\partial y} \quad \frac{\partial^3 \lambda_{yt}}{\partial x^2 \partial y} \quad \frac{\partial^3 \lambda_{yt}}{\partial y^3} \quad \frac{\partial \lambda_{xb}}{\partial x} \quad \frac{\partial^3 \lambda_{xb}}{\partial x^3} \quad \frac{\partial^3 \lambda_{xb}}{\partial x \partial y^2} \quad \frac{\partial \lambda_{yb}}{\partial y} \quad \frac{\partial^3 \lambda_{yb}}{\partial x^2 \partial y} \quad \frac{\partial^3 \lambda_{yb}}{\partial y^3} \quad \frac{\partial^2 w}{\partial x^2} \quad \frac{\partial^4 w}{\partial x^4} \quad \frac{\partial^4 w}{\partial x^2 \partial y^2} \quad \frac{\partial^2 w}{\partial y^2} \quad \frac{\partial^4 w}{\partial y^4} \right\}^T \tag{49}$$

4. Bending solution for a simply-supported plate

This section presents the solution for a simply-supported delaminated orthotropic plate depicted in Fig. 3 subject to a point force. In accordance with Lévy plate formulation (e.g: Reddy, 2004; Thai and Kim, 2012) the displacement parameters are approximated by trial functions:

$$\begin{Bmatrix} \theta_x(x,y) \\ \theta_y(x,y) \\ \lambda_x(x,y) \\ \lambda_y(x,y) \end{Bmatrix} = \sum_{n=1}^{\infty} \begin{Bmatrix} X_n(x,y) \sin \beta y \\ Y_n(x,y) \cos \beta y \\ Z_{xn}(x,y) \sin \beta y \\ Z_{yn}(x,y) \cos \beta y \end{Bmatrix}, \quad \begin{Bmatrix} u_0(x,y) \\ v_0(x,y) \\ q(x,y) \\ w(x,y) \end{Bmatrix} = \sum_{n=1}^{\infty} \begin{Bmatrix} U_{0n}(x,y) \sin \beta y \\ V_{0n}(x,y) \cos \beta y \\ Q_n(x,y) \sin \beta y \\ W_n(x,y) \sin \beta y \end{Bmatrix} \tag{50}$$

where $\beta = n\pi/b$. The state-space model is used to solve the system of differential equations for both the delaminated and uncracked plate portions.

4.1. Undelaminated plate portion

For the undelaminated plate portion the model developed in Sections 2 and 3 is utilized. The general form of the state-space model is:

$$\underline{Z}'^{(ud)} = \underline{\underline{T}}^{(ud)} \underline{Z}^{(ud)} + \underline{F}^{(ud)} \tag{51}$$

where the superscript (ud) refers to the undelaminated plate portion and $\underline{Z}$ is the state vector, $\underline{\underline{T}}$ is the system matrix, $\underline{F}$ is the vector of particular solutions, respectively. Utilizing Eq. (50) and taking it back into Eq. (43) results in a system of ODEs. The latter should be manipulated so that each equation contains the second derivative of only one displacement parameter. Then the system matrix $\underline{\underline{T}}^{(ud)}$ takes the form of:

$$\underline{\underline{T}}^{(ud)} = \begin{bmatrix}
0 & 1 & 0 & 0 & 0 & 0 & 0 & 0 & 0 & 0 & 0 & 0 & 0 & 0 & 0 & 0 & 0 & 0 & 0 & 0 \\
\hat{k}_1 & 0 & 0 & \hat{k}_2 & \hat{k}_3 & 0 & 0 & \hat{k}_4 & \hat{k}_5 & 0 & 0 & \hat{k}_6 & \hat{k}_7 & 0 & 0 & \hat{k}_8 & 0 & \hat{k}_9 & 0 & \hat{k}_{10} \\
0 & 0 & 0 & 1 & 0 & 0 & 0 & 0 & 0 & 0 & 0 & 0 & 0 & 0 & 0 & 0 & 0 & 0 & 0 & 0 \\
0 & \hat{l}_1 & \hat{l}_2 & 0 & 0 & \hat{l}_3 & \hat{l}_4 & 0 & 0 & \hat{l}_5 & \hat{l}_6 & 0 & 0 & \hat{l}_7 & \hat{l}_8 & 0 & \hat{l}_9 & 0 & \hat{l}_{10} & 0 \\
0 & 0 & 0 & 0 & 0 & 1 & 0 & 0 & 0 & 0 & 0 & 0 & 0 & 0 & 0 & 0 & 0 & 0 & 0 & 0 \\
\hat{m}_1 & 0 & 0 & \hat{m}_2 & \hat{m}_3 & 0 & 0 & \hat{m}_4 & \hat{m}_5 & 0 & 0 & \hat{m}_6 & \hat{m}_7 & 0 & 0 & \hat{m}_8 & 0 & \hat{m}_9 & 0 & \hat{m}_{10} \\
0 & 0 & 0 & 0 & 0 & 0 & 0 & 1 & 0 & 0 & 0 & 0 & 0 & 0 & 0 & 0 & 0 & 0 & 0 & 0 \\
0 & \hat{n}_1 & \hat{n}_2 & 0 & 0 & \hat{n}_3 & \hat{n}_4 & 0 & 0 & \hat{n}_5 & \hat{n}_6 & 0 & 0 & \hat{n}_7 & \hat{n}_8 & 0 & \hat{n}_9 & 0 & \hat{n}_{10} & 0 \\
0 & 0 & 0 & 0 & 0 & 0 & 0 & 0 & 0 & 1 & 0 & 0 & 0 & 0 & 0 & 0 & 0 & 0 & 0 & 0 \\
\hat{p}_1 & 0 & 0 & \hat{p}_2 & \hat{p}_3 & 0 & 0 & \hat{p}_4 & \hat{p}_5 & 0 & 0 & \hat{p}_6 & \hat{p}_7 & 0 & 0 & \hat{p}_8 & 0 & \hat{p}_9 & 0 & \hat{p}_{10} \\
0 & 0 & 0 & 0 & 0 & 0 & 0 & 0 & 0 & 0 & 0 & 1 & 0 & 0 & 0 & 0 & 0 & 0 & 0 & 0 \\
0 & \hat{q}_1 & \hat{q}_2 & 0 & 0 & \hat{q}_3 & \hat{q}_4 & 0 & 0 & \hat{q}_5 & \hat{q}_6 & 0 & 0 & \hat{q}_7 & \hat{q}_8 & 0 & \hat{q}_9 & 0 & \hat{q}_{10} & 0 \\
0 & 0 & 0 & 0 & 0 & 0 & 0 & 0 & 0 & 0 & 0 & 0 & 0 & 1 & 0 & 0 & 0 & 0 & 0 & 0 \\
\hat{r}_1 & 0 & 0 & \hat{r}_2 & \hat{r}_3 & 0 & 0 & \hat{r}_4 & \hat{r}_5 & 0 & 0 & \hat{r}_6 & \hat{r}_7 & 0 & 0 & \hat{r}_8 & 0 & \hat{r}_9 & 0 & \hat{r}_{10} \\
0 & 0 & 0 & 0 & 0 & 0 & 0 & 0 & 0 & 0 & 0 & 0 & 0 & 0 & 0 & 1 & 0 & 0 & 0 & 0 \\
0 & \hat{s}_1 & \hat{s}_2 & 0 & 0 & \hat{s}_3 & \hat{s}_4 & 0 & 0 & \hat{s}_5 & \hat{s}_6 & 0 & 0 & \hat{s}_7 & \hat{s}_8 & 0 & \hat{s}_9 & 0 & \hat{s}_{10} & 0 \\
0 & 0 & 0 & 0 & 0 & 0 & 0 & 0 & 0 & 0 & 0 & 0 & 0 & 0 & 0 & 0 & 0 & 1 & 0 & 0 \\
0 & 0 & 0 & 0 & 0 & 0 & 0 & 0 & 0 & 0 & 0 & 0 & 0 & 0 & 0 & 0 & 0 & 0 & 1 & 0 \\
0 & 0 & 0 & 0 & 0 & 0 & 0 & 0 & 0 & 0 & 0 & 0 & 0 & 0 & 0 & 0 & 0 & 0 & 0 & 1 \\
0 & 0 & 0 & 0 & 0 & \hat{t}_1 & \hat{t}_2 & 0 & 0 & \hat{t}_3 & \hat{t}_4 & 0 & 0 & \hat{t}_5 & \hat{t}_6 & 0 & \hat{t}_7 & 0 & \hat{t}_8 & 0
\end{bmatrix} \tag{52}$$

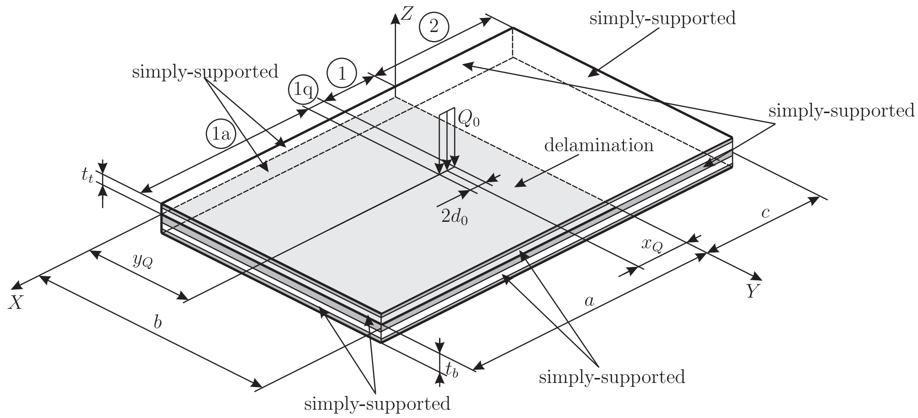

Fig. 3. A simply-supported asymmetrically delaminated plate subjected to a point force.

where the elements of the matrix are constants depending upon the top and bottom thicknesses, as well as the stiffness parameters of the plates. These are listed in Appendix B. The state vector and the vector of particular solutions are defined as:

$$\underline{Z}^{(ud)} = \{ U_0 \quad U_0' \quad V_0 \quad V_0' \quad X_{nb} \quad X_{nb}' \quad Y_{nb} \quad Y_{nb}' \quad Z_{xnt} \quad Z_{xnt}' \quad Z_{ynt} \quad Z_{ynt}' \quad Z_{xnb} \quad Z_{xnb}' \quad Z_{ynb} \quad Z_{ynb}' \quad W_n \quad W_n' \quad W_n'' \quad W_n''' \} \tag{53}$$

$$\underline{F}^{(ud)} = \{ 0 \quad \cdots \quad 0 \quad \hat{t}_9 Q_n \}^T \tag{54}$$

The general solution of Eq. (51) is (Reddy, 2004):

$$\underline{Z}^{(ud)}(x) = e^{\underline{\underline{T}}^{(ud)}x}\left(\underline{K}^{(ud)} + \int_{x_0}^{x} e^{-\underline{\underline{T}}^{(ud)}\xi}\underline{F}^{(ud)}(\xi)d\xi\right) = \underline{\underline{G}}^{(ud)}(x)\underline{K}^{(ud)} + \underline{H}^{(ud)}(x) \tag{55}$$

where $\underline{K}$ is the vector of constants (20).

4.2. Delaminated plate portion

The state-space model of the delaminated portion can be derived relatively simply based on Szekrényes (2014b). In the delaminated part (see Fig. 2) the SEKC does not enforce the two subplates to behave as a single plate, the parameters ($u_{0\delta}$, $v_{0\delta}$, $\theta_{x\delta}$, etc.) of the top and bottom plates in the delaminated part are independent of each other. Since the in-plane displacement functions are discontinuous in the delaminated region we can apply two (a top and a bottom) traditional ESLs for each region (‘1a’, ‘1q’ and ‘1’ in Fig. 3) with different thicknesses (t_t and t_b). The equilibrium equations of traditional Reddy plates (Reddy, 2004, p. 675) can be used in the latter case, however since the deflection of the top and bottom plates are assumed to be the same there is some coupling between the shear forces of the top and bottom plates, viz. an equation similar to Eq. (39) applies also to the delaminated portion (Szekrényes, 2014b). The system matrix of the delaminated portion is a 20×20 matrix.

5. Boundary and continuity conditions

The elements of the state vectors in Eq. (51) and that of the delaminated part can be referred to as:

$$Z_i^{(d)} = \sum_{j=1}^{20} G_{ij}^{(d)} K_j^{(d)} + H_j^{(d)}, \quad Z_i^{(ud)} = \sum_{j=1}^{20} G_{ij}^{(ud)} K_j^{(ud)} + H_j^{(ud)} \tag{56}$$

In accordance with Fig. 3, we have four different plate portions. The point force causes singularity in the PDEs, therefore a plate portion loaded by a constant line force was applied, the length d_0 was a very small value compared to the plate dimensions. In this case $Q_n = 2q_0/b\sin(\beta y_0)$ (Reddy, 2004), which was applied in the delaminated portion ‘1q’. Thus the three parts of the delaminated portion are denoted by ‘1a’, ‘1q’, ‘1’ and the undelaminated one is denoted by ‘2’, respectively. The boundary conditions (B.C.s) are formulated through the displacement parameters and the stress resultants. The latter can be expressed in the following forms:

$$\begin{Bmatrix} N_x \\ N_y \\ M_x \\ M_y \\ L_x \\ L_y \end{Bmatrix}_{(\delta)} = \sum_{n=1}^{\infty} \begin{Bmatrix} n_{xn} \\ n_{yn} \\ m_{xn} \\ m_{yn} \\ l_{xn} \\ l_{yn} \end{Bmatrix}_{(\delta)} \sin\beta y, \quad \begin{Bmatrix} P_x \\ P_y \\ Q_x \\ R_x \\ S_x \end{Bmatrix}_{(\delta)} = \sum_{n=1}^{\infty} \begin{Bmatrix} p_{xn} \\ p_{yn} \\ q_{xn} \\ r_{xn} \\ s_{xn} \end{Bmatrix}_{(\delta)} \sin\beta y \tag{57}$$

$$\begin{Bmatrix} N_{xy} \\ M_{xy} \\ L_{xy} \\ P_{xy} \end{Bmatrix}_{(\delta)} = \sum_{n=1}^{\infty} \begin{Bmatrix} n_{xyn} \\ m_{xyn} \\ l_{xyn} \\ p_{xyn} \end{Bmatrix}_{(\delta)} \cos\beta y, \quad \begin{Bmatrix} Q_y \\ R_y \\ S_y \end{Bmatrix}_{(\delta)} = \sum_{n=1}^{\infty} \begin{Bmatrix} q_{yn} \\ r_{yn} \\ s_{yn} \end{Bmatrix}_{(\delta)} \cos\beta y \tag{58}$$

i.e. n_{xn} is the function coefficient in the trial function of N_x, etc. For the present Problem 80 conditions need be formulated. Based on Fig. 3 the B.C.s are:

$$\begin{aligned}&W_n^{(1a)}(a)=0,\quad W_n^{\prime\prime(1a)}(a)=0,\quad Y_{n\delta}^{(1a)}(a)=0\\&V_{0n\delta}^{(1a)}(a)=0,\quad n_{xn\delta}^{(1a)}(a)=0,\quad m_{xn\delta}^{(1a)}(a)=0\end{aligned}\tag{59}$$

$$\begin{aligned}&W_n^{(2)}(-c)=0,\quad V_{0n}^{(2)}(-c)=0,\quad Y_{nb}^{(2)}(-c)=0\\&Z_{yn\delta}^{(2)}(-c)=0,\quad n_{x\delta}^{(2)}(-c)=0,\quad m_{xnt}^{(2)}(-c)=0,\quad p_{xn\delta}^{(2)}(a)=0\end{aligned}\tag{60}$$

where δ can take t and b, and so some of the equations involve two conditions, we have 20 B.C.s altogether. The continuity conditions between regions '1' and '2' are (considering Eqs. (10) and (11)):

$$\begin{aligned}&W_n^{(1)}(0)=W_n^{(2)}(0),W_n^{\prime(1)}(0)=W_n^{\prime(2)}(0)\\&W_n^{\prime\prime(1)}(0)=W_n^{\prime\prime(2)}(0),\quad W_n^{\prime\prime\prime(1)}(0)=W_n^{\prime\prime\prime(2)}(0)\end{aligned}\tag{61}$$

$$\begin{aligned}&U_{0nt}^{(1)}(0)=U_{0n}^{(2)}+(\Delta_tX_{nb}^{(2)}+\Phi_tZ_{xnt}^{(2)}+\Gamma_tZ_{xnb}^{(2)}+\Lambda_tW_n^{\prime(2)})\Big|_{x=0}\\&V_{0nt}^{(1)}(0)=V_{0n}^{(2)}+(\Delta_tY_{nb}^{(2)}+\Phi_tZ_{ynt}^{(2)}+\Gamma_tZ_{ynb}^{(2)}+\Lambda_t\beta W_n^{(2)})\Big|_{x=0}\end{aligned}\tag{62}$$

$$\begin{aligned}&U_{0nb}^{(1)}(0)=U_{0n}^{(2)}+(\Delta_bX_{nb}^{(2)}+\Gamma_bZ_{xnb}^{(2)}+\Lambda_bW_n^{\prime(2)})\Big|_{x=0}\\&V_{0nb}^{(1)}(0)=V_{0n}^{(2)}+(\Delta_bY_{nb}^{(2)}+\Gamma_bZ_{ynb}^{(2)}+\Lambda_b\beta W_n^{(2)})\Big|_{x=0}\end{aligned}\tag{63}$$

$$\begin{aligned}&X_{nb}^{(1)}(0)=X_{nb}^{(2)}(0),\quad Y_{nb}^{(1)}(0)=Y_{nb}^{(2)}(0),\\&-\frac{4}{3t_\delta^2}(X_{n\delta}^{(1)}+W_n^{\prime(1)})\Big|_{x=0}=Z_{xn\delta}^{(2)}(0),\quad -\frac{4}{3t_\delta^2}(Y_{n\delta}^{(1)}+\beta W_n^{(1)})\Big|_{x=0}=Z_{yn\delta}^{(2)}(0)\end{aligned}\tag{64}$$

As it can be seen, there is no need to impose continuity conditions with respect to $X_{nt}^{(1)}$ and $Y_{nt}^{(1)}$ (these are related to the delaminated portion and not eliminated from the displacement field). The reasons for that are the last two conditions of Eq. (64), which cause that the continuity of $X_{nt}^{(1)}$ and $Y_{nt}^{(1)}$ is automatically satisfied. The continuity conditions of the stress resultants must consider the coupling among them, therefore the equivalent stress resultants given by Eq. (40) are used:

$$\begin{aligned}&n_{xnt}^{(1)}+n_{xnb}^{(1)}\Big|_{x=0}=n_{xnt}^{(2)}+n_{xnb}^{(2)}\Big|_{x=0}\\&n_{xynt}^{(1)}+n_{xynb}^{(1)}\Big|_{x=0}=n_{xynt}^{(2)}+n_{xynb}^{(2)}\Big|_{x=0}\end{aligned}\tag{65}$$

$$\begin{aligned}&m_{xnt}^{(1)}-\frac{4}{3t_t^2}p_{xnt}^{(1)}\Big|_{x=0}=m_{xnt}^{(2)}+(\Delta_t-\Lambda_t)n_{xnt}^{(2)}\Big|_{x=0}\\&m_{xnb}^{(1)}-\frac{4}{3t_b^2}p_{xnb}^{(1)}\Big|_{x=0}=m_{xnb}^{(2)}+(\Delta_b-\Lambda_b)n_{xnb}^{(2)}\Big|_{x=0}\end{aligned}\tag{66}$$

$$\begin{aligned}&m_{xynt}^{(1)}-\frac{4}{3t_t^2}p_{xynt}^{(1)}\Big|_{x=0}=m_{xynt}^{(2)}+(\Delta_t-\Lambda_t)n_{xynt}^{(2)}\Big|_{x=0}\\&m_{xynb}^{(1)}-\frac{4}{3t_b^2}p_{xynb}^{(1)}\Big|_{x=0}=m_{xynb}^{(2)}+(\Delta_b-\Lambda_b)n_{xynb}^{(2)}\Big|_{x=0}\end{aligned}\tag{67}$$

As it can be seen, we can formulate 20 continuity conditions between regions '1' and '2'. It is important to mention that there are two continuity conditions with respect to the sum N_x and N_{xy} normal forces. Therefore the normal forces are not continuous across the cracked and uncracked portions. The magnitude of normal forces is determined by the kinematic continuity conditions. The continuity between the '1' and '1q' portions involves 20 conditions:

$$\begin{aligned}&W_n^{(1q)}(x_{01})=W_n^{(1)}(x_{01}),W_n^{\prime(1q)}(x_{01})=W_n^{\prime(1)}(x_{01})\\&W_n^{\prime\prime(1q)}(x_{01})=W_n^{\prime\prime(1)}(x_{01}),W_n^{\prime\prime\prime(1q)}(x_{01})=W_n^{\prime\prime\prime(1)}(x_{01})\\&U_{0n\delta}^{(1q)}(x_{01})=U_{0n\delta}^{(1)}(x_{01}),X_{n\delta}^{(1q)}(x_{01})=X_{n\delta}^{(1)}(x_{01})\\&V_{0n\delta}^{(1q)}(x_{01})=V_{0n\delta}^{(1)}(x_{01}),Y_{n\delta}^{(1q)}(x_{01})=Y_{n\delta}^{(1)}(x_{01})\end{aligned}\tag{68}$$

$$\begin{aligned}&n_{xn\delta}^{(1q)}(x_{01})=n_{xn\delta}^{(1)}(x_{01}),n_{xyn\delta}^{(1q)}(x_{01})=n_{xyn\delta}^{(1)}(x_{01})\\&m_{xn\delta}^{(1q)}-\frac{4}{3}t_\delta^2p_{xn\delta}^{(1q)}\Big|_{x=x_{01}}=m_{xn\delta}^{(1)}-\frac{4}{3}t_\delta^2p_{xn\delta}^{(1)}\Big|_{x=x_{01}}\\&m_{xyn\delta}^{(1q)}-\frac{4}{3}t_\delta^2p_{xyn\delta}^{(1q)}\Big|_{x=x_{01}}=m_{xyn\delta}^{(1)}-\frac{4}{3}t_\delta^2p_{xyn\delta}^{(1)}\Big|_{x=x_{01}}\end{aligned}\tag{69}$$

where $x_{01}=x_Q-d_0$. Further 20 conditions can be derived between '1q' and '1a', these are similar to those in Eq. (60), therefore these are not presented here. Thus we have $20+20+20+20=80$ conditions in all.

6. Energy release rate and mode mixity

The ERR can be determined based on the 3D J-integral (Murakami and Sato, 1983; Shivakumar and Raju, 1992). The J-integral have already been determined for first- and second-order plates with asymmetric delamination (Szekrényes, 2013d), therefore only the final results are presented here:

$$\begin{aligned}J_{II}=\frac{1}{2}\sum_{\delta=t,b}\Bigg\{&\left(N_{x1\delta}\varepsilon_{x1\delta}^{(0)}\Big|_{x=+0}-N_{x2\delta}\varepsilon_{x2\delta}^{(0)}\Big|_{x=-0}\right)\\&-\left(N_{y1\delta}\varepsilon_{y1\delta}^{(0)}\Big|_{x=+0}-N_{y2\delta}\varepsilon_{y2\delta}^{(0)}\Big|_{x=-0}\right)+\left(M_{x1\delta}\varepsilon_{x1\delta}^{(1)}\Big|_{x=+0}-M_{x2\delta}\varepsilon_{x2\delta}^{(1)}\Big|_{x=-0}\right)\\&-\left(M_{y1\delta}\varepsilon_{y1\delta}^{(1)}\Big|_{x=+0}-M_{y2\delta}\varepsilon_{y2\delta}^{(1)}\Big|_{x=-0}\right)+\left(L_{x1\delta}\varepsilon_{x1\delta}^{(2)}\Big|_{x=+0}-L_{x2\delta}\varepsilon_{x2\delta}^{(2)}\Big|_{x=-0}\right)\\&-\left(L_{y1\delta}\varepsilon_{y1\delta}^{(2)}\Big|_{x=+0}-L_{y2\delta}\varepsilon_{y2\delta}^{(2)}\Big|_{x=-0}\right)+\left(P_{x1\delta}\varepsilon_{x1\delta}^{(3)}\Big|_{x=+0}-P_{x2\delta}\varepsilon_{x2\delta}^{(3)}\Big|_{x=-0}\right)\\&-\left(P_{y1\delta}\varepsilon_{y1\delta}^{(3)}\Big|_{x=+0}-P_{y2\delta}\varepsilon_{y2\delta}^{(3)}\Big|_{x=-0}\right)\Bigg\}\end{aligned}\tag{70}$$

and:

Table 1
Elastic properties of single carbon/epoxy composite laminates.

	E_x (GPa)	E_y (GPa)	E_z (GPa)	G_{yz} (GPa)	G_{xz} (GPa)	G_{xy} (GPa)	ν_{yz} (–)	ν_{xz} (–)	ν_{xy} (–)
$\pm 45^{\circ f}$	16.39	16.39	16.4	5.46	5.46	16.4	0.5	0.5	0.3
0°	148	9.65	9.65	4.91	4.66	3.71	0.27	0.25	0.3

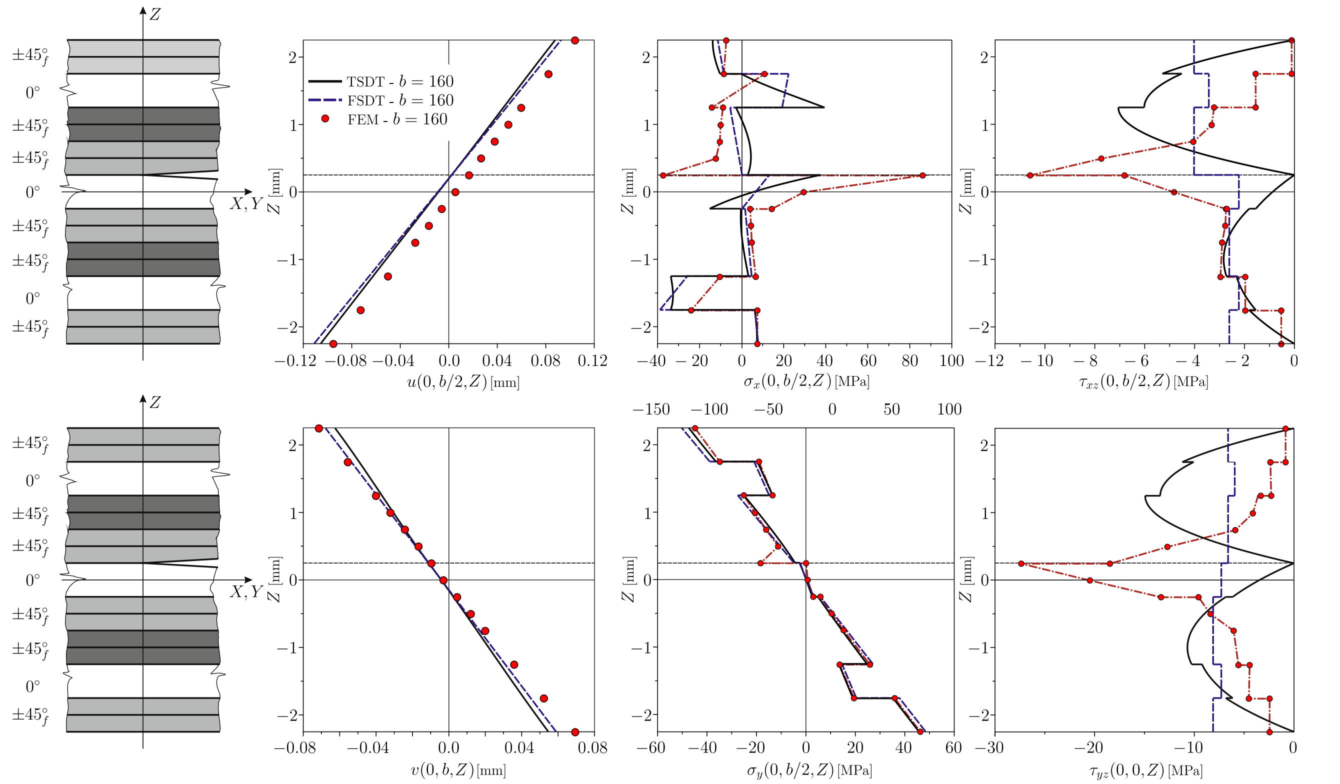

Fig. 4. Distribution of the in-plane displacements (u and v), normal stresses (σ_x and σ_y) and shear stresses (τ_{xz} and τ_{yz}) over the plate thickness for case I, $b = 160$ mm, lay-up: $\left[\pm 45^f/0/\pm 45^f_2/\bar{0}\right]_S$.

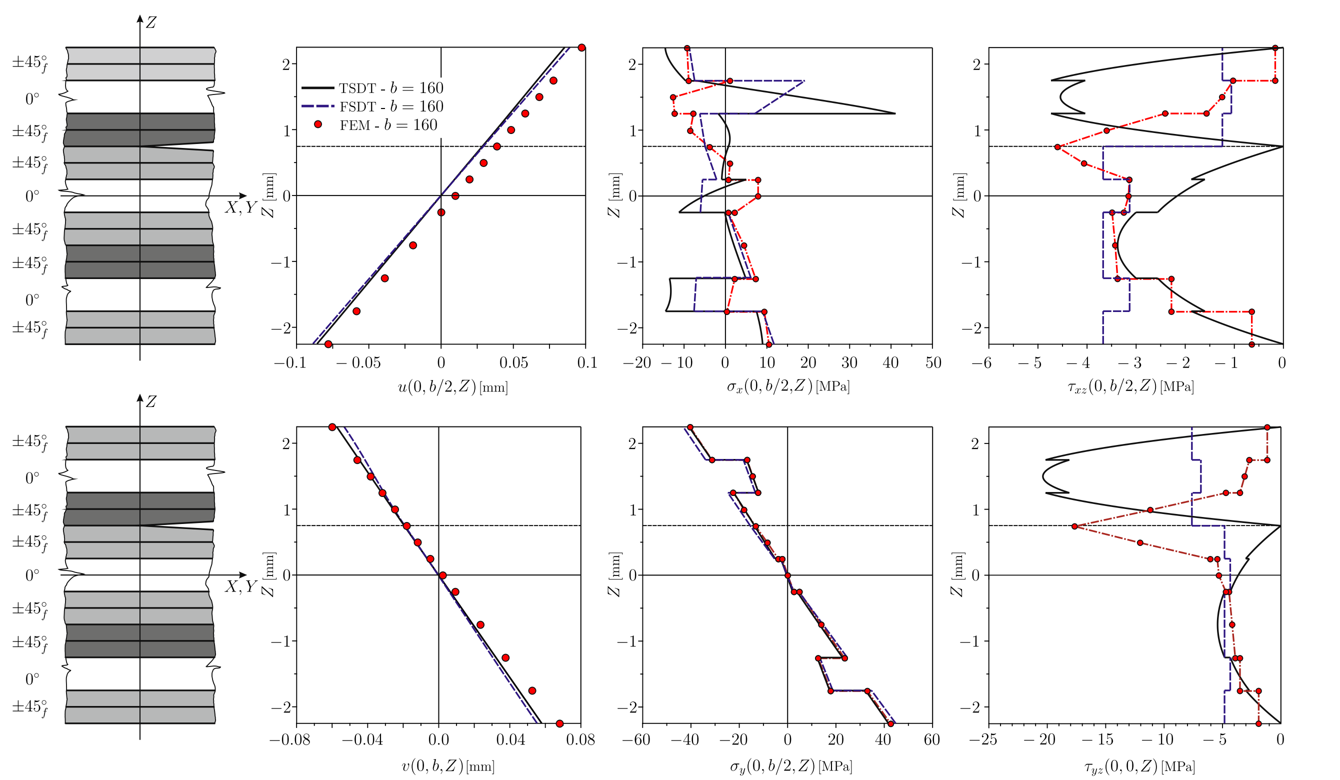

Fig. 5. Distribution of the in-plane displacements (u and v), normal stresses (σ_x and σ_y) and shear stresses (τ_{xz} and τ_{yz}) over the plate thickness for case II, $b = 160$ mm, lay-up: $\left[\pm 45^f/0/\pm 45^f_2/\bar{0}\right]_S$.

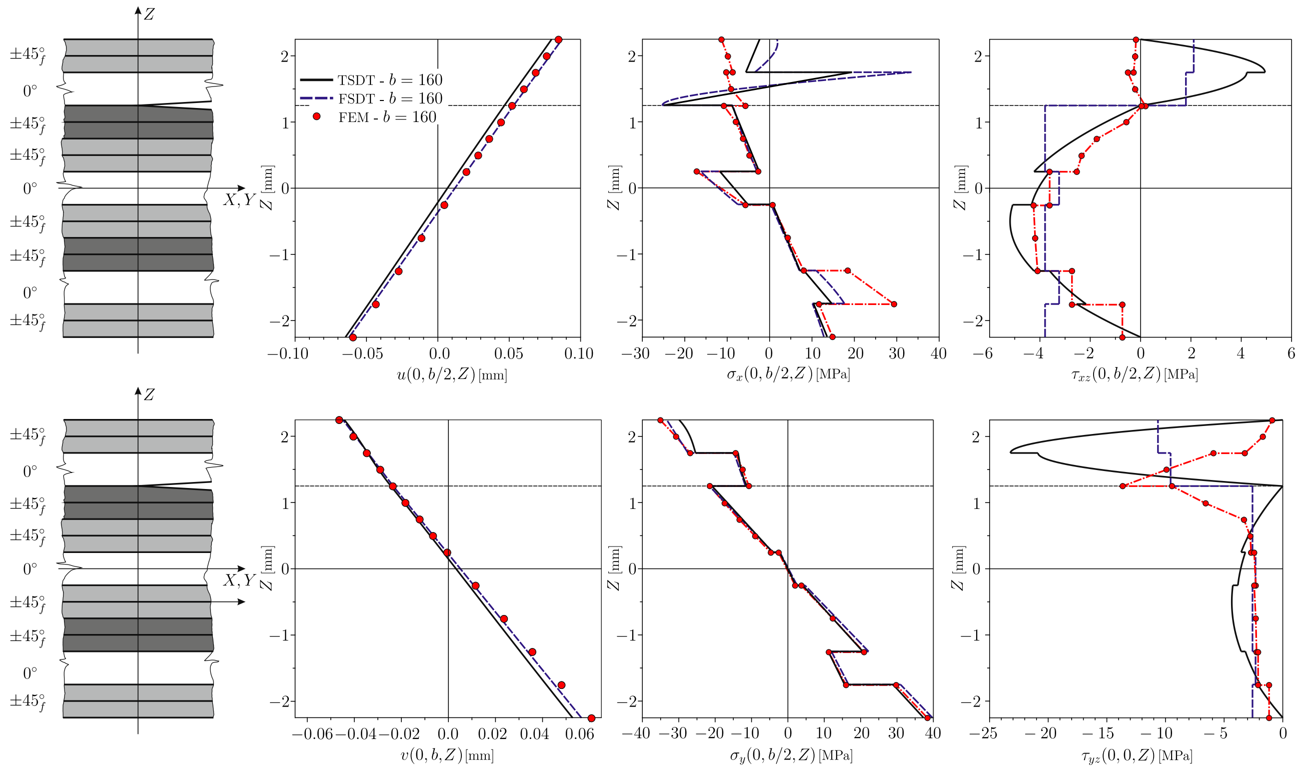

Fig. 6. Distribution of the in-plane displacements (u and v), normal stresses (σ_x and σ_y) and shear stresses (τ_{xz} and τ_{yz}) over the plate thickness for case III, $b = 160$ mm, lay-up: $\left[\pm 45^f/0/\pm 45_2^f/\bar{0}\right]_S$.

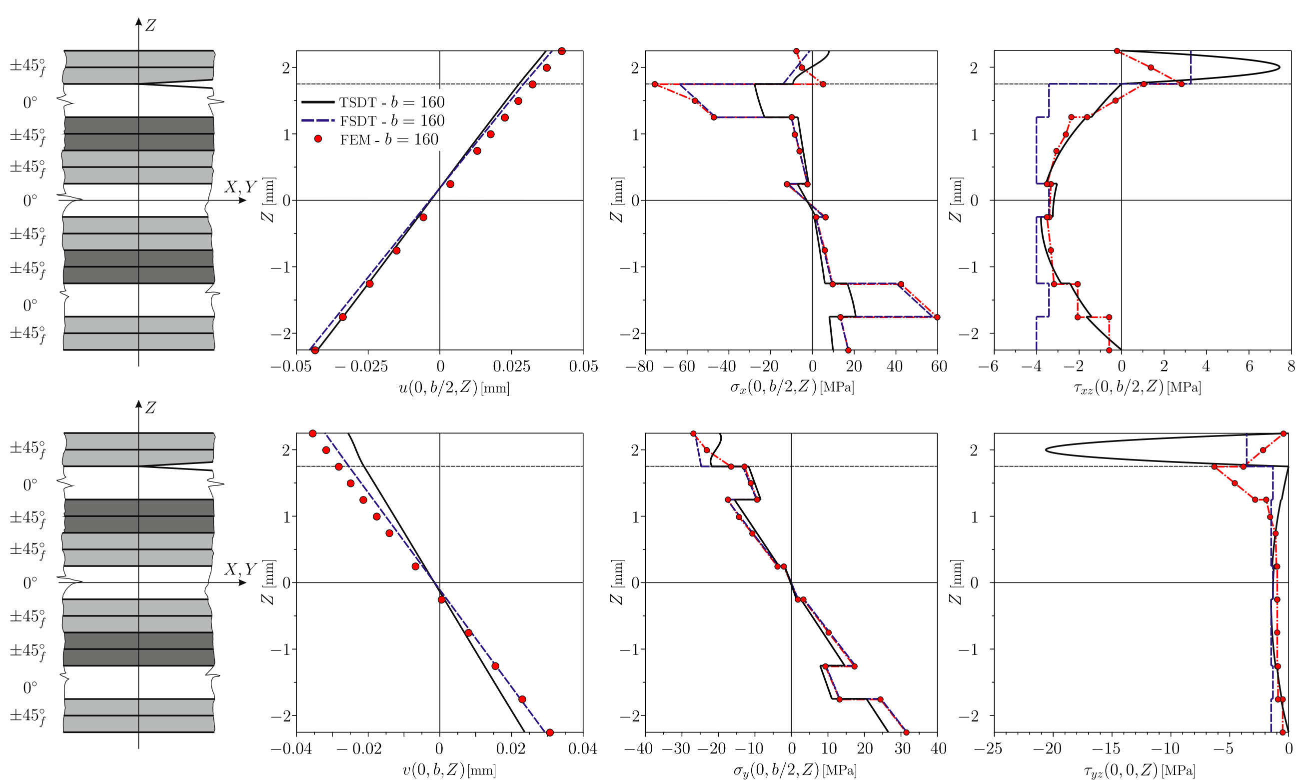

Fig. 7. Distribution of the in-plane displacements (u and v), normal stresses (σ_x and σ_y) and shear stresses (τ_{xz} and τ_{yz}) over the plate thickness for case IV, $b = 160$ mm, lay-up: $\left[\pm 45^f/0/\pm 45_2^f/\bar{0}\right]_S$.

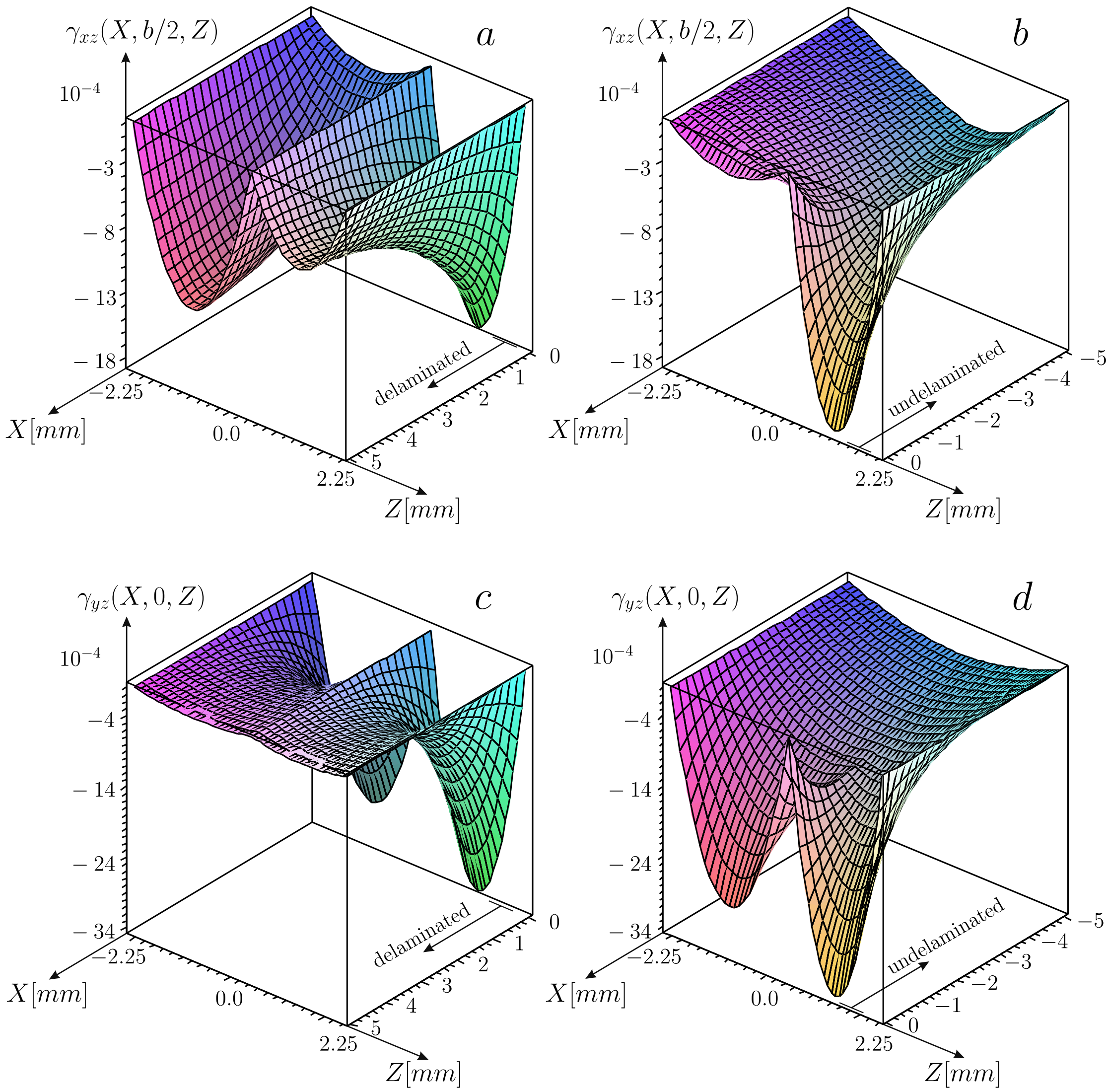

Fig. 8. Distribution of the shear strains γ_{xz} and γ_{yz} at the transition between the delaminated and uncracked regions at Y=b/2 and Y = 0 (case I, b = 100 mm, lay-up: $\left[\pm45^f/0/\pm45_2^f/\bar{0}\right]_S$).

$$
\begin{aligned}
J_{III} = \frac{1}{2}\sum_{\delta=t,b}\Bigg\{ &\left(N_{xy1\delta}\hat{\gamma}^{(0)}_{xy1\delta}\Big|_{x=+0} - N_{xy2\delta}\hat{\gamma}^{(0)}_{xy2\delta}\Big|_{x=-0}\right) \\
&+ \left(M_{xy1\delta}\hat{\gamma}^{(1)}_{xy1\delta}\Big|_{x=+0} - M_{xy2\delta}\hat{\gamma}^{(1)}_{xy2\delta}\Big|_{x=-0}\right) \\
&+ \left(L_{xy1\delta}\hat{\gamma}^{(2)}_{xy1\delta}\Big|_{x=+0} - L_{xy2\delta}\hat{\gamma}^{(2)}_{xy2\delta}\Big|_{x=-0}\right) \\
&+ \left(P_{xy1\delta}\hat{\gamma}^{(3)}_{xy1\delta}\Big|_{x=+0} - P_{xy2\delta}\hat{\gamma}^{(3)}_{xy2\delta}\Big|_{x=-0}\right)\Bigg\} \qquad (71)
\end{aligned}
$$

where the shear strains with the hat are defined as:

$$
\hat{\gamma}^{(0)}_{xy} = \frac{\partial u_0}{\partial y} - \frac{\partial v_0}{\partial x}, \quad \hat{\gamma}^{(1)}_{xy} = \frac{\partial \theta_x}{\partial y} - \frac{\partial \theta_y}{\partial x}, \quad \hat{\gamma}^{(2)}_{xy} = \frac{\partial \phi_x}{\partial y} - \frac{\partial \phi_y}{\partial x},
$$
$$
\hat{\gamma}^{(3)}_{xy} = \frac{\partial \lambda_x}{\partial y} - \frac{\partial \lambda_y}{\partial x} \qquad (72)
$$

Under static conditions $G_{II} = J_{II}$ and $G_{III} = J_{III}$. The mode mixity ($G_{II}/(G_{II}+G_{III})$ and $G_{III}/(G_{II}+G_{III})$) can also be calculated.

7. Results and discussions

In this section simply-supported plates with two different plate widths are analyzed with the following properties (refer to Fig. 2): $a = 105$ mm (crack length), $c = 45$ mm (uncracked length), $b = 100$ mm and $b = 160$ mm (plate widths), $t_t + t_b = 4.5$ mm (plate thickness), $Q_0 = 1000$ N (point force magnitude), $x_Q = 31$ mm, $y_Q = 50$ mm and $y_Q = 80$ mm (point of action coordinates of Q_0) and $d_0 = 0.1$ mm. The plate is made of a carbon/epoxy material, two different lay-ups were investigated: the lay-ups of the uncracked part were $[\pm45^f/0/\pm45_2^f/\bar{0}]_S$ and $[90/0/90_2/\bar{0}]_S$ (cross-ply laminate). A single layer was 0.5 mm thick. The properties of the individual laminae are given by Table 1 (Kollár and Springer, 2003). The $\pm45^f$ layers were isotropic, the 90 layers were obtained by rotating the 0 layers by 90° about the z axis. Four different positions of the delamination was studied, these were assigned as cases I–IV and are shown in Fig. 1. The computation was performed in the code MAPLE (Garvan, 2002) in accordance with the following points. The stiffness matrices of each single layer of the plate were determined based on the elastic properties of the laminates given in Table 1. The problem in Fig. 3 was solved varying the number of terms (N) in the trial function by creating a for-do cycle. Based on the displacement parameters the stress resultants and the stresses were calculated. Finally the ERRs were calculated using the J-integral. The convergence of the results was analyzed and it was found that after the 13th Fourier term there was no change in the displacement field, stresses, forces and ERRs.

7.1. Finite element model

In order to verify the analytical results finite element analyses were carried out. The 3D finite element models of the plate with different delamination positions were created in the code ANSYS 12 using 8 node linear solid elements. Similar 3D models are documented in the literature (de Morais and Pereira, 2008, 2009; Pereira and de Morais, 2009), therefore the models are not shown here. The global element size was 2 mm $\times$ 2 mm $\times$ 0.4 mm. In the vicinity of the crack tip a refined mesh was constructed including trapezoid shape elements. The z displacements of the contact nodes over the delaminated surface were imposed to be the same. The mode-II and mode-III ERRs were calculated by the virtual crack closure technique (VCCT) (e.g. Bonhomme et al., 2010), the size of the crack tip elements were $\Delta x = 0.25$ mm, $\Delta y = 2.0$ mm and $\Delta z = 0.25$ mm. For the determination of G_{II} and G_{III} along the delamination front a so-called MACRO was written in the ANSYS Design and Parametric Language (ADPL). The MACRO gets the nodal forces and displacements at the crack tip and at each pair of nodes, respectively, then by defining the size of crack tip elements it determines and plots the ERRs at each node along the crack front.

7.2. Displacement and stress fields – analysis vs. FE solution

In this section the analytical and numerical results are compared to each other. The analyses were carried out by using the present TSDT (Reddy) and a previous FSDT solution (Szekrényes, 2013d), respectively. Four cases were investigated, simultaneously two different plate widths and two lay-ups were applied. However, not all of these cases are documented in this paper, but the corresponding geometry and lay-up are always indicated in the legend of the subsequent figures. Fig. 4 depicts the results for case I with $b = 160$ mm for the $[\pm 45^f/0/\pm 45^f_2/\bar{0}]_S$ laminate. The displacements and stresses were evaluated in the vicinity of some points

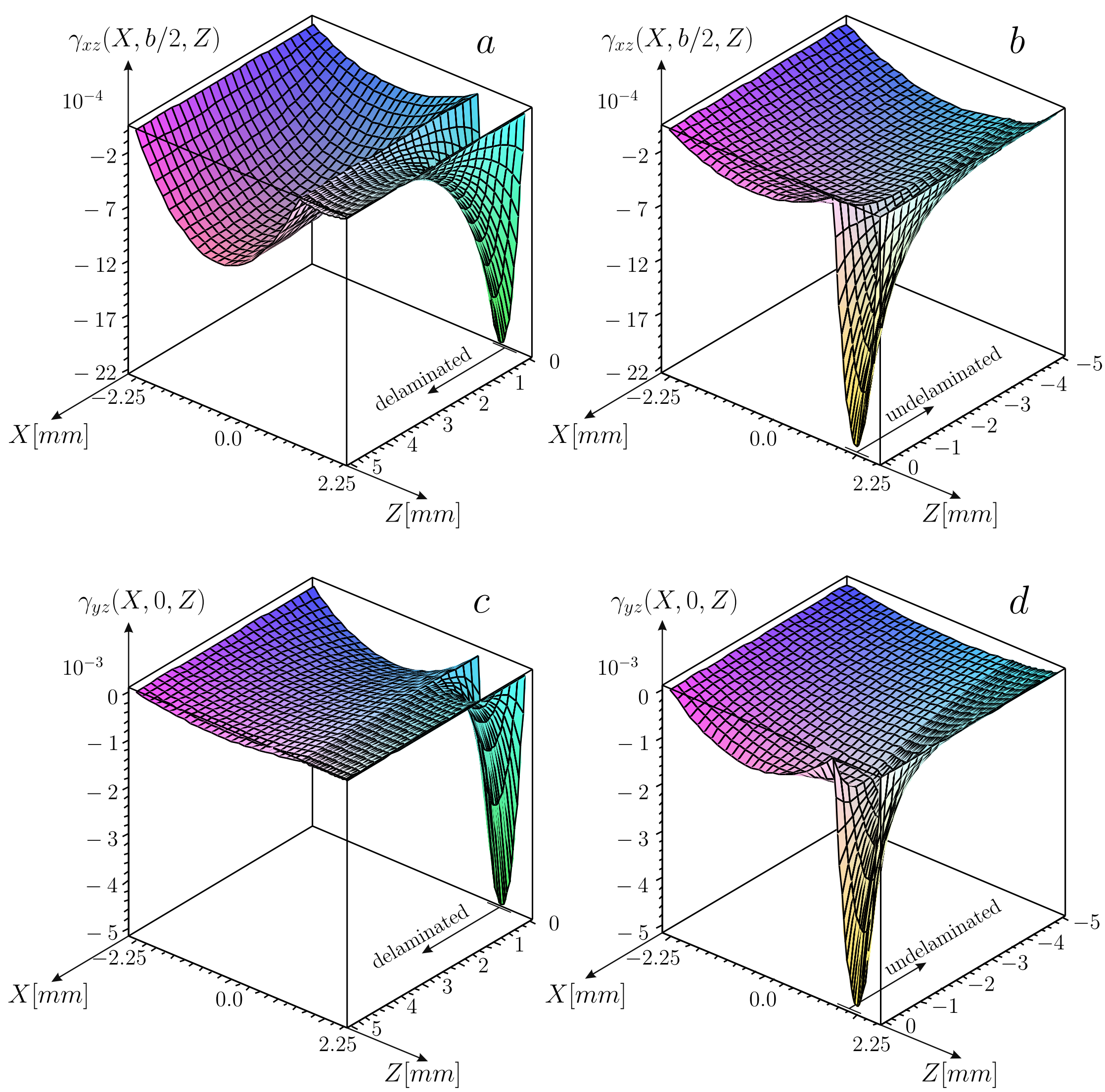

Fig. 9. Distribution of the shear strains γ_{xz} and γ_{yz} at the transition between the delaminated and uncracked regions at Y=b/2 and Y = 0 (case III, b = 100 mm, lay-up: $\left[\pm 45^f/0/\pm 45^f_2/0\right]_S$).

located at the delamination tip (refer to the legends again). It can be seen in Fig. 4 that the displacement distributions agree very well, in contrast the stresses are quite different. An immediate observation is that there is a misalignment between the numerically and analytically determined displacement distributions, more clearly, the intersection point of the displacement distributions by FEM are not the same as that of the analytical solution. It has to be mentioned that we can compare only the slope of the two solutions, because the intersection point slightly depends upon the boundary conditions related to the in-plane displacements. The rigid body motion of the plate in the X–Y plane can be eliminated in several different ways, e.g. in the present analysis the following conditions were imposed: $x = a,\ y = 0,\ z = -(t_t + t_b)/2 : u = 0,\ v = 0$ and $x = a,\ y = b,\ z = -(t_t + t_b)/2 : u = 0$. For σ_x the FE solution indicates a peak in the plane of the delamination, the peak by TSDT solution is significantly less. The FSDT approximation is quite similar to the TSDT for case I. For σ_y each solution agrees more or less. The approximation of shear stresses is again very contradictory. The FE solution shows a peak in the delamination plane. The major difference between the analytical solutions is that the shear stress by FSDT does not vanish at the top and bottom boundaries (the traction-free condition is violated). In contrast, the TSDT does satisfy the dynamic boundary conditions, the shear strains (and so the stresses) vanish even at the delamination tip. Although there are differences, the area under the curves is approximately the same, which is in fact the shear force. The further cases (II, III and IV) are presented in Figs. 5–7. The conclusions are similar to those for case I. Apparently, the shear stresses are better approximated by TSDT and it is the only solution that satisfies the dynamic conditions. In spite of that in case III the direction of τ_{xz} in the top plate does not agree with the FE result (Fig. 6), apart from that in case IV (Fig. 7) the shear stresses are somewhat overpredicted in the top plate again.

Figs. 8 and 9 plot the distribution of the shear strains in the neighborhood of the delamination tip (lay-up: $[\pm 45^f/0/\pm 45^f_2/\bar{0}]_S$). As expected the shear strains change suddenly at the transition between the delaminated and undelaminated plate portions. It has to be mentioned that the condition of shear strain continuity (Eq. (6)) in the delamination plane of the undelaminated part is very important to obtain accurate ERR distributions (see later). In the case of the FSDT the shear strains (and so the stresses) are discontinuous in the through-thickness direction, this leads to significant errors if the delamination gets closer to the top boundary surface of the plate. The results are similar in case III (Fig. 9), as well. The distribution of the interlaminar shear stress (τ_{xz} and τ_{yz}) in the delamination plane of the uncracked region are plotted in

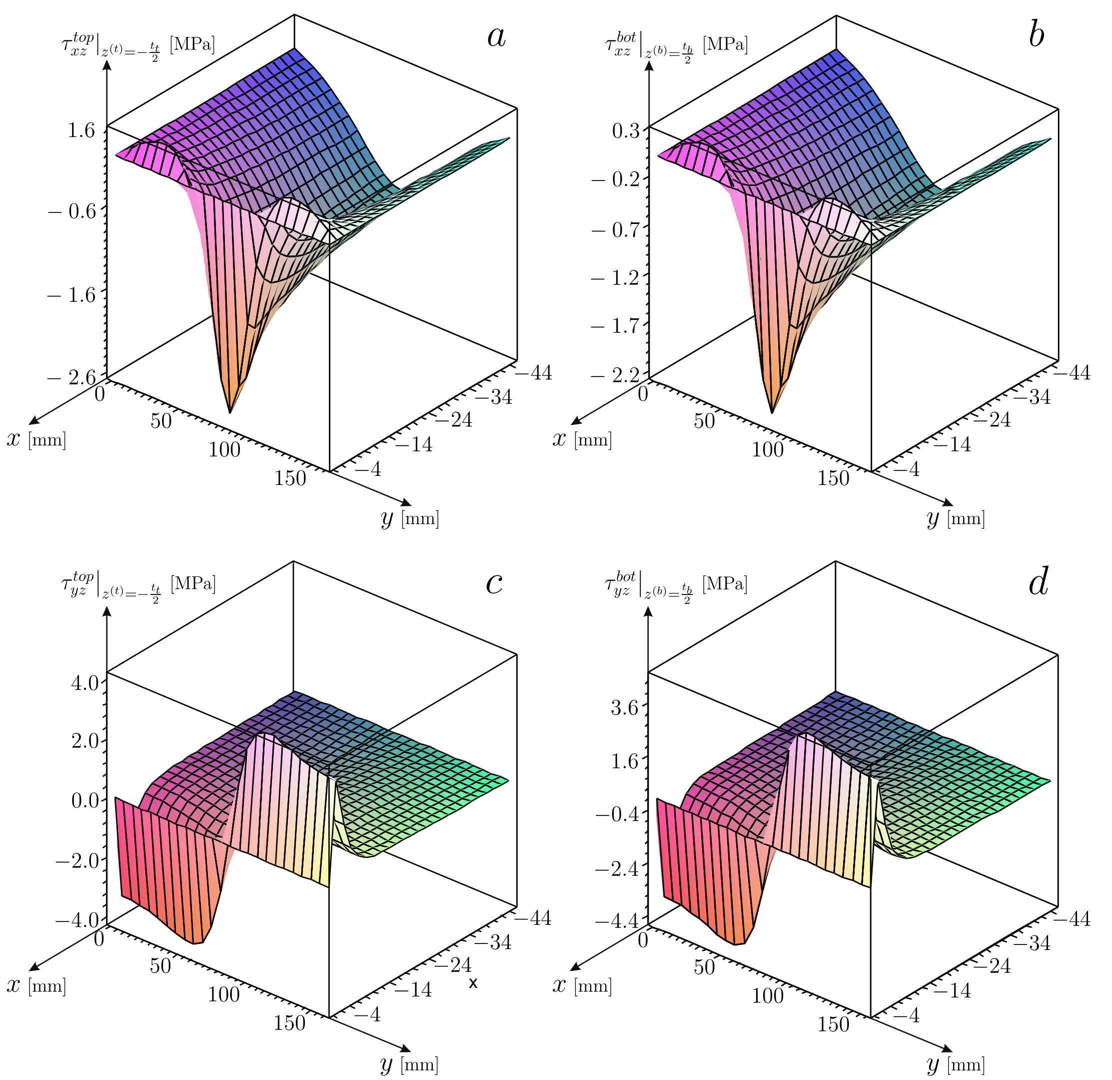

Fig. 10. Distribution of the interlaminar shear stress for case I, b = 160 mm, τ_{xz}^{top} (a), τ_{xz}^{bot} (b), τ_{yz}^{top} (c) and τ_{yz}^{bot} (d), lay-up: $\left[\pm 45^f/0/\pm 45^f_2/\bar{0}\right]_S$.

Figs. 10 and 11 for cases I and III with $b = 160$ mm (lay-up: $[\pm45^f/0/\pm45_2^f/\bar{0}]_S$). Satisfying the basic concepts of Reddy plates the shear stresses vanish along the delamination tip, which is followed by a sudden increase and a subsequent decay. Although it is possible to obtain these distributions by the FE model too, it would be a very lengthy process, the analytical solution is more reasonable in this case. For the cross-ply laminate the displacement and stress distributions are quite similar to those for the $[\pm45^f/0/\pm45_2^f/\bar{0}]_S$ lay-up, therefore only the results of the J-integral are presented for both lay-ups hereinafter.

7.3. Energy release rate and mode mixity

The ERR and the mode mixity is presented through Figs. 12 and 15 for both lay-ups. The solution by the VCCT, TSDT and the corresponding FSDT (Szekrényes, 2013d) results are compared to each other. In Fig. 12 it can be seen that for case I (Fig. 12(a), $[\pm45^f/0/\pm45_2^f/\bar{0}]_S$) the FSDT solution underpredicts G_{II} but agrees quite well with the TSDT in the case of G_{III}. On the contrary, the modified Reddy's TSDT agrees excellently with the numerical results for both components. Based on Fig. 13 for cases III and IV (i.e. when the bottom plate thickness is larger) it is shown that the FSDT overpredicts significantly the mode-III ERR, simultaneously, the mode-II ERR agrees better with the numerical and TSDT results. The major difference between the FSDT and TSDT solutions is the shear strain continuity at the interface plane, that is the reason for the differences in Fig. 13. In accordance with case III, the FSDT seems to be inaccurate in cases III and IV for both plate widths. Eventually, the TSDT approaches quite well both ERR components for each plate width, but if $b = 160$ mm, then the mode-II ERR is dissimilar to the FE solution at the edges. Compared to the VCCT results, the mode-III ERR is approximated very well by TSDT. Figs. 14 and 15 present the ERR and mode ratio distributions for the cross-ply laminate. It is interesting, that for cases I and II in Fig. 14 the FSDT agrees very well with the TSDT and VCCT results, even the mode ratios are almost the same. According to Fig. 15 the FSDT seems to be better for the cross-ply laminate than the TSDT. However, it has to be mentioned that one of the mode ratios is wrongly predicted for case IV with $b = 100$ mm in the middle region. Although the TSDT provides worst results in this case compared to the VCCT and FSDT, considering all of the cases investigated the TSDT captures better the problem of delaminated composite plates subjected to bending. Moreover it is the best solution among the higher-order plates models developed for the same problem (Szekrényes, 2013d) and captures very well the complex deformation around the delamination tip even if the delamination divides the plate into a relatively thin and a relatively thick layer.

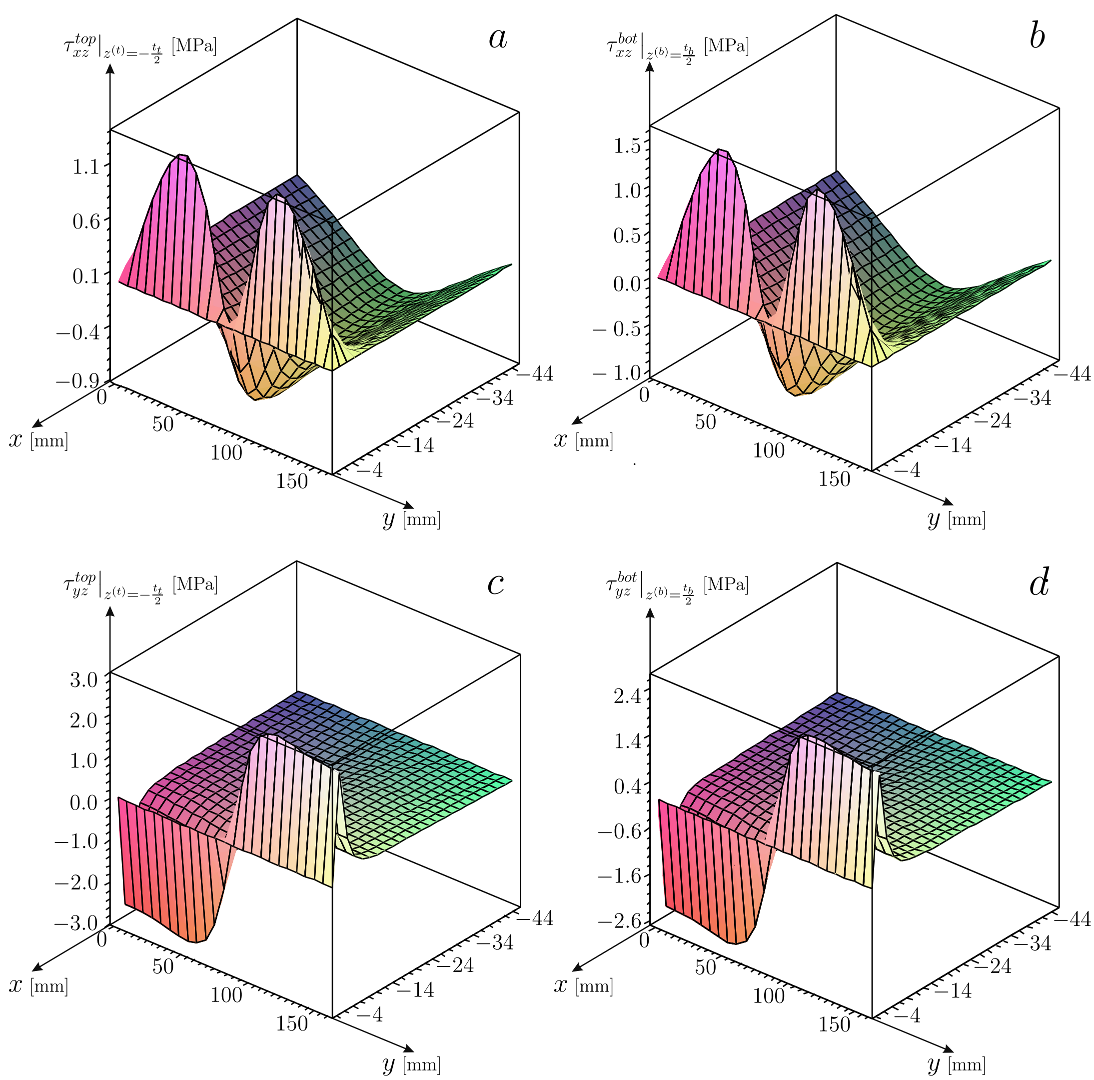

Fig. 11. Distribution of the interlaminar shear stress for case III, $b = 160$ mm, τ_{xz}^{top} (a), τ_{xz}^{bot} (b), τ_{yz}^{top} (c) and τ_{yz}^{bot} (d), lay-up: $\left[\pm45^f/0/\pm45_2^f/\bar{0}\right]_S$.

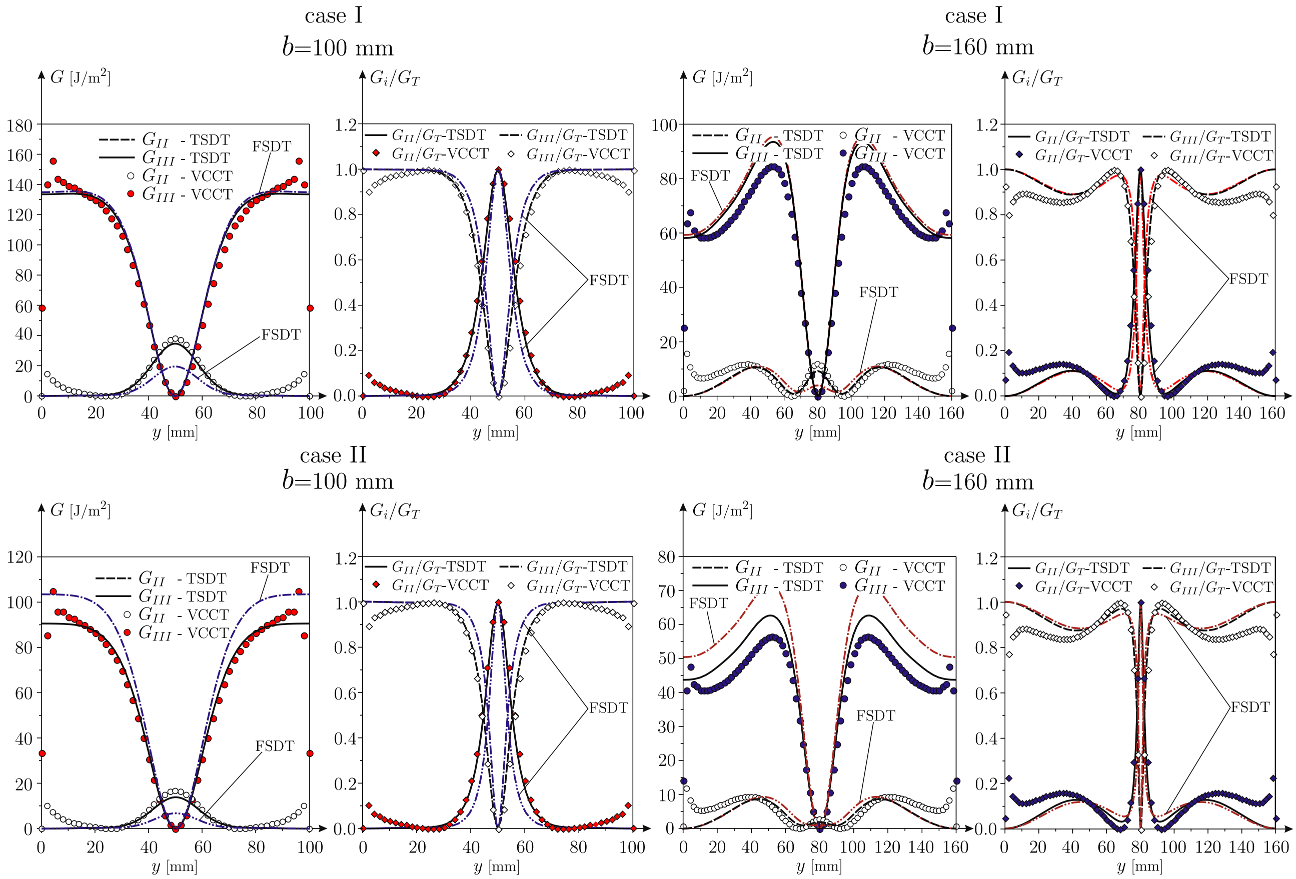

Fig. 12. Distribution of the energy release rates and mode mixity along the delamination front for cases I and II, lay-up: $\left[\pm 45^f/0/\pm 45^f_2/\bar{0}\right]_s$.

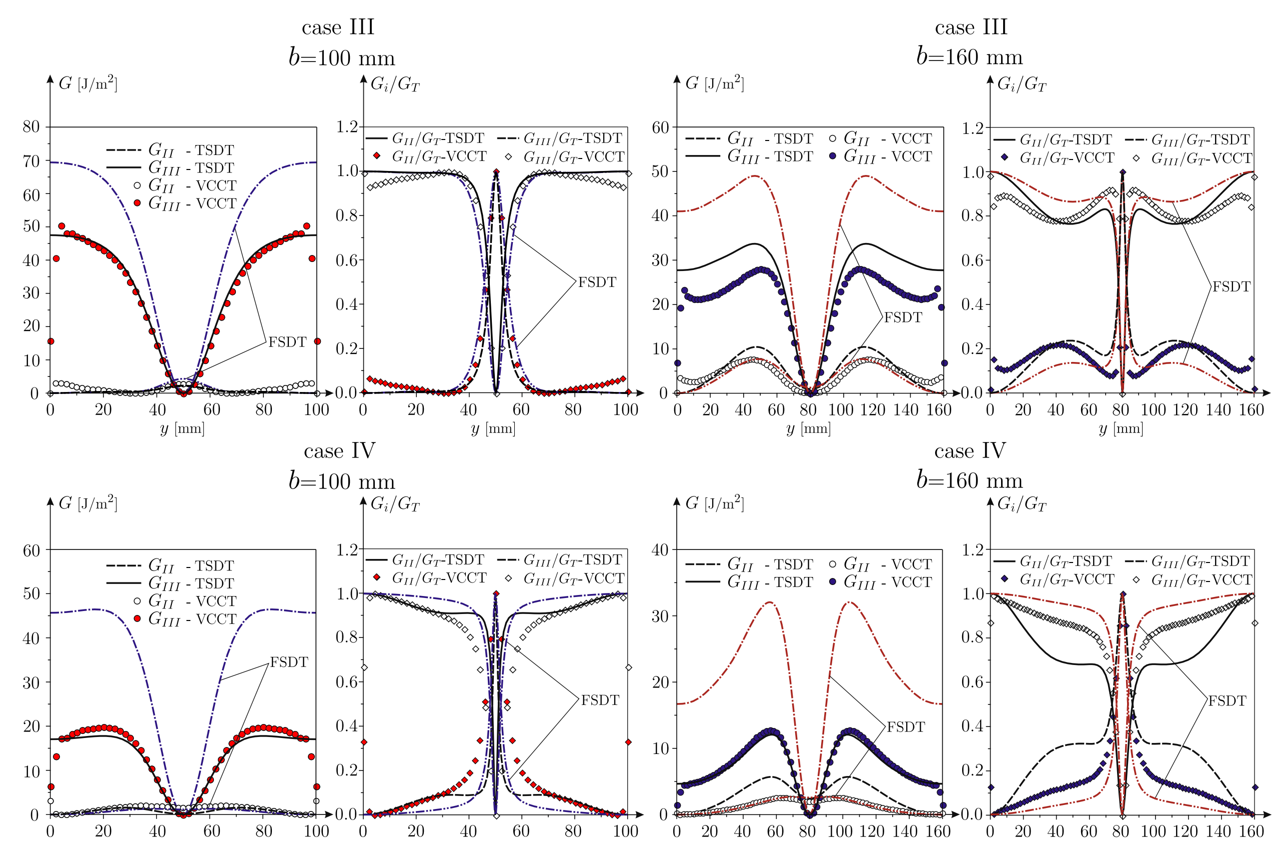

Fig. 13. Distribution of the energy release rates and mode mixity along the delamination front for cases III and IV, lay-up: $\left[\pm 45^f/0/\pm 45^f_2/\bar{0}\right]_s$.

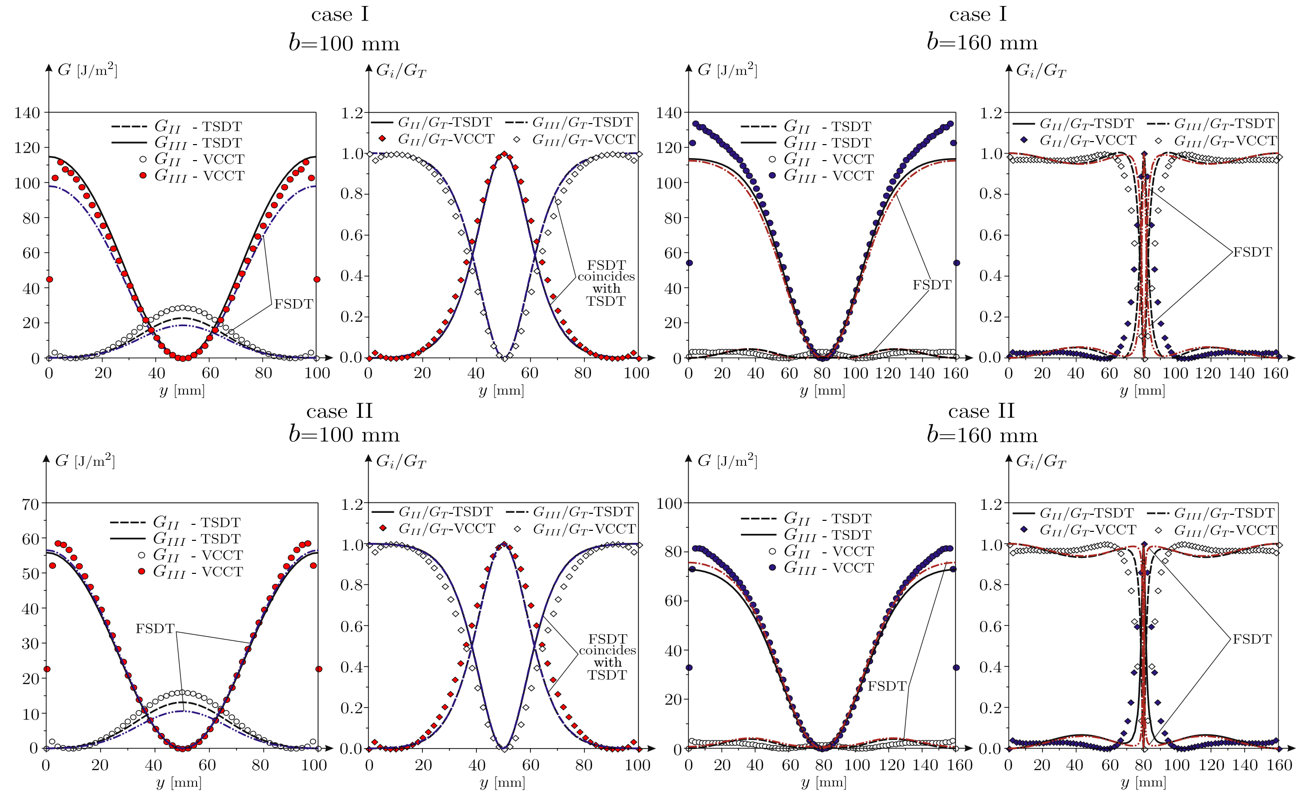

Fig. 14. Distribution of the energy release rates and mode mixity along the delamination front for cases I and II, lay-up: $[90/0/90_2/\bar{0}]_S$.

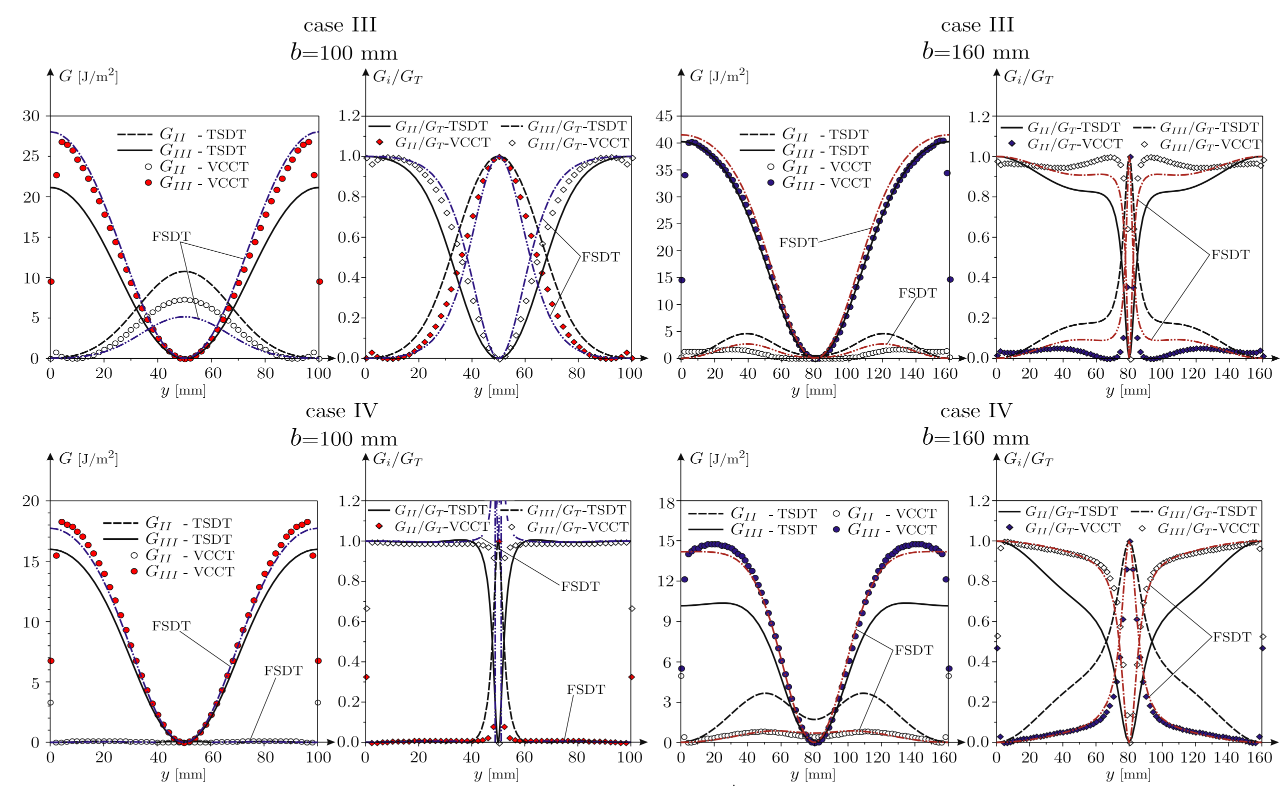

Fig. 15. Distribution of the energy release rates and mode mixity along the delamination front for cases III and IV, lay-up: $[90/0/90_2/\bar{0}]_S$.

8. Conclusions

This work presented an analytical model for delaminated orthotropic plates based on the third-order shear deformable theory by Reddy. The original theory was modified and the system of exact kinematic conditions was implemented into the theory. A novel condition involving the continuity of the shear strains across the interface plane was introduced and utilized in the development of the displacement field of the double-plate model. The main idea of the model is that the plane of the delamination divides the plate into two equivalent single layers. The kinematic conditions between these layers were established. The governing equations were derived and simply-supported plates with straight delamination front were analyzed using the Lévy plate formulation and the state-space model. The displacement and stress fields were calculated and compared to results by corresponding finite element and first-order plate theory analyses. It was shown that the present model is better than any of the previous plate models, however for the mode-II energy release rate distribution there are moderate differences between the numerical and analytical solutions if the delamination is very close to the free surface of the plate. Nevertheless, the present model is very reasonable and predicts very well the displacement field and the stress state. It was shown that the energy release rate can be accurately predicted only if the stress state is approximated by an as correct way as possible (viz., the satisfaction of the dynamic boundary conditions is important).

The developed model can be utilized in the following cases too. For some recently developed fracture mechanical plate bending systems (Lee, 1993; de Morais and Pereira, 2009) analytical solutions can be given in closed-form for the energy release rates, that may replace the finite element models with high element numbers. A possible plate finite element can be developed, which would make it possible to reduce the high element number in the vicinity of crack tips. By the reduction of the present analysis a possible beam model can be developed for the mode separation under mixed-mode I/II condition. An important aspect of the analysis is that it was shown that in the undelaminated part there are normal forces, as well. This indicates that for embedded delaminations the delaminated part is loaded by normal forces. The vibration analysis of beams and plates with embedded delaminations (the delamination has two tips and so it is closed) can be treated as a problem with time dependent stiffness, where the delaminated parts are loaded by periodic, nonconservative (i.e. follower) internal forces, and local instability can only be investigated by considering the normal forces. These tasks will be carried out in the near future.

Acknowledgments

This work was supported by the János Bolyai Research Scholarship of the Hungarian Academy of Sciences and the Hungarian National Scientific Research Fund (OTKA) under Grant No. 44615-066-15 (108414).

Appendix A. Coefficients for Eqs. (43) and (44)

The constant parameters in Eqs. (43) and (44) are defined in this Appendix. In the equations, e.g. the $a_7 = a_6\left((..)_{11}^{(\delta)} \Rightarrow (..)_{66}^{(\delta)}\right)$ notation means that a_7 can be obtained by replacing $A_{11}^{(t)}$, $B_{11}^{(t)}$, $D_{11}^{(t)}$, etc. with $A_{66}^{(t)}$, $B_{66}^{(t)}$, $D_{66}^{(t)}$, etc. in a_6.

$$a_1 = A_{11}^{(t)} + A_{11}^{(b)}, \quad a_2 = a_1\left((..)_{11}^{(\delta)} \Rightarrow (..)_{66}^{(\delta)}\right),$$
$$a_3 = a_1\left((..)_{11}^{(\delta)} \Rightarrow (..)_{12}^{(\delta)} + (..)_{66}^{(\delta)}\right)$$
$$a_4 = \sum_{\delta=t,b}\Delta_\delta A_{11}^{(\delta)} + B_{11}^{(\delta)} + \Lambda_\delta D_{11}^{(\delta)}, \quad a_5 = a_4\left((..)_{11}^{(\delta)} \Rightarrow (..)_{66}^{(\delta)}\right)$$
$$a_6 = a_4\left((..)_{11}^{(\delta)} \Rightarrow (..)_{12}^{(\delta)} + (..)_{66}^{(\delta)}\right), \quad a_7 = \Phi_t A_{11}^{(t)} + \Pi_t B_{11}^{(t)} + E_{11}^{(t)} \tag{A.1}$$

$$a_8 = a_7\left((..)_{11}^{(\delta)} \Rightarrow (..)_{66}^{(\delta)}\right), \quad a_9 = a_7\left((..)_{11}^{(\delta)} \Rightarrow (..)_{12}^{(\delta)} + (..)_{66}^{(\delta)}\right)$$
$$a_{10} = \sum_{\delta=t,b}\Gamma_\delta A_{11}^{(\delta)} + \Sigma_\delta B_{11}^{(\delta)} + \Psi_\delta D_{11}^{(\delta)}, \quad a_{11} = a_{10}\left((..)_{11}^{(\delta)} \Rightarrow (..)_{66}^{(\delta)}\right)$$
$$a_{12} = a_{10}\left((..)_{11}^{(\delta)} \Rightarrow (..)_{12}^{(\delta)} + (..)_{66}^{(\delta)}\right), \quad a_{13} = \sum_{\delta=t,b}\Lambda_\delta A_{11}^{(\delta)} + \Omega_\delta D_{11}^{(\delta)}$$
$$a_{14} = a_{13}\left((..)_{11}^{(\delta)} \Rightarrow (..)_{12}^{(\delta)} + 2(..)_{66}^{(\delta)}\right) \tag{A.2}$$

$$b_1 = a_3, \quad b_2 = a_2, \quad b_3 = a_1\left((..)_{11}^{(\delta)} \Rightarrow (..)_{22}^{(\delta)}\right), \quad b_4 = a_6, \quad b_5 = a_5,$$
$$b_6 = a_4\left((..)_{11}^{(\delta)} \Rightarrow (..)_{22}^{(\delta)}\right), \quad b_7 = a_9, \quad b_8 = a_8, \quad b_9 = a_7\left((..)_{11}^{(\delta)} \Rightarrow (..)_{22}^{(\delta)}\right)$$
$$b_{10} = a_{12}, \quad b_{11} = a_{11}, \quad b_{12} = a_{10}\left((..)_{11}^{(\delta)} \Rightarrow (..)_{22}^{(\delta)}\right), \quad b_{13} = a_{14}$$
$$b_{14} = a_{13}\left((..)_{11}^{(\delta)} \Rightarrow (..)_{22}^{(\delta)}\right) \tag{A.3}$$

$$c_4 = -\Pi_t(A_{55}^{(t)} + 2B_{55}^{(t)}\Omega_t) - 3D_{55}^{(t)} - 6E_{55}^{(t)}\Omega_t$$
$$c_5 = A_{11}^{(t)}\Delta_t\Phi_t + B_{11}^{(t)}(\Phi_t + \Delta_t\Pi_t) + D_{11}^{(t)}(\Phi_t\Omega_t + \Pi_t)$$
$$+ E_{11}^{(t)}(\Delta_t + \Pi_t\Omega_t) + F_{11}^{(t)} + G_{11}^{(t)}\Omega_t$$
$$c_6 = c_6\left((..)_{11}^{(\delta)} \Rightarrow (..)_{66}^{(\delta)}\right), \quad c_7 = c_5\left((..)_{11}^{(\delta)} \Rightarrow (..)_{12}^{(\delta)} + (..)_{66}^{(\delta)}\right) \tag{A.4}$$
$$c_8 = -A_{55}^{(t)}\Pi_t^2 - 6D_{55}^{(t)}\Pi_t - 9F_{55}^{(t)}$$
$$c_9 = A_{11}^{(t)}\Phi_t^2 + 2B_{11}^{(t)}\Phi_t\Pi_t + D_{11}^{(t)}\Pi_t^2 + 2E_{11}^{(t)}\Phi_t + 2F_{11}^{(t)}\Pi_t + H_{11}^{(t)}$$

$$c_{10} = c_9\left((..)_{11}^{(\delta)} \Rightarrow (..)_{66}^{(\delta)}\right), \quad c_{11} = c_9\left((..)_{11}^{(\delta)} \Rightarrow (..)_{12}^{(\delta)} + (..)_{66}^{(\delta)}\right)$$
$$c_{12} = -A_{55}^{(t)}\Pi_t\Sigma_t - 2B_{55}^{(t)}\Pi_t\Psi_t - 3D_{55}^{(t)}\Sigma_t - 6E_{55}^{(t)}\Psi_t$$
$$c_{13} = A_{11}^{(t)}\Phi_t\Gamma_t + B_{11}^{(t)}(\Phi_t\Sigma_t + \Pi_t\Gamma_t) + D_{11}^{(t)}(\Phi_t\Psi_t + \Pi_t\Sigma_t)$$
$$+ E_{11}^{(t)}(\Pi_t\Psi_t + \Gamma_t) + F_{11}^{(t)}\Sigma_t + G_{11}^{(t)}\Psi_t$$
$$c_{14} = c_{13}\left((..)_{11}^{(\delta)} \Rightarrow (..)_{66}^{(\delta)}\right), \quad c_{15} = c_{13}\left((..)_{11}^{(\delta)} \Rightarrow (..)_{12}^{(\delta)} + (..)_{66}^{(\delta)}\right), \quad c_{16} = c_4$$
$$c_{17} = A_{11}^{(t)}\Phi_t\Lambda_t + B_{11}^{(t)}\Pi_t\Lambda_t + D_{11}^{(t)}\Phi_t\Omega_t + E_{11}^{(t)}(\Pi_t\Omega_t + \Lambda_t)\Psi_t + G_{11}^{(t)}\Omega_t$$
$$c_{18} = c_{17}\left((..)_{11}^{(\delta)} \Rightarrow (..)_{12}^{(\delta)} + (..)_{66}^{(\delta)}\right) \tag{A.5}$$

$$d_1 = c_3, \quad d_2 = c_2, \quad d_3 = c_1\left((..)_{11}^{(\delta)} \Rightarrow (..)_{22}^{(\delta)}\right)$$
$$d_4 = c_7, \quad d_5 = d_{18} = c_4\left((..)_{55}^{(\delta)} \Rightarrow (..)_{44}^{(\delta)}\right),$$
$$d_6 = c_6, \quad d_7 = c_5\left((..)_{11}^{(\delta)} \Rightarrow (..)_{22}^{(\delta)}\right)$$
$$d_8 = c_{11}, \quad d_9 = c_8\left((..)_{55}^{(\delta)} \Rightarrow (..)_{44}^{(\delta)}\right),$$
$$d_{10} = c_{10}, \quad d_{11} = c_9\left((..)_{11}^{(\delta)} \Rightarrow (..)_{22}^{(\delta)}\right) \tag{A.6}$$
$$d_{12} = c_{15}, \quad d_{13} = c_{12}\left((..)_{55}^{(\delta)} \Rightarrow (..)_{44}^{(\delta)}\right),$$
$$d_{14} = c_{14}, \quad d_{15} = c_{13}\left((..)_{11}^{(\delta)} \Rightarrow (..)_{22}^{(\delta)}\right)$$
$$d_{16} = c_{18}, \quad b_{17} = c_{17}\left((..)_{11}^{(\delta)} \Rightarrow (..)_{22}^{(\delta)}\right)$$

$$\begin{aligned}
&e_1 = a_4, \quad e_2 = a_5, \quad e_3 = a_6,\\
&e_4 = e_{16} = -A_{55}^{(t)} - A_{55}^{(b)} - 4(B_{55}^{(t)}\Omega_t + B_{55}^{(b)}\Omega_b) - 4(D_{55}^{(t)}\Omega_t^2 + D_{55}^{(b)}\Omega_b^2)\\
&e_5 = A_{11}^{(t)}\Delta_t^2 + A_{11}^{(b)}\Delta_b^2 + 2(B_{11}^{(t)}\Delta_t + B_{11}^{(b)}\Delta_b) + D_{11}^{(t)}(1+2\Delta_t\Omega_t)\\
&\qquad + D_{11}^{(b)}(1+2\Delta_b\Omega_b) + 2(E_{11}^{(t)}\Omega_t + E_{11}^{(b)}\Omega_b) + F_{11}^{(t)}\Omega_t^2 + F_{11}^{(b)}\Omega_b^2\\
&e_6 = e_5\left((..)_{11}^{(\delta)} \Rightarrow (..)_{66}^{(\delta)}\right), \quad e_7 = e_5\left((..)_{11}^{(\delta)} \Rightarrow (..)_{12}^{(\delta)} + (..)_{66}^{(\delta)}\right),\\
&e_8 = c_4, \quad e_9 = c_5
\end{aligned} \tag{A.7}$$

$$\begin{aligned}
&e_{10} = c_6, \quad e_{11} = c_7,\\
&e_{12} = -A_{55}^{(t)}\Sigma_t - 2(B_{55}^{(t)}(\Psi_t + \Omega_t\Sigma_t) + B_{55}^{(b)}\Psi_b)\\
&\qquad - 4D_{55}^{(t)}\Omega_t\Psi_t - D_{55}^{(b)}(3+4\Omega_b\Psi_b) - 6E_{55}^{(b)}\Omega_b\\
&e_{13} = A_{11}^{(t)}\Delta_t\Gamma_t + A_{11}^{(b)}\Delta_b\Gamma_b + B_{11}^{(t)}(\Gamma_t + \Delta_t\Sigma_t) + B_{11}^{(b)}\Gamma_b + D_{11}^{(t)}(\Sigma_t\\
&\qquad + \Gamma_t\Omega_t + \Delta_t\Psi_t) + D_{11}^{(b)}(\Gamma_b\Omega_b + \Delta_b\Psi_b) + E_{11}^{(t)}(\Psi_t\\
&\qquad + \Omega_t\Sigma_t) + E_{11}^{(b)}(\Psi_b + \Delta_b) + F_{11}^{(t)}\Omega_t\Psi_t + F_{11}^{(b)}(1+\Omega_b\Psi_b) + G_{11}^{(b)}\Omega_b\\
&e_{14} = e_{13}\left((..)_{11}^{(\delta)} \Rightarrow (..)_{66}^{(\delta)}\right), \quad e_{15} = e_{13}\left((..)_{11}^{(\delta)} \Rightarrow (..)_{12}^{(\delta)} + (..)_{66}^{(\delta)}\right)\\
&e_{17} = A_{11}^{(t)}\Delta_t\Lambda_t + A_{11}^{(b)}\Delta_b\Lambda_b + B_{11}^{(t)}\Lambda_t + B_{11}^{(b)}\Lambda_b + D_{11}^{(t)}\Omega_t(\Delta_t + \Lambda_t)\\
&\qquad + D_{11}^{(b)}\Omega_b(\Delta_b + \Lambda_b) + E_{11}^{(t)}\Omega_t + E_{11}^{(b)}\Omega_b + F_{11}^{(t)}\Omega_t^2 + F_{11}^{(b)}\Omega_b^2\\
&e_{18} = e_{17}\left((..)_{11}^{(\delta)} \Rightarrow (..)_{12}^{(\delta)} + 2(..)_{66}^{(\delta)}\right)
\end{aligned} \tag{A.8}$$

$$\begin{aligned}
&f_1 = e_3, \quad f_2 = e_2, \quad f_3 = e_1\left((..)_{11}^{(\delta)} \Rightarrow (..)_{22}^{(\delta)}\right) f_4 = e_7,\\
&f_5 = f_{18} = e_4\left((..)_{55}^{(\delta)} \Rightarrow (..)_{44}^{(\delta)}\right) f_6 = e_6, \quad f_7 = e_5\left((..)_{11}^{(\delta)} \Rightarrow (..)_{22}^{(\delta)}\right),\\
&f_8 = e_{11}, \quad f_9 = e_8\left((..)_{55}^{(\delta)} \Rightarrow (..)_{44}^{(\delta)}\right) f_{10} = e_{10},\\
&f_{11} = e_9\left((..)_{11}^{(\delta)} \Rightarrow (..)_{22}^{(\delta)}\right), \quad f_{12} = c_{15}, \quad f_{13} = e_{12}\left((..)_{55}^{(\delta)} \Rightarrow (..)_{44}^{(\delta)}\right)\\
&f_{14} = e_{14}, \quad f_{15} = e_{13}\left((..)_{11}^{(\delta)} \Rightarrow (..)_{22}^{(\delta)}\right), \quad f_{16} = e_{18},\\
&f_{17} = e_{17}\left((..)_{11}^{(\delta)} \Rightarrow (..)_{22}^{(\delta)}\right)
\end{aligned} \tag{A.9}$$

$$\begin{aligned}
&g_1 = a_{10}, \quad g_2 = a_{11}, \quad g_3 = a_{12}, \quad g_4 = g_{16} = e_{12}, \quad g_5 = e_{13}, \quad g_6 = e_{14}\\
&g_7 = e_{15}, \quad g_8 = c_{12}, \quad g_9 = c_{13}, \quad g_{10} = c_{14}, \quad g_{11} = c_{15}\\
&g_{12} = -A_{55}^{(t)}\Sigma_t^2 - 4B_{55}^{(t)}\Sigma_t\Psi_t - 4(D_{55}^{(t)}\Psi_t^2 + D_{55}^{(b)}\Psi_b^2) - 12E_{55}^{(b)}\Psi_b - 9F_{55}^{(t)}\\
&g_{13} = A_{11}^{(t)}\Gamma_t^2 + A_{11}^{(b)}\Gamma_b^2 + 2B_{11}^{(t)}\Gamma_t\Sigma_t + D_{11}^{(t)}(2\Gamma_t\Psi_t + \Sigma_t^2) + 2D_{11}^{(b)}\Gamma_b\Psi_b\\
&\qquad + 2E_{11}^{(t)}\Sigma_t\Psi_t + 2E_{11}^{(b)}\Gamma_b + F_{11}^{(t)}\Psi_t^2 + F_{11}^{(b)}\Psi_b^2 + 2G_{11}^{(b)}\Psi_b + H_{11}^{(b)}\\
&g_{14} = g_{13}\left((..)_{11}^{(\delta)} \Rightarrow (..)_{66}^{(\delta)}\right), \quad g_{15} = g_{13}\left((..)_{11}^{(\delta)} \Rightarrow (..)_{12}^{(\delta)} + (..)_{66}^{(\delta)}\right)\\
&g_{17} = A_{11}^{(t)}\Gamma_t\Lambda_t + A_{11}^{(b)}\Gamma_b\Lambda_b + B_{11}^{(t)}\Sigma_t\Lambda_t + D_{11}^{(t)}(\Omega_t\Gamma_t + \Psi_t\Lambda_t)\\
&\qquad + D_{11}^{(b)}(\Omega_b\Gamma_b + \Psi_b\Lambda_b) + E_{11}^{(t)}\Omega_t\Sigma_t + E_{11}^{(b)}\Lambda_b + F_{11}^{(t)}\Omega_t\Psi_t\\
&\qquad + F_{11}^{(b)}\Omega_b\Psi_b + G_{11}^{(b)}\Omega_b,\\
&g_{18} = g_{17}\left((..)_{11}^{(\delta)} \Rightarrow (..)_{12}^{(\delta)} + 2(..)_{66}^{(\delta)}\right)
\end{aligned} \tag{A.10}$$

$$\begin{aligned}
&h_1 = a_{12}, \quad h_2 = a_{11}, \quad h_3 = b_{12}, \quad h_4 = g_7, \quad h_5 = h_{18} = f_{13},\\
&h_6 = g_6, \quad h_7 = f_{15}\\
&h_8 = g_{11}, \quad h_9 = d_{13}, \quad h_{10} = g_{10}, \quad h_{11} = d_{15}, \quad h_{12} = g_{15},\\
&h_{13} = g_{12}\left((..)_{55}^{(\delta)} \Rightarrow (..)_{44}^{(\delta)}\right)\\
&h_{14} = g_{14}, \quad h_{15} = g_{13}\left((..)_{11}^{(\delta)} \Rightarrow (..)_{22}^{(\delta)}\right), \quad h_{16} = g_{18},\\
&h_{17} = g_{17}\left((..)_{11}^{(\delta)} \Rightarrow (..)_{22}^{(\delta)}\right)
\end{aligned} \tag{A.11}$$

$$\begin{aligned}
&j_1 = -\sum_{\delta=t,b} A_{11}^{(\delta)}\Lambda_\delta + D_{11}^{(\delta)}\Omega_\delta, \quad j_2 = j_3 = j_1\left((..)_{11}^{(\delta)} \Rightarrow (..)_{12}^{(\delta)} + 2(..)_{66}^{(\delta)}\right)\\
&j_4 = j_1\left((..)_{11}^{(\delta)} \Rightarrow (..)_{22}^{(\delta)}\right)\\
&j_5 = j_{23} = A_{55}^{(t)} + A_{55}^{(b)} + 4B_{55}^{(t)}\Omega_t + 4B_{55}^{(b)}\Omega_b + 4D_{55}^{(t)}\Omega_t^2 + 4D_{55}^{(b)}\Omega_b^2\\
&j_6 = -A_{11}^{(t)}\Delta_t\Lambda_t - A_{11}^{(b)}\Delta_b\Lambda_b - B_{11}^{(t)}\Lambda_t - B_{11}^{(b)}\Lambda_b - D_{11}^{(t)}\Omega_t(\Delta_t + \Lambda_t)\\
&\qquad + D_{11}^{(b)}\Omega_b(\Delta_b + \Lambda_b) - E_{11}^{(t)}\Omega_t - E_{11}^{(b)}\Omega_b - F_{11}^{(t)}\Omega_t^2 - F_{11}^{(b)}\Omega_b^2\\
&j_7 = j_9 = j_6\left((..)_{11}^{(\delta)} \Rightarrow (..)_{12}^{(\delta)} + 2(..)_{6}^{(\delta)}\right),\\
&j_8 = j_{26} = j_4\left((..)_{55}^{(\delta)} \Rightarrow (..)_{44}^{(\delta)}\right)
\end{aligned} \tag{A.12}$$

$$\begin{aligned}
&j_{10} = j_6\left((..)_{11}^{(\delta)} \Rightarrow (..)_{22}^{(\delta)}\right), \quad j_{11} = A_{55}^{(t)}\Pi_t + 2B_{55}^{(t)}\Pi_t\Omega_t + 3D_{55}^{(t)} + 6E_{55}^{(t)}\Omega_t\\
&j_{12} = -A_{11}^{(t)}\Phi_t\Lambda_t - B_{11}^{(t)}\Lambda_t\Pi_t - B_{11}^{(b)}\Lambda_b - D_{11}^{(t)}\Phi_t\Omega_t - E_{11}^{(t)}(\Lambda_t + \Pi_t\Omega_t)\\
&\qquad - G_{11}^{(t)}\Omega_t\\
&j_{13} = j_{15} = j_{12}\left((..)_{11}^{(\delta)} \Rightarrow ((..)_{12}^{(\delta)} + 2(..)_{66}^{(\delta)})\right)\\
&j_{14} = j_{11}\left((..)_{55}^{(\delta)} \Rightarrow (..)_{44}^{(\delta)}\right), \quad j_{16} = j_{12}\left((..)_{11}^{(\delta)} \Rightarrow (..)_{22}^{(\delta)}\right)\\
&j_{17} = A_{55}^{(t)}\Sigma_t + 2B_{55}^{(t)}(\Omega_t\Sigma_t + \Psi_t) + 2B_{55}^{(b)}\Omega_b\Sigma_b + 4D_{55}^{(t)}\Omega_t\Psi_t\\
&\qquad + D_{55}^{(b)}(3+4\Omega_b\Psi_b) + 6E_{55}^{(b)}\Omega_b
\end{aligned} \tag{A.13}$$

$$\begin{aligned}
&j_{18} = -A_{11}^{(t)}\Gamma_t\Lambda_t - A_{11}^{(b)}\Gamma_b\Lambda_b - B_{11}^{(t)}\Sigma_t\Lambda_t - D_{11}^{(t)}(\Psi_t\Lambda_t + \Gamma_t\Omega_t)\\
&\qquad - D_{11}^{(b)}(\Psi_b\Lambda_b + \Gamma_b\Omega_b) - E_{11}^{(t)}\Omega_t\Sigma_t - E_{11}^{(b)}\Lambda_b - F_{11}^{(t)}\Omega_t\Psi_t\\
&\qquad - F_{11}^{(b)}\Omega_b\Psi_b - G_{11}^{(b)}\Omega_b\\
&j_{19} = j_{21} = -(A_{12}^{(t)} + 2A_{66}^{(t)})\Gamma_t\Lambda_t - (A_{12}^{(b)} + 2A_{66}^{(b)})\Gamma_b\Lambda_b\\
&\qquad - (B_{12}^{(t)} + 2B_{66}^{(t)})\Sigma_t\Lambda_t - (B_{12}^{(b)} + 2B_{66}^{(b)})\Sigma_b\Lambda_b - (E_{12}^{(t)} + 2E_{66}^{(t)})\Sigma_t\Omega_t\\
&\qquad - (E_{12}^{(b)} + 2E_{66}^{(b)})\Lambda_b - (F_{12}^{(t)} + 2F_{66}^{(t)})\Psi_t\Omega_t\\
&\qquad - (F_{12}^{(b)} + 2F_{66}^{(b)})\Psi_b\Omega_b - G_{12}^{(b)}\Omega_b\\
&j_{20} = j_{17}\left((..)_{55}^{(\delta)} \Rightarrow (..)_{44}^{(\delta)}\right), \quad j_{22} = j_{18}\left((..)_{11}^{(\delta)} \Rightarrow (..)_{22}^{(\delta)}\right)\\
&j_{24} = -A_{11}^{(t)}\Lambda_t^2 - A_{11}^{(b)}\Lambda_b^2 - 2D_{11}^{(t)}\Lambda_t\Omega_t - 2D_{11}^{(b)}\Lambda_b\Omega_b - F_{11}^{(t)}\Omega_t^2 - F_{11}^{(b)}\Omega_b^2\\
&j_{25} = j_{24}\left((..)_{11}^{(\delta)} \Rightarrow 2((..)_{12}^{(\delta)} + 2(..)_{66}^{(\delta)})\right),\\
&j_{27} = j_{25}\left((..)_{11}^{(\delta)} \Rightarrow (..)_{22}^{(\delta)}\right), j_{28} = 1
\end{aligned} \tag{A.14}$$

Appendix B. Coefficients for Eqs. (52)–(54)

The constants in Eqs. (52) and (54) are defined in this Appendix. First, we define the determinants below with three and six indices:

$$\begin{aligned}
&P_{i,j,k} = \begin{vmatrix} c_i & c_j & c_k \\ e_i & e_j & e_k \\ g_i & g_j & g_k \end{vmatrix}, \quad Q_{i,j,k}^{p,q,r} = \begin{vmatrix} a_p & a_q & a_r \\ e_i & e_j & e_k \\ g_i & g_j & g_k \end{vmatrix}\\
&R_{i,j,k}^{p,q,r} = \begin{vmatrix} a_p & a_q & a_r \\ c_i & c_j & c_k \\ g_i & g_j & g_k \end{vmatrix}, \quad S_{i,j,k}^{p,q,r} = \begin{vmatrix} a_p & a_q & a_r \\ c_i & c_j & c_k \\ e_i & e_j & e_k \end{vmatrix}
\end{aligned} \tag{B.1}$$

Moreover we have:

$$K_{i,j,k}=\begin{vmatrix} d_i & d_j & d_k\\ f_i & f_j & f_k\\ h_i & h_j & h_k\end{vmatrix},\quad L^{p,q,r}_{i,j,k}=\begin{vmatrix} b_p & b_q & b_r\\ f_i & f_j & f_k\\ h_i & h_j & h_k\end{vmatrix}$$
$$M^{p,q,r}_{i,j,k}=\begin{vmatrix} b_p & b_q & b_r\\ d_i & d_j & d_k\\ h_i & h_j & h_k\end{vmatrix},\quad N^{p,q,r}_{i,j,k}=\begin{vmatrix} b_p & b_q & b_r\\ d_i & d_j & d_k\\ f_i & f_j & f_k\end{vmatrix} \tag{B.2}$$

The denominators of the constants are defined by:

$$1/\Theta_1=-a_{10}P_{1,5,9}+c_{13}Q^{1,4,7}_{1,5,9}-e_{13}R^{1,4,7}_{1,5,9}+g_{13}S^{1,4,7}_{1,5,9}$$
$$1/\Theta_2=b_{11}K_{2,6,10}-d_{14}L^{2,5,8}_{2,6,10}+f_{14}M^{2,5,8}_{2,6,10}-h_{14}N^{2,5,8}_{2,6,10} \tag{B.3}$$

Thus, the constants denoted by $\hat{k}$, $\hat{l}$, $\hat{m}$, $\hat{n}$, $\hat{p}$, $\hat{q}$, $\hat{r}$ and $\hat{s}$ are:

$$\hat{k}_1=\beta^2\Theta_1\left(-a_{10}P_{2,5,9}+c_{13}Q^{2,4,7}_{2,5,9}-e_{13}R^{2,4,7}_{2,5,9}+g_{13}S^{2,4,7}_{2,5,9}\right)$$
$$\hat{k}_2=\beta\Theta_1\left(-a_{10}P_{3,5,9}+c_{13}Q^{3,4,7}_{3,5,9}-e_{13}R^{3,4,7}_{3,5,9}+g_{13}S^{3,4,7}_{3,5,9}\right)$$
$$\hat{k}_3=\beta^2\Theta_1(a_{10}P_{5,6,9}-a_4P_{6,9,13}-a_7P_{5,6,13}+a_5P_{5,9,13})$$
$$-\Theta_1(-a_{10}P_{4,5,9}-a_4P_{4,9,13}+a_7P_{4,5,13}) \tag{B.4}$$
$$\hat{k}_4=\beta\Theta_1\left(a_{10}P_{5,7,9}-c_{13}Q^{4,6,7}_{5,7,9}+e_{13}R^{4,6,7}_{5,7,9}+g_{13}S^{4,6,7}_{5,7,9}\right)$$
$$\hat{k}_5=\beta^2\Theta_1(-a_{10}P_{5,9,10}+a_4P_{9,10,13}-a_7P_{5,10,13}+a_8P_{5,9,13})$$
$$-\Theta_1(a_{10}P_{5,8,9}-a_4P_{8,9,13}-a_7P_{5,8,13})$$

$$\hat{k}_6=\beta\Theta_1\left(-a_{10}P_{5,9,11}+c_{13}Q^{4,7,9}_{5,9,11}-e_{13}R^{4,7,9}_{5,9,11}+g_{13}S^{4,7,9}_{5,9,11}\right)$$
$$\hat{k}_7=\beta^2\Theta_1(-a_{10}P_{5,9,14}-a_4P_{9,13,14}+a_7P_{5,13,14}-a_{11}P_{5,9,13})$$
$$-\Theta_1(-a_{10}P_{5,9,12}+a_4P_{9,12,13}-a_7P_{5,12,13})$$
$$\hat{k}_8=\beta\Theta_1\left(-a_{10}P_{5,9,15}+c_{13}Q^{4,7,12}_{5,9,15}-e_{13}R^{4,7,12}_{5,9,15}+g_{13}S^{4,7,12}_{5,9,15}\right) \tag{B.5}$$
$$\hat{k}_9=\beta^2\Theta_1(-a_{10}P_{5,9,18}-a_4P_{9,13,18}+a_7P_{5,13,18}+a_{14}P_{5,9,13})$$
$$-\Theta_1(-a_{10}P_{5,9,16}-a_4P_{9,13,16}+a_7P_{5,13,16})$$
$$\hat{k}_{10}=\Theta_1\left(a_{10}P_{5,9,17}-c_{13}Q^{4,7,13}_{5,9,17}+e_{13}R^{4,7,13}_{5,9,17}-g_{13}S^{4,7,13}_{5,9,17}\right)$$

$$\hat{l}_1=\beta\Theta_2\left(b_{11}K_{1,6,10}-d_{14}L^{1,5,8}_{1,6,10}+f_{14}M^{1,5,8}_{1,6,10}-h_{14}N^{1,5,8}_{1,6,10}\right)$$
$$\hat{l}_2=\beta^2\Theta_2\left(-b_{11}K_{3,6,10}+d_{14}L^{3,5,8}_{3,6,10}-f_{14}M^{3,5,8}_{3,6,10}+h_{14}N^{3,5,8}_{3,6,10}\right)$$
$$\hat{l}_3=\beta\Theta_2\left(b_{11}K_{4,6,10}-d_{14}L^{4,5,8}_{4,6,10}+f_{14}M^{4,5,8}_{4,6,10}-h_{14}N^{4,5,8}_{4,6,10}\right) \tag{B.6}$$
$$\hat{l}_4=\beta^2\Theta_2(b_{11}K_{6,7,10}-b_5K_{7,10,14}-b_8K_{6,7,14}+b_6K_{6,10,14})$$
$$-\Theta_2(-b_{11}K_{5,6,10}-b_5K_{5,10,14}+b_8K_{5,6,14})$$
$$\hat{l}_5=\beta\Theta_2\left(-b_{11}K_{6,8,10}+d_{14}L^{5,7,8}_{6,8,10}-f_{14}M^{5,7,8}_{6,8,10}+h_{14}N^{5,7,8}_{6,8,10}\right)$$

$$\hat{l}_6=\beta^2\Theta_2(-b_{11}K_{6,10,11}+b_5K_{10,11,14}-b_8K_{6,11,14}+b_9K_{6,10,14})$$
$$-\Theta_2(b_{11}K_{6,9,10}-b_5K_{9,10,14}-b_8K_{6,9,14})$$
$$\hat{l}_7=\beta\Theta_2(b_{11}K_{6,10,12}-b_{10}K_{6,10,14}-b_5K_{10,12,14}+b_8K_{6,12,14})$$
$$\hat{l}_8=\beta^2\Theta_2(-b_{11}K_{6,10,15}-b_5K_{10,14,15}+b_8K_{6,14,15}+b_{12}K_{6,10,14})$$
$$-\Theta_2(-b_{11}K_{6,10,13}+b_5K_{6,13,14}-b_8K_{6,13,14}) \tag{B.7}$$
$$\hat{l}_9=\beta^2\Theta_2(-b_{11}K_{6,10,17}+b_5K_{10,14,17}-b_8K_{6,14,17}-b_{14}K_{6,10,14})$$
$$-\Theta_2(b_{11}K_{6,10,18}+b_5K_{10,14,18}-b_8K_{6,14,18})$$
$$\hat{l}_{10}=\beta\Theta_2(b_{11}K_{6,10,16}-b_{13}K_{6,10,14}+b_5K_{10,14,16}-b_8K_{6,14,16})$$

$$\hat{m}_1=\beta^2\Theta_1\left(-a_{10}P_{1,2,9}+c_{13}Q^{1,2,7}_{1,2,9}-e_{13}R^{1,2,7}_{1,2,9}+g_{13}S^{1,2,7}_{1,2,9}\right)$$
$$\hat{m}_2=\beta\Theta_1\left(-a_{10}P_{1,3,9}+c_{13}Q^{1,3,7}_{1,3,9}-e_{13}R^{1,3,7}_{1,3,9}+g_{13}S^{1,3,7}_{1,3,9}\right)$$
$$\hat{m}_3=\beta^2\Theta_1(-a_{10}P_{1,6,9}+a_1P_{6,9,13}+a_7P_{1,6,13}-a_5P_{1,9,13})$$
$$-\Theta_1(-a_{10}P_{1,4,9}+a_1P_{4,9,13}+a_7P_{1,4,13}) \tag{B.8}$$
$$\hat{m}_4=\beta\Theta_1\left(-a_{10}P_{1,7,9}+c_{13}Q^{1,6,7}_{1,7,9}-e_{13}R^{1,6,7}_{1,7,9}+g_{13}S^{1,6,7}_{1,7,9}\right)$$
$$\hat{m}_5=\beta^2\Theta_1(a_{10}P_{1,9,10}-a_4P_{9,10,13}+a_7P_{1,10,13}-a_8P_{1,9,13})$$
$$-\Theta_1(-a_{10}P_{1,8,9}+a_1P_{8,9,13}+a_7P_{1,8,13})$$

$$\hat{m}_6=\beta\Theta_1\left(a_{10}P_{1,9,11}-c_{13}Q^{1,7,9}_{1,9,11}+e_{13}R^{1,7,9}_{1,9,11}-g_{13}S^{1,7,9}_{1,9,11}\right)$$
$$\hat{m}_7=\beta^2\Theta_1(a_{10}P_{1,9,14}+a_1P_{9,13,14}-a_7P_{1,13,14}-a_{11}P_{1,9,13})$$
$$-\Theta_1(a_{10}P_{1,9,12}-a_1P_{9,12,13}+a_7P_{1,12,13})$$
$$\hat{m}_8=\beta\Theta_1\left(a_{10}P_{1,9,15}-c_{13}Q^{1,7,12}_{1,9,15}+e_{13}R^{1,7,12}_{1,9,15}-g_{13}S^{1,7,12}_{1,9,15}\right) \tag{B.9}$$
$$\hat{m}_9=\beta^2\Theta_1(a_{10}P_{1,9,18}+a_1P_{9,13,18}-a_7P_{1,13,18}-a_{14}P_{1,9,13})$$
$$-\Theta_1(a_{10}P_{1,9,16}+a_1P_{9,13,16}-a_7P_{1,13,16})$$
$$\hat{m}_{10}=\Theta_1\left(-a_{10}P_{1,9,17}+c_{13}Q^{1,7,13}_{1,9,17}-e_{13}R^{1,7,13}_{1,9,17}+g_{13}S^{1,7,13}_{1,9,17}\right)$$

$$\hat{n}_1=\beta\Theta_2\left(-b_{11}K_{1,2,10}+d_{14}L^{1,2,8}_{1,2,10}-f_{14}M^{1,2,8}_{1,2,10}+h_{14}N^{1,2,8}_{1,2,10}\right)$$
$$\hat{n}_2=\beta^2\Theta_2\left(-b_{11}K_{2,3,10}+d_{14}L^{2,3,8}_{2,3,10}-f_{14}M^{2,3,8}_{2,3,10}+h_{14}N^{2,3,8}_{2,3,10}\right)$$
$$\hat{n}_3=\beta\Theta_2\left(b_{11}K_{2,4,10}-d_{14}L^{4,5,8}_{2,4,10}+f_{14}M^{4,5,8}_{4,6,10}-h_{14}N^{4,5,8}_{4,6,10}\right) \tag{B.10}$$
$$\hat{n}_4=\beta^2\Theta_2(-b_{11}K_{2,7,10}+b_2K_{7,10,14}+b_8K_{2,7,14}-b_6K_{2,10,14})$$
$$-\Theta_2(-b_{11}K_{2,5,10}+b_2K_{5,10,14}+b_8K_{2,5,14})$$
$$\hat{n}_5=\beta\Theta_2\left(b_{11}K_{2,8,10}-d_{14}L^{2,7,8}_{2,8,10}+f_{14}M^{2,7,8}_{2,8,10}-h_{14}N^{2,7,8}_{2,8,10}\right)$$

$$\hat{n}_6=\beta^2\Theta_2(b_{11}K_{2,10,11}-b_2K_{10,11,14}+b_8K_{2,11,14}-b_9K_{2,10,14})$$
$$-\Theta_2(-b_{11}K_{2,9,10}+b_2K_{9,10,14}+b_8K_{2,9,14})$$
$$\hat{n}_7=\beta\Theta_2(-b_{11}K_{2,10,12}+b_{10}K_{2,10,14}-b_2K_{10,12,14}-b_8K_{2,12,14})$$
$$\hat{n}_8=\beta^2\Theta_2(b_{11}K_{2,10,15}-b_2K_{10,14,15}-b_8K_{2,14,15}-b_{12}K_{2,10,14})$$
$$-\Theta_2(b_{11}K_{2,10,13}-b_2K_{10,13,14}+b_8K_{2,13,14})$$
$$\hat{n}_9=\beta^2\Theta_2(-b_{11}K_{2,10,17}-b_2K_{10,14,17}-b_8K_{2,14,17}+b_{14}K_{2,10,14})$$
$$-\Theta_2(-b_{11}K_{2,10,18}-b_2K_{10,14,18}+b_8K_{2,14,18})$$
$$\hat{n}_{10}=\beta\Theta_2(-b_{11}K_{2,10,16}+b_{13}K_{2,10,14}-b_2K_{10,14,16}+b_8K_{2,14,16}) \tag{B.11}$$

$$\hat{p}_1=\beta^2\Theta_1\left(a_{10}P_{1,5,9}-c_{13}Q^{1,4,7}_{1,5,9}+e_{13}R^{1,4,7}_{1,5,9}-g_{13}S^{1,4,7}_{1,5,9}\right)$$
$$\hat{p}_2=\beta\Theta_1\left(a_{10}P_{1,3,5}-c_{13}Q^{1,3,4}_{1,3,5}+e_{13}R^{1,3,4}_{1,3,5}-g_{13}S^{1,3,4}_{1,3,5}\right)$$
$$\hat{p}_3=\beta^2\Theta_1(-a_{10}P_{1,5,6}+a_1P_{5,6,13}-a_4P_{1,6,13}+a_5P_{1,5,13})$$
$$-\Theta_1(a_{10}P_{1,4,5}-a_1P_{4,5,13}-a_4P_{1,4,13}) \tag{B.12}$$
$$\hat{p}_4=\beta\Theta_1\left(-a_{10}P_{1,5,7}+c_{13}Q^{1,4,6}_{1,5,7}-e_{13}R^{1,4,6}_{1,5,7}+g_{13}S^{1,4,6}_{1,5,7}\right)$$
$$\hat{p}_5=\beta^2\Theta_1(-a_{10}P_{1,5,10}+a_1P_{5,10,13}-a_4P_{1,10,13}+a_8P_{1,5,13})$$
$$-\Theta_1(-a_{10}P_{1,5,8}+a_1P_{5,8,13}-a_4P_{1,8,13})$$

$$\hat{p}_6=\beta\Theta_1\left(-a_{10}P_{1,5,11}+c_{13}Q^{1,4,9}_{1,5,11}-e_{13}R^{1,4,9}_{1,5,11}+g_{13}S^{1,4,9}_{1,5,11}\right)$$
$$\hat{p}_7=\beta^2\Theta_1(-a_{10}P_{1,5,14}-a_1P_{5,13,14}+a_4P_{1,13,14}+a_{11}P_{1,5,13})-\Theta_1(-a_{10}P_{1,5,12}+a_1P_{5,12,13}-a_4P_{1,12,13})$$
$$\hat{p}_8=\beta\Theta_1\left(-a_{10}P_{1,5,15}+c_{13}Q^{1,4,12}_{1,5,15}-e_{13}R^{1,4,12}_{1,5,15}+g_{13}S^{1,4,12}_{1,5,15}\right)\quad\text{(B.13)}$$
$$\hat{p}_9=\beta^2\Theta_1(-a_{10}P_{1,5,18}-a_1P_{5,13,18}+a_4P_{1,13,18}+a_{14}P_{1,5,13})-\Theta_1(-a_{10}P_{1,5,16}-a_1P_{5,13,16}+a_4P_{1,13,16})$$
$$\hat{p}_{10}=\Theta_1\left(a_{10}P_{1,5,17}-c_{13}Q^{1,4,13}_{1,5,17}+e_{13}R^{1,4,13}_{1,5,17}-g_{13}S^{1,4,13}_{1,5,17}\right)$$

$$\hat{q}_1=\beta\Theta_2\left(b_{11}K_{1,2,6}-d_{14}L^{1,2,5}_{1,2,6}+f_{14}M^{1,2,5}_{1,2,6}-h_{14}N^{1,2,5}_{1,2,6}\right)$$
$$\hat{q}_2=\beta^2\Theta_2\left(b_{11}K_{2,3,6}-d_{14}L^{2,3,5}_{2,3,6}+f_{14}M^{2,3,5}_{2,3,6}-h_{14}N^{2,3,5}_{2,3,6}\right)$$
$$\hat{q}_3=\beta\Theta_2\left(-b_{11}K_{2,4,6}+d_{14}L^{2,4,5}_{2,4,6}+f_{14}M^{2,4,5}_{2,4,6}-h_{14}N^{2,4,5}_{2,4,6}\right)\quad\text{(B.14)}$$
$$\hat{q}_4=\beta^2\Theta_2(-b_{11}K_{2,6,7}+b_2K_{6,7,14}-b_5K_{2,7,14}+b_6K_{2,6,14})-\Theta_2(b_{11}K_{2,5,6}-b_2K_{5,6,14}-b_5K_{2,5,14})$$
$$\hat{q}_5=\beta\Theta_2\left(b_{11}K_{2,6,8}-d_{14}L^{2,5,7}_{2,6,8}+f_{14}M^{2,5,7}_{2,6,8}-h_{14}N^{2,5,7}_{2,6,8}\right)$$

$$\hat{q}_6=\beta^2\Theta_2(-b_{11}K_{2,6,11}+b_2K_{6,11,14}-b_5K_{2,11,14}+b_9K_{2,6,14})-\Theta_2(-b_{11}K_{2,6,9}+b_2K_{6,9,14}-b_5K_{2,9,14})$$
$$\hat{q}_7=\beta\Theta_2(b_{11}K_{2,6,12}-b_{10}K_{2,6,14}-b_2K_{6,12,14}+b_5K_{2,12,14})$$
$$\hat{q}_8=\beta^2\Theta_2(-b_{11}K_{2,6,15}-b_2K_{6,14,15}+b_5K_{2,14,15}+b_{12}K_{2,6,14})-\Theta_2(-b_{11}K_{2,6,13}+b_2K_{6,13,14}-b_5K_{2,13,14})\quad\text{(B.15)}$$
$$\hat{q}_9=\beta^2\Theta_2(b_{11}K_{2,6,17}+b_2K_{6,14,17}-b_5K_{2,14,17}-b_{14}K_{2,6,14})-\Theta_2(b_{11}K_{2,6,18}+b_2K_{6,14,18}-b_5K_{2,14,18})$$
$$\hat{q}_{10}=\beta\Theta_2(b_{11}K_{2,6,16}-b_{13}K_{2,6,14}+b_2K_{6,14,16}-b_5K_{2,14,16})$$

$$\hat{r}_1=\beta^2\Theta_1(a_1P_{2,5,9}-a_2P_{1,5,9}+a_4P_{1,2,9}-a_7P_{1,2,5})$$
$$\hat{r}_2=\beta\Theta_1(a_1P_{3,5,9}-a_3P_{1,5,9}+a_4P_{1,3,9}-a_7P_{1,3,5})$$
$$\hat{r}_3=\beta^2\Theta_1(-a_1P_{5,6,9}+a_4P_{1,6,9}+a_7P_{1,5,6}-a_5P_{1,5,9})-\Theta_1(a_1P_{1,4,9}+a_4P_{1,4,9}-a_6P_{1,4,5})\quad\text{(B.16)}$$
$$\hat{r}_4=\beta\Theta_1(-a_1P_{5,7,9}+a_4P_{1,7,9}-a_6P_{1,5,9}+a_7P_{1,5,7})$$
$$\hat{r}_5=\beta^2\Theta_1(a_1P_{5,9,10}-a_4P_{1,9,10}+a_7P_{1,5,10}-a_8P_{1,5,9})-\Theta_1(-a_1P_{5,8,9}+a_4P_{1,8,9}+a_7P_{1,5,8})$$

$$\hat{r}_6=\beta\Theta_1\left(-a_9P_{1,5,9}+c_{11}Q^{1,4,7}_{1,5,9}-e_{11}R^{1,4,7}_{1,5,9}+g_{11}S^{1,4,7}_{1,5,9}\right)$$
$$\hat{r}_7=\beta^2\Theta_1(a_1P_{5,9,14}-a_4P_{1,9,14}+a_7P_{1,5,14}-a_{11}P_{1,5,9})-\Theta_1(a_1P_{5,9,12}-a_4P_{1,9,12}+a_7P_{1,5,12})$$
$$\hat{r}_8=\beta\Theta_1\left(-a_{12}P_{1,5,9}+c_{15}Q^{1,4,7}_{1,5,9}-e_{15}R^{1,4,7}_{1,5,9}+g_{15}S^{1,4,7}_{1,5,9}\right)\quad\text{(B.17)}$$
$$\hat{r}_9=\beta^2\Theta_1(a_1P_{1,9,18}-a_4P_{1,9,18}+a_7P_{1,5,18}-a_{14}P_{1,5,9})-\Theta_1(a_1P_{1,5,16}-a_4P_{1,9,16}+a_7P_{1,5,16})$$
$$\hat{r}_{10}=\Theta_1\left(a_{13}P_{1,5,9}-c_{17}Q^{1,4,7}_{1,5,9}+e_{17}R^{1,4,7}_{1,5,9}-g_{17}S^{1,4,7}_{1,5,9}\right)$$

$$\hat{s}_1=\beta\Theta_2\left(-b_8K_{1,2,6}+d_{11}L^{1,2,5}_{1,2,6}-f_{10}M^{1,2,5}_{1,2,6}+h_{10}N^{1,2,5}_{1,2,6}\right)$$
$$\hat{s}_2=\beta^2\Theta_2\left(-b_8K_{2,3,6}+d_{10}L^{2,3,5}_{2,3,6}-f_{10}M^{2,3,5}_{2,3,6}+h_{10}N^{2,3,5}_{2,3,6}\right)$$
$$\hat{s}_3=\beta\Theta_2\left(b_8K_{2,4,6}-d_{10}L^{2,4,5}_{2,4,6}+f_{10}M^{2,4,5}_{2,4,6}-h_{10}N^{2,4,5}_{2,4,6}\right)\quad\text{(B.18)}$$
$$\hat{s}_4=\beta^2\Theta_2(-b_2K_{6,7,10}+b_5K_{2,7,10}+b_8K_{2,6,7}-b_6K_{2,6,10})-\Theta_2(b_2K_{5,6,10}+b_5K_{2,5,10}-b_8K_{2,5,6})$$
$$\hat{s}_5=\beta\Theta_2\left(-b_8K_{2,6,8}+d_{10}L^{2,5,7}_{2,6,8}-f_{10}M^{2,5,7}_{2,6,8}+h_{10}N^{2,5,7}_{2,6,8}\right)$$

$$\hat{s}_6=\beta^2\Theta_2(b_2K_{6,10,11}-b_5K_{2,10,11}+b_8K_{2,6,11}-b_9K_{2,6,10})-\Theta_2(-b_2K_{6,9,10}+b_5K_{2,9,10}+b_8K_{2,6,9})$$
$$\hat{s}_7=\beta\Theta_2\left(b_{10}K_{2,6,10}-d_{12}L^{2,5,8}_{2,6,10}+f_{12}M^{2,5,8}_{2,6,10}-h_{12}N^{2,5,8}_{2,6,10}\right)$$
$$\hat{s}_8=\beta^2\Theta_2(b_2K_{6,10,15}-b_5K_{2,10,15}+b_8K_{2,6,15}-b_{12}K_{2,6,10})-\Theta_2(b_2K_{6,10,13}-b_5K_{2,10,13}+b_8K_{2,6,13})\quad\text{(B.19)}$$
$$\hat{s}_9=\beta^2\Theta_2(-b_2K_{6,10,17}+b_5K_{2,10,17}-b_8K_{2,6,17}+b_{14}K_{2,6,10})-\Theta_2(-b_2K_{6,10,18}+b_5K_{2,10,18}-b_8K_{2,6,18})$$
$$\hat{s}_{10}=\beta\Theta_2\left(b_{13}K_{2,6,10}-d_{16}L^{2,5,8}_{2,6,10}+f_{16}M^{2,5,8}_{2,6,10}-h_{16}N^{2,5,8}_{2,6,10}\right)$$

For the constants denoted by $\hat{t}$ we define the denominator below:

$$1/\Theta_3=j_{12}\hat{p}_{10}+j_{24}+j_1\hat{k}_{10}+j_6\hat{m}_{10}+j_{18}\hat{r}_{10}\quad\text{(B.20)}$$

The constants are:

$$\begin{aligned}\hat{t}_1=\Theta_3\Big[&\left(-\hat{p}_2\hat{l}_1-\hat{p}_4\hat{n}_1-\hat{p}_6\hat{q}_1-\hat{p}_8\hat{s}_1-p_1\right)j_{12}\\&+\left(-\hat{r}_4\hat{n}_1-\hat{r}_6\hat{q}_1-\hat{r}_8\hat{s}_1-\hat{r}_2\hat{l}_1-\hat{r}_1\right)j_{18}\\&+\left(-\hat{k}_8\hat{s}_1-\hat{k}_2\hat{l}_1-\hat{k}_4\hat{n}_1-\hat{k}_6\hat{q}_1-\hat{k}_1\right)j_1\\&+\left(-\hat{m}_6\hat{q}_1-\hat{m}_8\hat{s}_1-\hat{m}_1-\hat{m}_2\hat{l}_1-\hat{m}_4\hat{n}_1\right)j_6\\&+\beta\left(\hat{s}_1j_{21}+\hat{n}_1j_9+\hat{q}_1j_{15}+\hat{l}_1j_3+\beta j_2\right)\Big]\end{aligned}\quad\text{(B.21)}$$

$$\begin{aligned}\hat{t}_2=\Theta_3\Big[&\left(-\hat{p}_2\hat{l}_2-\hat{p}_4\hat{n}_2-\hat{p}_6\hat{q}_2-\hat{p}_8\hat{s}_2\right)j_{12}\\&+\left(-\hat{r}_4\hat{n}_2-\hat{r}_6\hat{q}_2-\hat{r}_8\hat{s}_2-\hat{r}_2\hat{l}_2\right)j_{18}\\&+\left(-\hat{k}_2\hat{l}_2-\hat{k}_4\hat{n}_2-\hat{k}_6\hat{q}_2-\hat{k}_8\hat{s}_2\right)j_1\\&+\left(-\hat{m}_4\hat{n}_2-\hat{m}_6\hat{q}_2-\hat{m}_8\hat{s}_2-\hat{m}_2\hat{l}_2\right)j_6\\&-\beta\left(\beta^2j_4-j_3\hat{l}_2-\hat{s}_2j_{21}-\hat{n}_2j_9-\hat{q}_2j_{15}\right)\Big]\end{aligned}\quad\text{(B.22)}$$

$$\begin{aligned}\hat{t}_3=\Theta_3\Big[&\left(-\hat{p}_3-\hat{p}_4\hat{n}_3-\hat{p}_8\hat{s}_3-\hat{p}_2\hat{l}_3-\hat{p}_6q_3\right)j_{12}\\&+\left(-\hat{q}_3\hat{r}_6-\hat{r}_3-\hat{r}_8\hat{s}_3-\hat{r}_2\hat{l}_3-\hat{r}_4\hat{n}_3\right)j_{18}\\&+\left(-\hat{k}_2\hat{l}_3-\hat{k}_6\hat{q}_3-\hat{k}_8\hat{s}_3-\hat{k}_4\hat{n}_3-\hat{k}_3\right)j_1\\&+\left(-\hat{m}_2\hat{l}_3-\hat{m}_8\hat{s}_3-\hat{m}_6\hat{q}_3-\hat{m}_3-\hat{m}_4\hat{n}_3\right)j_6\\&+j_{21}\beta\hat{s}_3-j_5+j_{15}\beta\hat{q}_3+j_3\beta\hat{l}_3+j_7\beta^2+j_9\beta\hat{n}_3\Big]\end{aligned}\quad\text{(B.23)}$$

$$\begin{aligned}\hat{t}_4=\Theta_3\Big[&-j_{10}\beta^3+\left(j_{15}\hat{q}_4+j_3\hat{l}_4+j_{21}\hat{s}_4+j_9\hat{n}_4+j_8\right)\beta\\&+\left(-\hat{p}_2\hat{l}_4-\hat{p}_4\hat{n}_4-\hat{p}_6\hat{q}_4-\hat{p}_8\hat{s}_4\right)j_{12}\\&+\left(-\hat{r}_4\hat{n}_4-\hat{r}_6\hat{q}_4-\hat{r}_8\hat{s}_4-\hat{r}_2\hat{l}_4\right)j_{18}\\&+\left(-\hat{k}_2\hat{l}_4-\hat{k}_4\hat{n}_4-\hat{k}_6\hat{q}_4-\hat{k}_8\hat{s}_4\right)j_1\\&-j_6\left(\hat{m}_2\hat{l}_4+\hat{m}_4\hat{n}_4+\hat{m}_8\hat{s}_4+\hat{m}_6\hat{q}_4\right)\Big]\end{aligned}\quad\text{(B.24)}$$

$$\begin{aligned}\hat{t}_5=\Theta_3\Big[&\left(-\hat{p}_8\hat{s}_5-\hat{p}_6\hat{q}_5-\hat{p}_4\hat{n}_5-\hat{p}_2\hat{l}_5-p_5\right)j_{12}\\&+\left(-\hat{r}_2\hat{l}_5-\hat{r}_5-\hat{n}_5\hat{r}_4-\hat{r}_6\hat{q}_5-\hat{r}_8\hat{s}_5\right)j_{18}\\&+\left(-\hat{k}_4\hat{n}_5-\hat{k}_6\hat{q}_5-\hat{k}_2\hat{l}_5-\hat{k}_8\hat{s}_5-\hat{k}_5\right)j_1\\&+\left(-\hat{m}_5-\hat{m}_4\hat{n}_5-\hat{m}_8\hat{s}_5-\hat{m}_2\hat{l}_5-\hat{m}_6\hat{q}_5\right)j_6\\&+j_{15}\beta\hat{q}_5+j_{21}\beta\hat{s}_5+j_9\beta\hat{n}_5-j_{11}+j_3\beta\hat{l}_5+j_{13}\beta^2\Big]\end{aligned}\quad\text{(B.25)}$$

$$\begin{aligned}\hat{t}_6 = \Theta_3\Big[&-j_{16}\beta^3 + \Big(j_{14} + j_9\hat{n}_6 + j_{15}\hat{q}_6 + j_3\hat{l}_6 + j_{21}\hat{s}_6\Big)\beta \\ &+\Big(-\hat{p}_2\hat{l}_6 - \hat{p}_4\hat{n}_6 - \hat{p}_6\hat{q}_6 - \hat{p}_8\hat{s}_6\Big)j_{12} \\ &+\Big(-r_2\hat{l}_6 - \hat{r}_4\hat{n}_6 - \hat{r}_6\hat{q}_6 - \hat{r}_8\hat{s}_6\Big)j_{18} \\ &+\Big(-\hat{k}_4\hat{n}_6 - \hat{k}_2\hat{l}_6 - \hat{k}_6\hat{q}_6 - \hat{k}_8\hat{s}_6\Big)j_1 \\ &-j_6\Big(\hat{m}_8\hat{s}_6 + \hat{m}_2\hat{l}_6 + \hat{m}_6\hat{q}_6 + \hat{m}_4\hat{n}_6\Big)\Big]\end{aligned} \tag{B.26}$$

$$\begin{aligned}\hat{t}_7 = \Theta_3\Big[&\Big(-\hat{p}_4\hat{n}_7 - \hat{p}_8\hat{s}_7 - \hat{p}_2\hat{l}_7 - \hat{p}_7 - \hat{q}_7 p_6\Big)j_{12} \\ &+\Big(-\hat{r}_2\hat{l}_7 - \hat{r}_6\hat{q}_7 - \hat{r}_7 - \hat{r}_4\hat{n}_7 - \hat{r}_8\hat{s}_7\Big)j_{18} \\ &+\Big(-\hat{k}_4\hat{n}_7 - \hat{k}_2\hat{l}_7 - \hat{k}_6\hat{q}_7 - \hat{k}_8\hat{s}_7 - \hat{k}_7\Big)j_1 \\ &+\Big(-\hat{m}_2\hat{l}_7 - \hat{m}_7 - \hat{m}_4\hat{n}_7 - \hat{m}_8\hat{s}_7 - \hat{m}_6\hat{q}_7\Big)j_6 \\ &+j_{19}\beta^2 + j_9\beta\hat{n}_7 + j_3\beta\hat{l}_7 + j_{21}\beta\hat{s}_7 + j_{15}\beta\hat{q}_7 - j_{17}\Big]\end{aligned} \tag{B.27}$$

$$\begin{aligned}\hat{t}_8 = \Theta_3\Big[&-j_{22}\beta^3 + \Big(j_{20} + j_{15}\hat{q}_8 + j_3\hat{l}_8 + j_{21}\hat{s}_8 + j_9\hat{n}_8\Big)\beta \\ &+\Big(-\hat{p}_2\hat{l}_8 - \hat{p}_4\hat{n}_8 - \hat{p}_6\hat{q}_8 - \hat{p}_8\hat{s}_8\Big)j_{12} \\ &+\Big(-r_2\hat{l}_8 - \hat{r}_4\hat{n}_8 - \hat{r}_6\hat{q}_8 - \hat{r}_8\hat{s}_8\Big)j_{18} \\ &+\Big(-\hat{k}_2\hat{l}_8 - \hat{k}_4\hat{n}_8 - \hat{k}_6\hat{q}_8 - \hat{k}_8\hat{s}_8\Big)j_1 \\ &-j_6\Big(\hat{m}_6\hat{q}_8 + \hat{m}_8\hat{s}_8 + \hat{m}_2\hat{l}_8 + \hat{m}_4\hat{n}_8\Big)\Big]\end{aligned} \tag{B.28}$$

$$\begin{aligned}\hat{t}_9 = \Theta_3\Big[&-j_{27}\beta^4 + j_{26}\beta^2 + \Big(j_{15}\hat{q}_9 + j_3\hat{l}_9 + j_{21}\hat{s}_9 + j_9\hat{n}_9\Big)\beta \\ &+\Big(-\hat{p}_2\hat{l}_9 - \hat{p}_4\hat{n}_9 - \hat{p}_6\hat{q}_9 - \hat{p}_8\hat{s}_9\Big)j_{12} \\ &+\Big(-\hat{r}_2\hat{l}_9 - \hat{r}_4\hat{n}_9 - \hat{r}_6\hat{q}_9 - \hat{r}_8\hat{s}_9\Big)j_{18} \\ &+\Big(-\hat{k}_2\hat{l}_9 - \hat{k}_4\hat{n}_9 - \hat{k}_6\hat{q}_9 - \hat{k}_8\hat{s}_9\Big)j_1 \\ &-j_6\Big(\hat{m}_6\hat{q}_9 + \hat{m}_8\hat{s}_9 + \hat{m}_2\hat{l}_9 + \hat{m}_4\hat{n}_9\Big)\Big]\end{aligned} \tag{B.29}$$

$$\begin{aligned}\hat{t}_{10} = \Theta_3\Big[&\Big(-\hat{p}_9 - \hat{p}_2\hat{l}_{10} - \hat{p}_4\hat{n}_{10} - \hat{p}_6\hat{q}_{10} - \hat{p}_8\hat{s}_{10}\Big)j_{12} \\ &-\Big(\hat{r}_9 + \hat{r}_6\hat{q}_{10} + \hat{r}_2\hat{l}_{10} + \hat{r}_8\hat{s}_{10} + \hat{r}_4\hat{n}_{10}\Big)j_{18} \\ &-\Big(\hat{k}_2\hat{l}_{10} + \hat{k}_4\hat{n}_{10} + \hat{k}_6\hat{q}_{10} + \hat{k}_8\hat{s}_{10} + \hat{k}_9\Big)j_1 \\ &-\Big(\hat{m}_4\hat{n}_{10} + \hat{m}_8\hat{s}_{10} + \hat{m}_9 + \hat{m}_2\hat{l}_{10} + \hat{m}_6\hat{q}_{10}\Big)j_6 \\ &+j_{21}\beta\hat{s}_{10} + j_9\beta\hat{n}_{10} - j_{23} + j_3\beta\hat{l}_{10} + j_{15}\beta\hat{q}_{10} + j_{25}\beta^2\Big]\end{aligned} \tag{B.30}$$

$$\hat{t}_{11} = -1/\Theta_3 \tag{B.31}$$

References

Adams, D.F., Carlsson, L.A., Pipes, R.B., 2000. Experimental Characterization of Advanced Composite Materials, third ed. CRC Press, Boca Raton, London, New York, Washington, DC.

Anderson, T.L., 2005. Fracture Mechanics – Fundamentals and Applications, third ed. CRC Press, Taylor & Francis Group, Boca Raton, London, New York, Singapore.

Andrews, M.G., Massabò, R., Cavicchi, A., Cox, B.N., 2009. Dynamic interaction effects of multiple delaminations in plates subject to cylindrical bending. Int. J. Solids Struct. 49, 1815–1833.

Argüelles, A., Viña, J., Canteli, A.F., Bonhomme, J., 2011. Influence of resin type on the delamination behavior of carbon fiber reinforced composites under mode-II loading. Int. J. Damage Mech. 20, 963–977.

Arrese, A., Carbajal, N., Vargas, G., Mujika, F., 2010. A new method for determining mode II R-curve by the end-notched flexure test. Eng. Fract. Mech. 77, 51–70.

Batista, M., 2012. Comparison of Reissner, Mindlin and Reddy plate models with exact three dimensional solution for simply supported isotropic and transverse inextensible rectangular plate. Meccanica 47, 257–268.

Bennati, S., Colleluori, M., Corigliano, D., Valvo, P.S., 2009. An enhanced beam-theory model of the asymmetric double cantilever beam (ADCB) test for composite laminates. Compos. Sci. Technol. 69, 1735–1745.

Bennati, S., Fisicaro, P., Valvo, P.S., 2013a. An enhanced beam-theory model of the mixed-mode bending (MMB) test. Part I: Literature review and mechanical model. Meccanica 48, 443–462.

Bennati, S., Fisicaro, P., Valvo, P.S., 2013b. An enhanced beam-theory model of the mixed-mode bending (MMB) test. Part II: Applications and results. Meccanica 48, 465–484.

Bonhomme, J., Argüelles, A., Castrillo, M.A., Viña, J., 2010. Computational models for mode I composite fracture failure: the virtual crack closure technique versus the two-step extension method. Meccanica 45, 297–304.

Budzik, M.K., Jumel, J., Salem, N.B., Shanahan, M.E.R., 2013. Instrumented end notched flexure – crack propagation and process zone monitoring. Part II: Data reduction and experimental. Int. J. Solids Struct. 50, 310–319.

Cherepanov, G.P., 1997. Methods of Fracture Mechanics: Solid Matter Physics. Kluwer Academic Publishers, Dordrecht, Boston, London.

Chirica, I., 2013. Torsion dynamic behaviour of the ship hull made out of layered composites. Math. Prob. Eng., 1–7 (Article ID 793412).

Chirica, I., Musat, S.D., Chirica, R., Beznea, E.F., 2011. Torsional behaviour of the ship hull composite model. Comput. Mater. Sci. 50, 1381–1386.

Chou, P.C., Pagano, N.J., 1967. Elasticity – Tensor, Dyadic, and Engineering Approaches. D. Van Nostrand Company Inc., Princeton, NJ, Toronto, London.

da Silva, L.F.M., Estevez, V.H.C., Chavez, F.J.P., 2011. Fracture toughness of a structural adhesive under mixed mode loadings. Materialwiss. Werkstofftech. 42, 460–470.

Davidson, B.D., Sediles, F.O., 2011. Mixed-modeI-II-III delamination toughness determination via a shear-torsion-bending test. Compos. Part A: Appl. Sci. Manuf. 42, 589–603.

Davidson, B.D., Yu, L., Hu, H., 2000. Determination of energy release rate and mode mix in three-dimensional layered structures using plate theory. Int. J. Fract. 105, 81–104.

Davidson, B.D., Sediles, F.O., Humphrey, K.D., 2010. A shear-torsion-bending test for mixed-mode I-II-III delamination toughness determination, in: 25th Technical Conference of the American Society for Composites and 14th US–Japan Conference on Composite Materials, 20–22 September 2010, Dayton, Ohio, USA, pp. 1001–1020.

de Morais, A.B., Pereira, A.B., 2008. Mixed mode II + III interlaminar fracture of carbon/epoxy laminates. Compos. Sci. Technol. 68, 2022–2027.

de Morais, A.B., Pereira, A.B., 2009. Mode III interlaminar fracture of carbon/epoxy laminates using a four-point bending plate test. Compos. Part A: Appl. Sci. Manuf. 40, 1741–1746.

de Morais, A.B., Pereira, A.B., de Moura, M.F.S.F., 2011. Mode III interlaminar fracture of carbon/epoxy laminates using the six-point edge crack torsion (6ECT). Compos. Part A: Appl. Sci. Manuf. 42, 1793–1799.

de Moura, M.F.S.F., Fernandez, M.V.C., de Morais, A.B., Campilho, R.D.S.G., 2009. Numerical analysis of the edge crack torsion test for mode III interlaminar fracture of composite laminates. Eng. Fract. Mech. 76, 469–478.

Fernández, M.V., Moura, M.F.S.F., da Silva, L.F.M., Marques, A.T., 2013. Mixed-mode fatigue/fracture characterization of composite bonded joints using the single-leg bending test. Compos. Part A: Appl. Sci. Manuf. 44, 63–69.

Ferreira, A.J.M., Roque, C.M.C., Carrera, E., Cinefra, M., Polit, O., 2011. Two higher order zig-zag theories for the accurate analysis of bending, vibration and buckling response of laminated plates by radial basis functions collocation and a unified formulation. J. Compos. Mater. 45, 2523–2536.

Garvan, F., 2002. The Maple Book. Chapman & Hall/CRC, Boca Raton, London, New York, Washington DC.

Giannis, S., Adams, R.D., Clark, L.J., Taylor, M.A., 2008. The use of a modified peel specimen to assess the peel resistance of aircraft fuel tank sealants. Int. J. Adhes. Adhes. 28, 158–175.

Hamed, M.A., Nosier, A., Farrahi, G.H., 2006. Separation of delamination modes in composite beams with symmetric delaminations. Mater. Des. 27, 900–910.

Hills, D.A., Kelly, P.A., Dai, D.N., Korsunsky, A.M., 1996. Solution of Crack Problems, The Distributed Dislocation Technique. Kluwer Academic Publishers, Dordrecht, Boston, London.

Ho, S.L., Tay, A.A.O., 201. A numerical analysis of penny-shaped delaminations in an encapsulated silicon module. In: Proceedings – Electronic Componentsand Technology Conference, pp. 1115–1121.

Islam, M.M., Kapania, R.K., 2011. Delamination growth using cohesive zone model for adhesive bonding under compression. In: Proulx, T. (Ed.), Experimental and Applied Mechanics. Springer, New York, pp. 527–536.

Johnston, A.L., Davidson, B.D., Simon, K.K., 2012. Evaluation of new test methods for the determination of G_{IIIc} of laminated polymeric composites. In: 27th Annual Technical Conference of the American Society for Composites 2012, Held Jointly with 15th Joint US-Japan Conference on Composite Materials and ASTM-D30 Meeting, pp. 120–139.

Jones, R.M., 1999. Mechanics of Composite Materials, second ed. Taylor & Francis Inc., Philadelphia, London.

Jumel, J., Budzik, M.K., Shanahan, M.E.R., 2011a. Beam on elastic foundation with anticlastic curvature: application to analysis of mode I fracture tests. Eng. Fract. Mech. 78, 3253–3269.

Jumel, J., Budzik, M.K., Shanahan, M.E.R., 2011b. Process zone in the single cantilever beam under transverse loading. Part I: Theoretical analysis. Theor. Appl. Fract. Mech. 56, 7–12.

Jumel, J., Budzik, M.K., Salem, N.B., Shanahan, M.E.R., 2013. Instrumented end notched flexure – crack propagation and process zone monitoring. Part I: Modelling and analysis. Int. J. Solids Struct. 50, 297–309.

Kenane, M., Benmedakhene, S., Azari, Z., 2010. Fracture and fatigue study of unidirectional glass/epoxy laminate under different mode of loading. Fatigue Fract. Eng. Mater. Struct. 33, 285–293.
Kharazi, M., Ovesy, H.R., Taghizadeh, M., 2010. Buckling of the composite laminates containing through-the-width delaminations using different plate theories. Compos. Struct. 92, 1176–1183.
Kiani, M., Shiozaki, H., Motoyama, K., 2013. Using experimental data to improve crash modeling for composite materials. in: Conference Proceedings of the Society for Experimental Mechanics Series, pp. 215–226.
Kim, S., Kim, J.S., Yoon, H., 2011. Experimental and numerical investigations of mode I delamination behaviors of woven fabric composites with carbon, kevlar and their hybrid fibers. Int. J. Precis. Eng. Manuf. 12, 321–329.
Kollár, L.P., Springer, G.S., 2003. Mechanics of Composite Structures. Cambridge University Press, Cambridge, New York, Melbourne, Madrid, Cape Town, Singapore, São Paolo.
Kondo, A., Sato, Y., Suemasu, H., Gouzu, K., Aoki, Y., 2010. Characterization of fracture resistance of carbon/epoxy composite laminates during mixed-mode II and III stable damage propagation. J. Jpn. Soc. Compos. Mater. 36, 179–188.
Kondo, A., Sato, Y., Suemasu, H., Aoki, Y., 2011. Fracture resistance of carbon/epoxy composite laminates under mixed-mode II and III failure and its dependence on fracture morphology. Adv. Compos. Mater. 20, 405–418.
Kumar, Y., Lal, R., 2012. Vibrations of nonhomogeneous orthotropic rectangular plates with bilinear thickness variation resting on Winkler foundation. Meccanica 47, 893–915.
Kutnar, A., Kamke, F.A., Nairn, J.A., Sernek, M., 2008. Mode II fracture behavior of bonded viscoelastic thermal compressed wood. Wood Fiber Sci. 40, 362–373.
Lee, S.M., 1993. An edge crack torsion method for mode III delamination fracture testing. J. Compos. Technol. Res. 15, 193–201.
Lee, L.J., Tu, D.W., 1993. J integral for delaminated composite laminates. Compos. Sci. Technol. 47, 185–192.
Luo, Q., Tong, L., 2009. Energy release rates for interlaminar delamination in laminates considering transverse shear effects. Compos. Struct. 89, 235–244.
Marat-Mendes, R.M., Freitas, M.M., 2009. Characterisation of the edge crack torsion (ECT) test for the measurement of the mode III interlaminar fracture toughness. Eng. Fract. Mech. 76, 2799–2809.
Marat-Mendes, R., Freitas, M.D., 2013. Fractographic analysis of delamination in glass/fibre epoxy composites. J. Compos. Mater. 47, 1437–1448.
Massabò, R., Campi, F., 2013. Modeling laminated composites with cohesive interfaces: a homogenization approach. In: Proceedings of the XXI congress of the Italian Association of Theoretical and Applied Mechanics, Torino, September 2013, pp. 1–10.
Mehrabadi, F.A., 2013. Analysis of pure mode III and mixed mode (III + II) interlaminar crack growth in polymeric woven fabrics. Mater. Des. 44, 429–437.
Mehrabadi, F.A., Khosravan, M., 2013. Mode III interlaminar fracture in woven glass/epoxy composite laminates. World Acad. Sci. Eng. Technol. 73, 479–483.
Miura, M., Shindo, Y., Takeda, T., Narita, F., 2012. Interlaminar fracture characterization of woven glass/epoxy composites under mixed-mode II/III loading conditions at cryogenic temperatures. Eng. Fract. Mech. 96, 615–625.
Mladensky, A.S., Rizov, V., 2013a. Analysis of mixed mode II/III crack in bilayered composite beam. J. Theor. Appl. Mech. 42, 41–52.
Mladensky, A.S., Rizov, V., 2013b. Analytical investigation of nonlinear interlaminar fracture in trilayered polymer composite beam under mode II crack loading conditions using the J-integral approach. Arch. Appl. Mech. 83, 1637–1658.
Murakami, T., Sato, T., 1983. Three-dimensional J-integral calculations of part-through surface crack problems. Comput. Struct. 17, 731–736.
Nettles, A.T., 1991. Basic mechanics of laminated composite plates. Technical Report, NASA, Marshall Space Flight Center, MSFC, Alabama 35812, USA, NASA Reference, Publication 1351.
Nikbakht, M., Choupani, N., 2008. Fracture toughness characterization of carbon-epoxy composite using Arcan specimen. World Acad. Sci. Eng. Technol. 41, 738–744.
Nikbakht, M., Choupani, N., Hosseini, S.R., 2010. 2D and 3D interlaminar fracture assessment under mixed-mode loading conditions. Mater. Sci. Eng. A 516, 162–168.
Peng, L., Zhang, J., Zhao, L., Bao, R., Yang, H., Fei, B., 2011. Mode I delamination growth of multidirectional composite laminates under fatigue loading. J. Compos. Mater. 45, 1077–1090.
Pereira, A.B., de Morais, A.B., 2009. Mixed-mode I + III interlaminar fracture of carbon/epoxy laminates. Compos. Part A: Appl. Sci. Manuf. 40, 518–523.
Pereira, A.B., de Morais, A.B., de Moura, M.F.S.F., 2011. Design and analysis of a new six-point edge crack torsion (6ECT) specimen for mode III interlaminar fracture characterisation. Compos. Part A: Appl. Sci. Manuf. 42, 131–139.
Reddy, J.N., 2004. Mechanics of Laminated Composite Plates and Shells – Theory and Analysis. CRC Press, Boca Raton, London, New York, Washington DC.
Rizov, V., Mladensky, A.S., 2012. Analysis of mode II crack in bilayered composite beam. J. Theor. Appl. Mech. 42, 67–78.
Rizov, V., Shindo, Y., Horiguchi, K., Narita, F., 2006. Mode III interlaminar fracture behaviour of glass fiber reinforced polymer woven laminates at 293 to 4 K. Appl. Compos. Mater. 13, 287–304.
Romhany, G., Szebenyi, G., 2012. Interlaminar fatigue crack growth behavior of MWCNT/carbon fiber reinforced hybrid composites monitored via newly developed acoustic emission method. Express Polym. Lett. 6, 572–580.
Saeedi, N., Sab, K., Caron, J.F., 2012a. Delaminated multilayered plates under uniaxial extension. Part I: Analytical analysis using a layerwise stress approach. Int. J. Solids Struct. 49, 3711–3726.
Saeedi, N., Sab, K., Caron, J.F., 2012b. Delaminated multilayered plates under uniaxial extension. Part II: Efficient layerwise mesh strategy for the prediction of delamination onset. Int. J. Solids Struct. 49, 3727–3740.
Salem, N.B., Budzik, M.K., Jumel, J., Shanahan, M.E.R., Lavelle, F., 2013. Investigation of the crack front process zone in the double cantilever beam test with backface strain monitoring technique. Eng. Fract. Mech. 98, 272–283.
Sankar, B.V., Sonik, V., 1995. Pointwise energy release rate in delaminated plates. AIAA J. 33, 1312–1318.
Shahrjerdi, A., Bayat, M., Mustapha, F., Sapuan, S.M., Zahari, R., 2010. Second-order shear deformation theory to analyze stress distribution for solar functionally graded plates. Mech. Based Des. Struct. Mach. 38, 348–361.
Shahrjerdi, A., Mustapha, F., Bayat, M., Majid, D.L.A., 2011. Free vibration analysis of solar functionally graded plates with temperature-dependent material properties using second order shear deformation theory. J. Mech. Sci. Technol. 25, 1–15.
Shivakumar, K.N., Raju, I.S., 1992. An equivalent domain integral method for three-dimensional mixed-mode fracture problems. Eng. Fract. Mech. 42, 935–959.
Sorensen, L., Botsis, J., Gmür, T., Cugnoni, J., 2007. Delamination detection and characterisation of bridging tractions using long FBG optical sensors. Compos. Part A: Appl. Sci. Manuf. 38, 2087–2096.
Suemasu, H., Tanikado, Y., 2012. Delamination propagation behavior and the fracture toughness of composite laminates under shear fracture mode. In: 27th Annual Technical Conference of the American Society for Composites 2012, Held Jointly with 15th Joint US-Japan Conference on Composite Materials and ASTM-D30 Meeting, pp. 367–379.
Suemasu, H., Kondo, A., Gozu, K., Aoki, Y., 2010. Novel test method for mixed mode II and III interlaminar fracture toughness. Adv. Compos. Mater. 19, 349–361.
Szekrényes, A., 2007a. Delamination fracture analysis in the G_{II}–G_{III} plane using prestressed composite beams. Int. J. Solids Struct. 44, 3359–3378.
Szekrényes, A., 2007b. Improved analysis of unidirectional composite delamination specimens. Mech. Mater. 39, 953–974.
Szekrényes, A., 2009a. Improved analysis of the modified split-cantilever beam for mode III fracture. Int. J. Mech. Sci. 51, 682–693.
Szekrényes, A., 2009b. Interlaminar fracture analysis in the G_I–G_{III} plane using prestressed composite beams. Compos. Part A: Appl. Sci. Manuf. 40, 1621–1631.
Szekrényes, A., 2011. Interlaminar fracture analysis in the G_I–G_{II}–G_{III} space using prestressed composite beams. J. Reinf. Plast. Compos. 30, 1655–1669.
Szekrényes, A., 2012a. Interlaminar fracture analysis in the G_{II}–G_{III} plane using prestressed composite beams. Compos. Part A: Appl. Sci. Manuf. 43, 95–103.
Szekrényes, A., 2012b. Interlaminar stresses and energy release rates in delaminated orthotropic composite plates. Int. J. Solids Struct. 49, 2460–2470.
Szekrényes, A., 2013a. Analysis of classical and first-order shear deformable cracked orthotropic plates. J. Compos. Mater. (available online).
Szekrényes, A., 2013b. Interface crack between isotropic Kirchhoff plates. Meccanica 48, 507–526.
Szekrényes, A., 2013c. Interface fracture in orthotropic composite plates using second-order shear deformation theory. Int. J. Damage Mech. 22, 1161–1185.
Szekrényes, A., 2013d. The system of exact kinematic conditions and application to delaminated first-order shear deformable plates. Int. J. Mech. Sci. 77, 17–29.
Szekrényes, A., 2014b. Application of Reddy's third-order theory to delaminated orthotropic composite plates. Eur. J. Mech. A/Solids 43, 9–24.
Szekrényes, A., in press. Stress and fracture analysis in delaminated orthotropic composite plates using third-order shear deformation theory. Appl. Math. Model.
Thai, H.T., Choi, D.H., 2013. A simple first-order shear deformation theory for laminated composite plates. Compos. Struct. 106, 754–763.
Thai, H.T., Kim, S.E., 2012. Lévy-type solution for free vibration analysis of orthotropic plates based on two variable refined plate theory. Appl. Math. Model. 36, 3870–3882.
Yoshihara, H., Satoh, A., 2009. Shear and crack tip deformation correction for the double cantilever beam and three-point end-notched flexure specimens for mode I and mode II fracture toughness measurement of wood. Eng. Fract. Mech. 76, 335–346.
Yu, W., 2005. Mathematical construction of a Reissner–Mindlin plate theory for composite laminates. Int. J. Solids Struct. 42, 6680–6699.
Zhou, W., Liang, X., Li, Y., You, S., Liu, R., Chai, H., Lv, Z., 2013. Acoustic emission monitoring for delaminated composites under bending damage failure condition. Appl. Mech. Mater. 310, 51–54.